

WIENER-HOPF METHOD APPLIED TO A DIELECTRIC CYLINDER ASYMMETRICALLY
EXCITED BY A CIRCULAR METALLIC WAVEGUIDE

by

Luís Filipe Ferreira Martins Camelo

A dissertation submitted in partial fulfillment
of the requirements for the degree of
Doctor of Philosophy
(Electrical Engineering)
in The University of Michigan
1982

Doctoral Committee:

Professor Thomas B.A. Senior, Co-chairman
Research Scientist Dipak L. Sengupta, Co-chairman
Professor Albert E. Heins
Professor Charles B. Sharpe
Professor Chen-To Tai

ABSTRACT

WIENER-HOPF METHOD APPLIED TO A DIELECTRIC CYLINDER ASYMMETRICALLY EXCITED BY A CIRCULAR METALLIC WAVEGUIDE

by

Luís Filipe Ferreira Martins Camelo

Co-chairmen: Thomas B.A. Senior, Dipak L. Sengupta

The problem of an infinite dielectric cylinder, clad by a semi-infinite metallic circular waveguide, and excited by means of an azimuthally asymmetric mode propagating down the guide towards its open end, is formulated using the Wiener-Hopf technique. The method introduced by Jones is used, and leads to a pair of coupled Wiener-Hopf equations, whose solution depends on the factorization of a second order square matrix, into two square matrices analytic in the upper and lower half-planes, respectively. That factorization appears to be beyond the capabilities of presently known methods. Instead, a perturbation solution is sought for the case of a dielectric with relative permittivity close to unity.

The coupled Wiener-Hopf equations are expanded in Taylor series, in the propagation constant around the free space value. New sets of coupled Wiener-Hopf equations are found for the zeroth- and the first-order terms of the series expansions of the unknown

functions. For each one of these sets of equations, a redefinition of the unknown functions, as linear combinations of the previous unknown functions, leads to the uncoupling of the equations. Then, the solutions for the zeroth- and the first-order terms of the unknown functions are found by solving, in each case, two independent Wiener-Hopf problems.

These solutions are inverse Fourier transformed, to yield the zeroth- and the first-order terms of the components of the surface current density. The zeroth- and first-order terms of the reflection coefficients inside the metallic guide are then identified, and computations are carried out for the reflection coefficient of the dominant mode.

The solutions of the zeroth- and first-order Wiener-Hopf equations are used to yield the zeroth- and first-order terms of the Fourier transforms of the components of the electric and magnetic fields for every point in space. These functions are inverse Fourier transformed, for points in the far field, by evaluating the integrals asymptotically, using the method of steepest descents. Expressions for the zeroth- and first-order terms of the far field components are found.

DEDICATION

To my parents.

ACKNOWLEDGEMENTS

The author would like to acknowledge the support of his colleagues at the Radiation Laboratory during the work that led to the completion of this dissertation. Thanks are due to Dr. D. L. Sengupta and Professor T.B.A. Senior for having helped in the selection of this topic, and for their support and invaluable advice, during the many times the author felt temporarily discouraged by the innumerable difficulties of the problem. Special thanks go to Mrs. Wanita Rasey, who expertly typed the manuscript.

TABLE OF CONTENTS

	<u>Page</u>
DEDICATION	ii
ACKNOWLEDGEMENTS	iii
LIST OF FIGURES	vi
LIST OF TABLES	vii
LIST OF SYMBOLS	viii
LIST OF APPENDICES	xiii
CHAPTER I. INTRODUCTION	1
1.1 Introductory Remarks and Survey of Previous Work	1
1.2 Outline of the Problem to be Solved	6
CHAPTER II. FORMULATION OF THE PROBLEM	10
2.1 Formulation of the Coupled Wiener-Hopf Equations	10
2.2 Factorization of the Matrix	23
2.3 Simplification for the Case $\epsilon_1 = \epsilon_0$	28
2.4 Simplification for the Symmetrical Case ($m = 0$)	34
CHAPTER III. TAYLOR SERIES SOLUTION FOR $\epsilon_1 - \epsilon_0 \ll \epsilon_0$	35
3.1 Wiener-Hopf Equations for the Zeroth- and First-Order Terms of the Series	35
3.2 Solution of the Wiener-Hopf Equations for the Zeroth-Order Terms	40
3.3 Solution of the Wiener-Hopf Equations for the First-Order Terms	50
CHAPTER IV. REFLECTION COEFFICIENTS INSIDE THE METALLIC GUIDE	58
4.1 Inverse Fourier Transformation of $\mathcal{A}_{\phi_0}^U(n)$ and $\mathcal{A}_{z_0}^U(n)$	58
4.2 Inverse Fourier Transformation of $\mathcal{A}_{\phi_1}^U(n)$ and $\mathcal{A}_{z_1}^U(n)$	64
4.3 Reflection Coefficients; Zeroth and First Order Terms	73
4.4 Some Numerical Computations for the TE ₁₁ Mode	80

	<u>Page</u>
CHAPTER V. FIELDS OUTSIDE THE METALLIC GUIDE	87
5.1 Some Properties of the Field Components for $z > 0$	87
5.2 Zeroth Order Asymptotic Far Field	92
5.3 First Order Asymptotic Far Field Outside the Dielectric	102
CHAPTER VI. COMMENTS AND CONCLUSIONS	105
APPENDICES	107
LIST OF REFERENCES	140

LIST OF FIGURES

<u>Figure</u>		<u>Page</u>
1.1	Geometry and coordinate system of the problem.	3
2.1	Choice of branch and branch cuts, such that $\text{Im } \nu_0 \geq 0$. The shaded area represents the physical region, for which $\text{Re } \nu_0 \geq 0$ as well.	15
4.1	Variation with $k_0 a$ of the complex functions Γ_{10}^{TE} and $1/a \Gamma_{11}^{\text{TE}}$.	83
5.1	Paths of integration in the α -plane. The Regions numbered I, II, III, and IV are the images of the first, second, third and fourth quadrants of the η -plane through $\eta = k_0 \cos \alpha$, with k_0 real. The primed regions are such that $\nu_0 = k_0 \sin \alpha$ has negative imaginary part, with $\text{Im } \nu_0$ positive in the unprimed regions.	97
B.1	Branch cuts and paths of integration for the additive decomposition of $R_1(\eta)$ and $S_1(\eta)$. The dashed lines represent alternative branch cuts, which are used in Appendix B.	114
B.2	Deformation of the paths of integration γ_1 and γ_2 into γ_1' and γ_2' , respectively, showing the capture of the residues of the poles on the branches of the hyperbola.	119

LIST OF TABLES

<u>Table</u>		<u>Page</u>
4.1	Numerical Values for $\Gamma_1^{\text{TE}} = \Gamma_{10}^{\text{TE}} + \Gamma_{11}^{\text{TE}} \Delta k + \dots$	82

LIST OF SYMBOLS

a	Radius of the cylinder.
a^-	Limit $\rho \rightarrow a$ from values $\rho < a$.
a^+	Limit $\rho \rightarrow a$ from values $\rho > a$.
$A_n(k)$	Amplitude factor for a TM_{mn} reflected mode.
$B_n(k)$	Amplitude factor for a TE_{mn} reflected mode.
c, c'	Paths of integration, Fig. 5.1.
$E_\rho(\rho, z), E_\phi(\rho, z), E_z(\rho, z)$	Total electric field components.
$E_\rho^i(\rho, z), E_\phi^i(\rho, z), E_z^i(\rho, z)$	Incident electric field components.
$\mathcal{E}_\rho(\rho, z), \mathcal{E}_\phi(\rho, z), \mathcal{E}_z(\rho, z)$	Scattered electric field components in cylindrical coordinates.
$\mathcal{E}_r(r, \theta), \mathcal{E}_\phi(r, \theta), \mathcal{E}_\theta(r, \theta)$	Scattered electric field components in spherical coordinates.
F.T.	Fourier transform(s).
$H_\rho(\rho, z), H_\phi(\rho, z), H_z(\rho, z)$	Total magnetic field components.
$H_\rho^i(\rho, z), H_\phi^i(\rho, z), H_z^i(\rho, z)$	Incident magnetic field components.
$\mathcal{H}_\rho(\rho, z), \mathcal{H}_\phi(\rho, z), \mathcal{H}_z(\rho, z)$	Scattered magnetic field components in cylindrical coordinates.
$\mathcal{H}_r(r, \theta), \mathcal{H}_\phi(r, \theta), \mathcal{H}_\theta(r, \theta)$	Scattered magnetic field components in spherical coordinates.
$H_m^{(1)}(x), H_m^{(2)}(x)$	mth order Hankel functions of the first and second kinds.

$\text{Im} ()$	Imaginary part of ().
$I_{\phi}(n,\rho), I_z(n,\rho), \dots$	Functions proportional to the F.T. of the scattered magnetic field components of the same subscripts.
$\mathcal{I}_{\phi}(n,a), \mathcal{I}_z(n,a)$	Functions proportional to the F.T. of the discontinuity of the z and the ϕ components of the scattered magnetic fields at $\rho = a$, respectively.
$\mathcal{I}_{\phi}^U(n), \mathcal{I}_z^U(n)$	Functions proportional to the F.T. of the surface current density components of the same subscripts.
$\mathcal{I}_{\phi 0}^U(n), \mathcal{I}_{z 0}^U(n), \mathcal{I}_{\phi 1}^U(n),$ $\mathcal{I}_{z 1}^U(n)$	Zeroth and first order terms of the functions of the previous entry.
$\mathcal{I}_{10}^U(n), \mathcal{I}_{20}^U(n), \mathcal{I}_{11}^U(n), \mathcal{I}_{21}^U(n)$	Linear combinations of the functions of the previous entry.
$J_m(x)$	mth order Bessel function of the first kind.
$J_{\phi}(z), J_z(z)$	Current density components associated with the scattered fields.
$J_{\phi}^{\text{TE}}(z), J_z^{\text{TE}}(z), J_z^{\text{TM}}(z)$	Current density components associated with the reflected waveguide modes.
$J_{\phi}^i(z), J_z^i(z), J_{\phi}^{i\text{TE}}(z),$ $J_z^{i\text{TE}}(z), J_z^{i\text{TM}}(z)$	Current density components associated with the incident waveguide modes.
k_0, k_1	Propagation constants in free-space and in the dielectric.

m	Number of periods of the ϕ -variation.
$o(\), O(\)$	Order behaviors for a given limit.
p_{mn}	n th zero of $J_m(x)$.
$\mathcal{P}_\eta [\]$	Cauchy principal value integration at η .
q_{mn}	n th zero of $J'_m(x)$.
r	Spherical radial coordinate.
$\text{Re} (\)$	Real part of $(\)$.
$R_{\phi 0}^E(\theta), R_{\theta 0}^E(\theta), R_{\phi 1}^E(\theta), R_{\theta 1}^E(\theta)$	θ - varying part of the components of the electric far field.
$V_\phi(\eta, \rho), V_Z(\eta, \rho), \dots$	Functions proportional to the F.T. of the scattered electric field components.
$V_\phi^L(\eta), V_Z^L(\eta), \dots$	Same as above, with $\rho = a$.
$V_{1c}^L(\eta), V_{20}^L(\eta), V_{11}^L(\eta), V_{21}^L(\eta)$	Linear combinations of the zeroth and first order terms of the functions of the previous entry.
$Y_m(x)$	m th order Bessel function of the second kind.
z	Cylindrical coordinate along the axis.
α	Complex variable, $\eta = k_0 \cos \alpha$.
α_m	Arbitrary amplitude factor for the TE_{m1} incident mode.
β_m	Arbitrary amplitude factor for the TM_{m1} incident mode.
$\gamma_1, \gamma_2, \gamma_1', \gamma_2'$	Paths of integration, Figs. B.1 and B.2.
Γ_n^{TE}	Reflection coefficient for the TE_{mn} mode, TE_{m1} incidence.

Γ_n^{TE}	Conversion coefficient for the TM_{mn} mode, TE_{m1} incidence.
Γ_n^{TM}	Reflection coefficient for the TM_{mn} mode, TM_{m1} incidence.
Γ_n^{TM}	Conversion coefficient for the TE_{mn} mode, TM_{m1} incidence.
Δk	$k_1 - k_0$
ϵ_0, ϵ_1	Electric permittivities of free space and of the dielectric.
ϵ_r	Relative permittivity of the dielectric, ϵ_1/ϵ_0 .
η	Complex F.T. variable.
θ	Spherical coordinate, angle with respect to the z-axis.
λ_{mn1}	Propagation constant of the TE_{mn} mode in the dielectric-filled metal guide.
λ_{mn} or λ_{mno}	Propagation constant of the TE_{mn} mode in the air-filled metal guide.
μ or μ_0	Magnetic permeability of free space.
μ_{mn1}	Propagation constant of the TM_{mn} mode in the dielectric-filled metal guide.
μ_{mn} or μ_{mno}	Propagation constant of the TM_{mn} mode in the air-filled metal guide.
v_0	$(k_0^2 - \eta^2)^{1/2}$
v_1	$(k_1^2 - \eta^2)^{1/2}$

ξ	Complex variable.
ρ	Cylindrical radial coordinate.
τ_c	$(k_0^2 - \xi^2)^{1/2}$
τ_1	$(k_1^2 - \xi^2)^{1/2}$
ϕ	Azimuthal angular coordinate in both the spherical and the cylindrical systems.
ϕ_0	Arbitrary polarization angle.
ω	Angular frequency of excitation.

LIST OF APPENDICES

<u>Appendix</u>		<u>Page</u>
A	Factorization of $x(n)$ and $y(n)$.	107
B	Additive Decomposition of $R_1(n)$ and $S_1(n)$	110
C	Some Properties of the Transforms of the Fields for $\rho < a$.	132
D	Some Properties of the Transforms of the Fields for $\rho > a$.	137

CHAPTER I. INTRODUCTION

1.1 Introductory Remarks and Survey of Previous Work

Dielectric-rod antennas are of considerable interest at microwave frequencies, and they have been treated by many authors, of which only a few will be mentioned here. Some early treatments (Kiely [1]) considered the radiation field to be due to the field distribution along the surface of the dielectric rod. Later, it was realized that the radiation originates mainly at the discontinuities. The strong forward lobe of the radiation pattern can be justified by considering the surface wave field at the plane where the dielectric rod ends. This field extends far beyond the cross-section of the rod, and constitutes a rather enlarged equivalent aperture, accounting for the improved gain (Brown and Spector [2], James [3]). More recently, a modal analysis of the radiation field was carried out by Yaghjian and Kornhauser [4]. The feeding problem, however, was not adequately addressed by any of the aforementioned works.

A very complete treatment of this type of antennas was presented by Andersen [5], who considered the excitation to be an equivalent magnetic current ring around the rod, and carried out a rigorous analysis based on that premise. A dipole excitation of a dielectric cylinder was rigorously treated by Yip [6], with concern for the waveguiding characteristics of the rod rather than the antenna characteristics.

It is clear that an exact mathematical treatment of the junction between a dielectric-filled circular metallic waveguide and a dielectric cylinder of the same radius, (Fig. 1.1.), is of great interest in understanding the properties of a dielectric-rod antenna.

The Fourier transform method of Wiener-Hopf is particularly suitable for that purpose, and has been used extensively. Very adequate treatments of this method may be found in [7], [8], [9], [10] and [11]. Applications of this method to discontinuities inside cylindrical waveguide regions may be found in [12], [13] and [14].

Acoustical radiation from open-ended cylindrical waveguides has been treated by Levine and Schwinger [15], Weinstein [16] and Rawlins [17], among others. The electromagnetic radiation from an open-ended air-filled cylindrical guide was treated by Weinstein [16]. The excitation was a mode propagating down the guide toward the open-end, and he considered both the cases of azimuthally symmetric (no ϕ -variation) and asymmetric ($\cos m\phi$ variation) modes. Ledebner [18] considered the radiation of an azimuthally symmetric electromagnetic mode from a coaxial line where the inner conductor is clad with a dielectric shell, and the outer conductor is terminated at $z = 0$. Angulo and Chang [19] studied the case of Fig. 1.1 excited by an azimuthally symmetric mode from inside the metallic guide. Pearson [20] treated the scattering of a plane wave by a semi-infinite air-filled metallic cylindrical guide.

The problem to be treated in this work considers the structure of Fig. 1.1, and the excitation is an electromagnetic

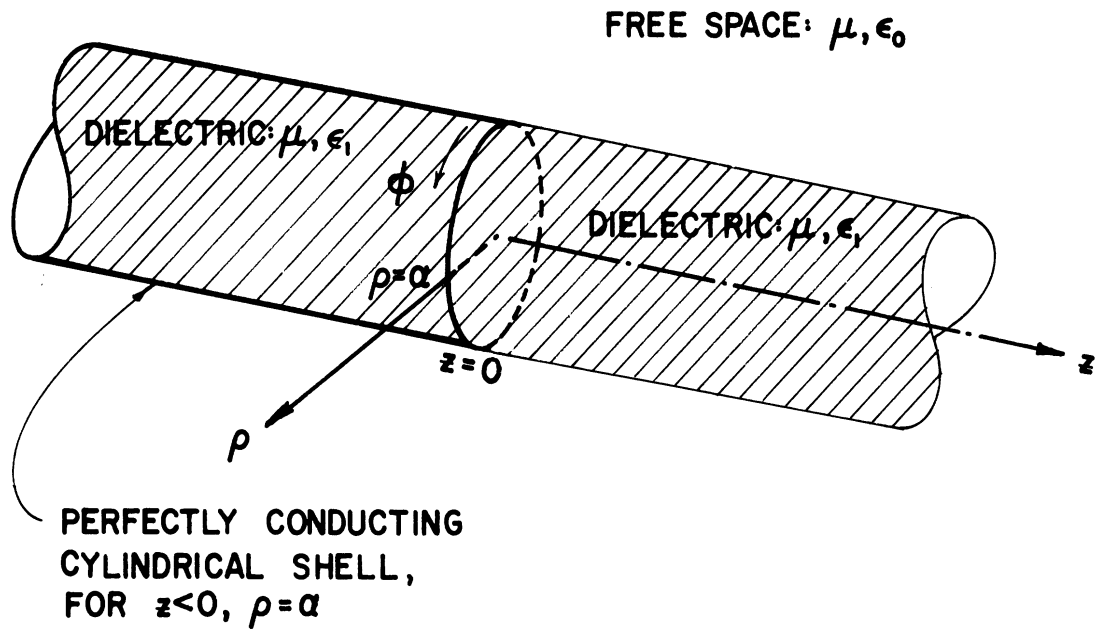


Fig. 1.1: Geometry and coordinate system of the problem.

mode propagating down the metallic guide in the positive z -direction. This mode will be assumed to have an m th order ϕ -variation.

This problem is an extension of [19], in that it considers an asymmetric mode excitation, instead of a symmetric mode. It is also an extension of both [20] and Chapter IV of [16], because it considers an asymmetric excitation, but it includes a dielectric rod inside the metallic guide, which extends to infinity

The major difficulty of the present problem is that it leads to two coupled Wiener-Hopf equations. Reference [19] leads to a single equation; [16] and [20] also lead to coupled equations, but it is possible to uncouple them by choosing suitable linear combinations of the unknown functions (in a manner similar to the problem treated by Senior, [21], for example).

The factorization of a matrix, which is involved in a coupled Wiener-Hopf problem, can only be accomplished in very special cases, (as treated in Section 2.2 of the present work). Heins [22] and, more recently, Hurd [23], Daniele [24] and Rawlins [25], have addressed this problem. This is a topic of active research at present, (see, for example, Heins [26]).

It is known ([1], [5]) that the preferred surface wave mode of the dielectric cylinder, as far as maximizing the forward radiation and minimizing the side-lobe levels are concerned, is the hybrid HE_{11} mode. This is also the dominant mode of the dielectric rod, with zero cutoff frequency, and its field components vary with ϕ as $\cos \phi$ or $\sin \phi$.

The dielectric rod is excited by means of a metallic waveguide, like in Fig. 1.1. An examination of the field distributions of the modes of the metallic guide, in a plane normal to the axis, points to the TE_{11} and TM_{11} modes as the most appropriate to excite an HE_{11} mode in the dielectric rod. It should be noted further that the dominant mode in a circular guide is the TE_{11} and, if a first order ϕ -variation is imposed, the next mode to propagate, for increasing frequency, is the TM_{11} . If the excitation is achieved by means of a small electric dipole in a transverse plane, centered on the axis inside the metallic waveguide, and far enough from the discontinuity, the only field to reach the open end is a TE_{11} mode if $1.84118 < k_1 a < 3.83171$. A TM_{11} mode will also reach the open end if $3.83171 < k_1 a$. Note that an electric dipole on axis will preferably excite first order ϕ -varying modes (similar to Yip [6]).

As a result of the previous considerations, it may be concluded that an azimuthally asymmetric excitation of the structure of Fig. 1.1 is of much more relevance, to the study of a real dielectric rod antenna, than a symmetrical excitation, (as [19], for instance). This constitutes the main motivation for this work.

As a last remark, it should be said that much of the attractiveness of this problem, to the author, was the fact that the mathematical tools and problems encountered resemble some of the problems in the field of optical fibers, which have been of interest to the author in the recent past.

1.2 Outline of the Problem to be Solved

The structure of Fig. 1.1 will be analyzed, when the excitation consists of two modes propagating inside the metallic guide in the positive z-direction. An mth order ϕ -variation is assumed for the field components, and the TE_{m1} and TM_{m1} modes are the exciting modes considered. Throughout all this work, the ρ and z components of the electric field and the ϕ component of the magnetic field are assumed to have a ϕ variation given by the factor $\sin(m\phi + \phi_0)$. Similarly, the ϕ component of the electric field and the ρ and the z components of the magnetic field have a ϕ variation given by the factor $\cos(m\phi + \phi_0)$. In that manner, the ρ component of the incident electric field, for example, will be represented as $\sin(m\phi + \phi_0) E_{\rho}^i(\rho, z)$, and analogously for the remaining field components. In the above, ϕ_0 is an arbitrary value of angle which determines the polarization of the fields. A time-varying factor $e^{-i\omega t}$ has been omitted throughout this work.

With A^* representing an arbitrary amplitude for the components of the incident TM_{m1} mode, and B^* for the TE_{m1} mode, the incident field components are

$$E_z^i = A^* J_m \left(\frac{p_{m1}}{a} \rho \right) e^{i\mu_{m11} z}, \quad (1.1)$$

$$H_z^i = B^* J_m \left(\frac{q_{m1}}{a} \rho \right) e^{i\lambda_{m11} z}, \quad (1.2)$$

$$E_{\rho}^i = \frac{i\mu_{m11} a}{p_{m1}} A^* J_m' \left(\frac{p_{m1}}{a} \rho \right) e^{i\mu_{m11} z} - \frac{i\omega\mu_0 a^2}{q_{m1}^2 \rho} B^* J_m \left(\frac{q_{m1}}{a} \rho \right) e^{i\lambda_{m11} z}, \quad (1.3)$$

$$H_{\rho}^i = -\frac{i\omega\varepsilon_1 ma^2}{p_{m1}^2 \rho} A * J_m \left(\frac{p_{m1}}{a} \rho \right) e^{i\mu_{m11} z} + \frac{i\lambda_{m11} a}{q_{m1}} B * J'_m \left(\frac{q_{m1}}{a} \rho \right) e^{i\lambda_{m11} z}, \quad (1.4)$$

$$E_{\phi}^i = \frac{i\mu_{m11} ma^2}{p_{m1}^2 \rho} A * J_m \left(\frac{p_{m1}}{a} \rho \right) e^{i\mu_{m11} z} - \frac{i\omega\mu a}{q_{m1}} B * J'_m \left(\frac{q_{m1}}{a} \rho \right) e^{i\lambda_{m11} z} \quad (1.5)$$

and

$$H_{\phi}^i = \frac{i\omega\varepsilon_1 a}{p_{m1}} A * J'_m \left(\frac{p_{m1}}{a} \rho \right) e^{i\mu_{m11} z} - \frac{i\lambda_{m11} ma^2}{q_{m1}^2 \rho} B * J_m \left(\frac{q_{m1}}{a} \rho \right) e^{i\lambda_{m11} z}. \quad (1.6)$$

The following notation was used in (1.1) through (1.6):

p_{mn} is the n th zero of $J_m(x)$, q_{mn} is the n th zero of $J'_m(x)$, μ_{mn1} and λ_{mn1} are the guided propagation constants of the TM_{mn} and the TE_{mn} modes, respectively, i.e.,

$$\mu_{mn1} = \left[k_1^2 - \left(\frac{p_{mn}}{a} \right)^2 \right]^{1/2} \quad (1.7a)$$

and

$$\lambda_{mn1} = \left[k_1^2 - \left(\frac{q_{mn}}{a} \right)^2 \right]^{1/2}, \quad (1.7b)$$

where $k_1 = \omega\sqrt{\mu\varepsilon_1}$. The corresponding notations $k_0 = \omega\sqrt{\mu\varepsilon_0}$,

$$\mu_{mno} = \left[k_0^2 - \left(\frac{p_{mn}}{a} \right)^2 \right]^{1/2}$$

and

$$\lambda_{mno} = \left[k_o^2 - \left(\frac{q_{mn}}{a} \right)^2 \right]^{1/2}$$

will be used throughout this work when $\epsilon = \epsilon_o$. Actually, as the zero-subscripted quantities will occur so often, the following simplified notation will also be used:

$$\mu_{mn} = \mu_{mno} \quad (1.8a)$$

and

$$\lambda_{mn} = \lambda_{mno} \quad (1.8b)$$

Similarly, as all the media considered have the same magnetic permeability as free space, it is represented by μ instead of μ_o , here and in the future.

As will be concluded in Section 2.1, it is more convenient to use the pair (α_m, β_m) of arbitrary amplitudes of the modes, instead of (A^*, B^*) , where the new constants are defined by

$$\alpha_m = \frac{B^* J_m(q_{m1})}{i \sqrt{2\pi}} \quad (1.9a)$$

and

$$\beta_m = \frac{A^* J_m'(p_{m1}) a^2}{\sqrt{2\pi} p_{m1}} \quad (1.9b)$$

When $A^* = \beta_m = 0$, the only incident mode is the TE_{m1} , and when $B^* = \alpha_m = 0$, the only incident mode is the TM_{m1} .

As a last remark, the components of the surface current density, associated with the incident fields, are easily obtained from (1.1) through (1.6), namely

$$J_{\phi}^i(z) = H_z^i(\rho = a^-, z) \quad (1.10a)$$

and

$$J_z^i(z) = -H_{\phi}^i(\rho = a^-, z) \quad , \quad (1.10b)$$

where the ϕ -variation has been factored out, and where $\rho = a^-$ refers to the inside surface of the metallic shell, for $z < 0$.

CHAPTER II. FORMULATION OF THE PROBLEM

2.1 Formulation of the Coupled Wiener-Hopf Equations

The Wiener-Hopf equations will be formulated by starting with Maxwell's equations in differential form, and taking their Fourier transforms with respect to the coordinate z .

An m th order azimuthal variation of the components of the fields is assumed for the exciting modes, and by symmetry considerations it is concluded that all the fields have a variation in ϕ of that type. Namely, the fields are assumed to be

$$E_{\rho} = \sin(m\phi + \phi_0)(E_{\rho}^i + \mathcal{E}_{\rho}) \quad , \quad (2.1a)$$

$$E_{\phi} = \cos(m\phi + \phi_0)(E_{\phi}^i + \mathcal{E}_{\phi}) \quad , \quad (2.1b)$$

$$E_z = \sin(m\phi + \phi_0)(E_z^i + \mathcal{E}_z) \quad (2.1c)$$

and

$$H_{\rho} = \cos(m\phi + \phi_0)(H_{\rho}^i + \mathcal{H}_{\rho}) \quad , \quad (2.2a)$$

$$H_{\phi} = \sin(m\phi + \phi_0)(H_{\phi}^i + \mathcal{H}_{\phi}) \quad , \quad (2.2b)$$

$$H_z = \cos(m\phi + \phi_0)(H_z^i + \mathcal{H}_z) \quad . \quad (2.2c)$$

In these expressions, all the ϕ variation has been factored out. The incident field components, after factoring out the ϕ -varying parts, are $E_{\rho}^i(\rho, z)$, $E_{\phi}^i(\rho, z)$, etc.... The remaining

fields, $\mathcal{E}_\rho(\rho, z)$, $\mathcal{E}_\phi(\rho, z)$, etc..., will be called the scattered fields. It is assumed that the incident fields exist for all values of z and for $\rho < a$, being zero for $\rho > a$, and that the scattered fields are the difference between the total fields and the incident fields.

The components of the scattered fields can be represented as Fourier transform integrals, as follows:

$$\mathcal{E}_z(\rho, z) = -\frac{1}{\sqrt{2\pi}} \int_{-\infty}^{\infty} V_z(\eta, \rho) e^{i\eta z} d\eta, \quad (2.3)$$

$$\mathcal{E}_\phi = -\frac{1}{\sqrt{2\pi}} \int_{-\infty}^{\infty} \frac{V_\phi(\eta, \rho)}{\rho} e^{i\eta z} d\eta, \quad (2.4)$$

$$\mathcal{H}_z = \frac{1}{\sqrt{2\pi}} \int_{-\infty}^{\infty} I_z(\eta, \rho) e^{i\eta z} d\eta, \quad (2.5)$$

$$\mathcal{H}_\phi = \frac{1}{\sqrt{2\pi}} \int_{-\infty}^{\infty} \frac{I_\phi(\eta, \rho)}{\rho} e^{i\eta z} d\eta, \quad (2.6)$$

By using these integral representations, and Maxwell's differential equations, it is concluded that

$$\mathcal{E}_\rho = \frac{1}{\sqrt{2\pi}} \int_{-\infty}^{\infty} \left[\frac{m}{i\omega\epsilon} \frac{I_z(\eta, \rho)}{\rho} + \frac{\eta}{\omega\epsilon} \frac{I_\phi(\eta, \rho)}{\rho} \right] e^{i\eta z} d\eta, \quad (2.7)$$

$$\mathcal{H}_\rho = -\frac{1}{\sqrt{2\pi}} \int_{-\infty}^{\infty} \left[\frac{m}{i\omega\mu} \frac{V_z(\eta, \rho)}{\rho} - \frac{\eta}{\omega\mu} \frac{V_\phi(\eta, \rho)}{\rho} \right] e^{i\eta z} d\eta. \quad (2.8)$$

Maxwell's equations further yield the following relations among the several Fourier transformed functions, in each one of the two media:

$$\rho \frac{\partial V_Z(\eta, \rho)}{\partial \rho} = - \frac{v^2}{i\omega\epsilon} I_\phi(\eta, \rho) - \frac{\eta m}{\omega\epsilon} I_Z(\eta, \rho) \quad , \quad (2.9a)$$

$$\frac{\partial V_\phi(\eta, \rho)}{\partial \rho} = - \frac{\eta m}{\omega\epsilon} \frac{I_\phi(\eta, \rho)}{\rho} + \frac{\rho(k^2 - \frac{m^2}{\rho^2})}{i\omega\epsilon} I_Z(\eta, \rho) \quad , \quad (2.9b)$$

$$\frac{\partial I_\phi(\eta, \rho)}{\partial \rho} = - \frac{\eta m}{\omega\mu} \frac{V_\phi(\eta, \rho)}{\rho} - \frac{\rho(k^2 - \frac{m^2}{\rho^2})}{i\omega\mu} V_Z(\eta, \rho) \quad , \quad (2.9c)$$

$$\rho \frac{\partial I_Z(\eta, \rho)}{\partial \rho} = - \frac{\eta m}{\omega\mu} V_Z(\eta, \rho) + \frac{v^2}{i\omega\mu} V_\phi(\eta, \rho) \quad , \quad (2.9d)$$

where $k = \omega\sqrt{\mu\epsilon}$ and $v^2 = k^2 - \eta^2$.

After some simple manipulations, this set of equations becomes

$$\frac{\partial^2 I_Z(\eta, \rho)}{\partial \rho^2} + \frac{1}{\rho} \frac{\partial I_Z(\eta, \rho)}{\partial \rho} + (v^2 - \frac{m^2}{\rho^2}) I_Z(\eta, \rho) = 0 \quad , \quad (2.10a)$$

$$\frac{\partial^2 V_Z(\eta, \rho)}{\partial \rho^2} + \frac{1}{\rho} \frac{\partial V_Z(\eta, \rho)}{\partial \rho} + (v^2 - \frac{m^2}{\rho^2}) V_Z(\eta, \rho) = 0 \quad (2.10b)$$

and

$$V_\phi(\eta, \rho) = \frac{i m \eta}{v^2} V_Z(\eta, \rho) + \frac{i \omega \mu}{v^2} \rho \frac{\partial I_Z(\eta, \rho)}{\partial \rho} \quad , \quad (2.11a)$$

$$I_{\phi}(\eta, \rho) = -\frac{i\omega\epsilon}{v^2} \rho \frac{\partial V_Z(\eta, \rho)}{\partial \rho} - \frac{i\eta m}{v^2} I_Z(\eta, \rho) \quad (2.11b)$$

Equations (2.10a) and (2.10b) are of the Bessel type, and their solutions are

$$V_Z(\eta, \rho) = \frac{V_Z(\eta, a)}{J_m(v_1 a)} J_m(v_1 \rho) \quad \text{for } \rho < a \quad (2.12a)$$

$$= \frac{V_Z(\eta, a)}{H_m^{(1)}(v_0 a)} H_m^{(1)}(v_0 \rho) \quad \text{for } \rho > a \quad (2.12b)$$

and

$$I_Z(\eta, \rho) = \frac{I_Z(\eta, a^-)}{J_m(v_1 a)} J_m(v_1 \rho) \quad \text{for } \rho < a \quad (2.13a)$$

$$= \frac{I_Z(\eta, a^+)}{H_m^{(1)}(v_0 a)} H_m^{(1)}(v_0 \rho) \quad \text{for } \rho > a \quad (2.13b)$$

The subscript notation, v_0 and v_1 , refers to the values in the two different media, for which $\epsilon = \epsilon_0$ and $\epsilon = \epsilon_1$, respectively. In a similar fashion, the propagation constants will be denoted by k_0 and k_1 .

The expressions (2.12a) and (2.12b) already satisfy the continuity condition of $\mathcal{E}_Z(\rho, z)$ across the surface $\rho = a$. As for $\mathcal{H}_Z(\rho, z)$, no such condition exists, and hence the limit values $I_Z(\eta, a^-)$ and $I_Z(\eta, a^+)$ are different, in principle. $I_Z(\eta, a^-)$ and $I_Z(\eta, a^+)$ are the limit values of $I_Z(\eta, \rho)$ as $\rho \rightarrow a$ from values of ρ less than a or greater than a , respectively.

Care was also taken in the choice of the appropriate Bessel functions, so that the fields remain finite for $\rho = 0$, and the radiation condition is satisfied as $\rho \rightarrow \infty$. It must be noted here that the choice of the branch of $v_0 = (k_0^2 - \eta^2)^{1/2}$ is such that

$$\text{Im } v_0 \geq 0 \quad (2.14)$$

and that, within that branch (Fig. 2.1), the physical region is such that $\text{Re } v_0 \geq 0$, which means outward propagation, and includes the second and fourth quadrants of the η -plane, plus the areas between the axes and the branches of the hyperbola $\text{Re } \eta \times \text{Im } \eta = \text{Re } k_0 \times \text{Im } k_0$.

It is assumed that k_0 and k_1 have small positive imaginary parts, in order to ensure convergence of all the integrals. For the final results, however, these imaginary parts are forced to vanish, yielding the lossless case. In (2.12) and (2.13), as well as for the remaining components of the transformed fields, the apparent branch points at $\eta = \pm k_1$ are cancelled and do not actually occur.

From (2.11), (2.12) and (2.13), the expressions for $V_\phi(\eta, \rho)$ and $I_\phi(\eta, \rho)$ can be written as follows:

$$V_\phi(\eta, \rho) = \frac{i}{v_1^2 J_m(v_1 a)} \left[m_\eta V_Z(\eta, a) J_m(v_1 \rho) + \omega \mu v_1 I_Z(\eta, a) J'_m(v_1 \rho) \right] \text{ for } \rho < a \quad (2.15a)$$

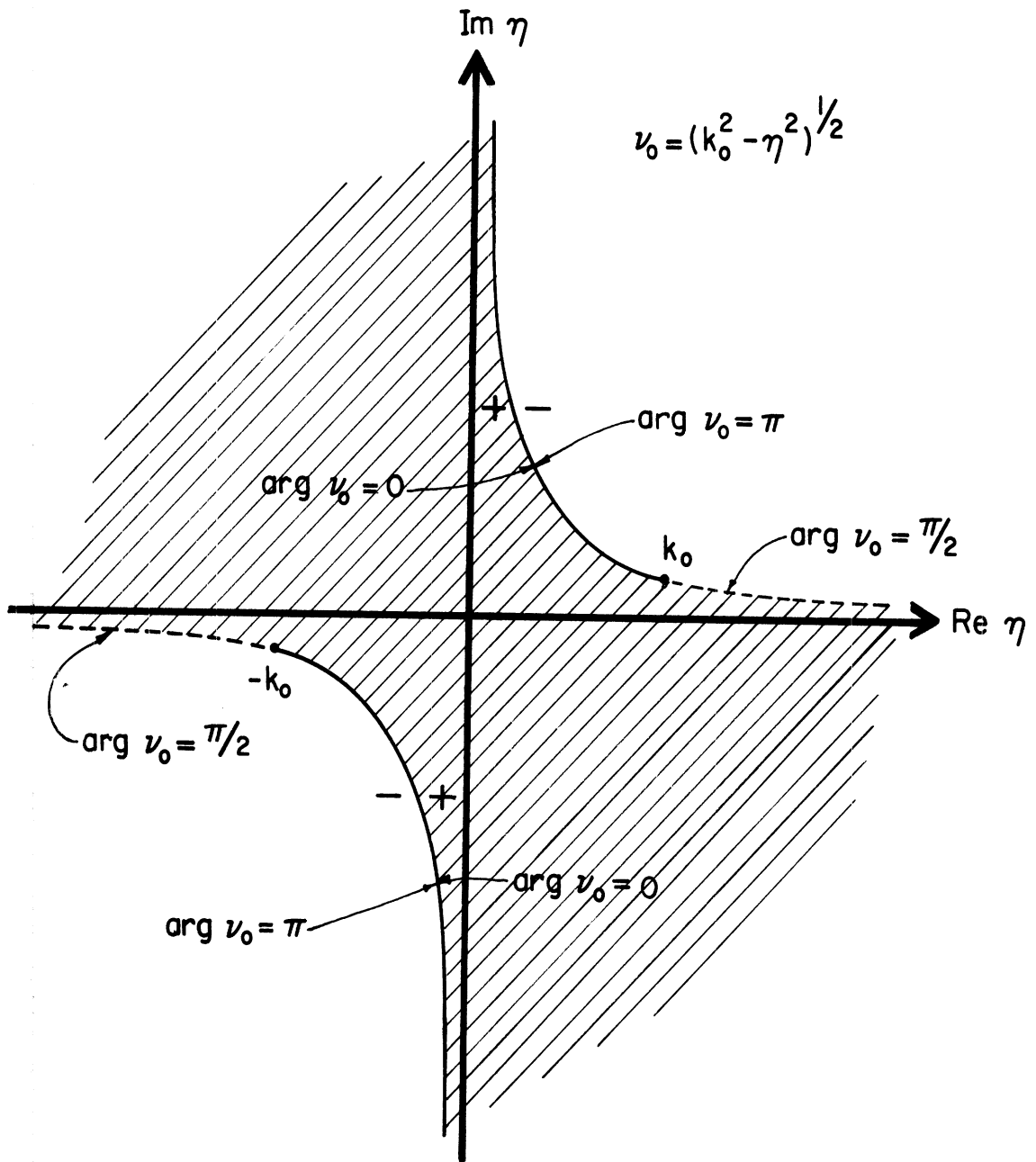


Fig. 2.1: Choice of branch and branch cuts, such that $\text{Im } \nu_0 \geq 0$.

The shaded area represents the physical region, for which $\text{Re } \nu_0 \geq 0$ as well.

$$V_{\phi}(\eta, \rho) = \frac{i}{v_0^2 H_m^{(1)}(v_0 a)} \left[m\eta V_z(\eta, a) H_m^{(1)}(v_0 \rho) + \omega \mu v_0 I_z(\eta, a+)_{\rho} H_m^{(1)'}(v_0 \rho) \right] \text{ for } \rho > a \quad (2.15b)$$

and

$$I_{\phi}(\eta, \rho) = - \frac{i}{v_1^2 J_m(v_1 a)} \left[\omega \epsilon_1 v_1 V_z(\eta, a)_{\rho} J_m'(v_1 \rho) + m\eta I_z(\eta, a-) J_m(v_1 \rho) \right] \text{ for } \rho < a \quad (2.16a)$$

$$= - \frac{i}{v_0^2 H_m^{(1)}(v_0 a)} \left[\omega \epsilon_0 v_0 V_z(\eta, a)_{\rho} H_m^{(1)'}(v_0 \rho) + m\eta I_z(\eta, a+) H_m^{(1)}(v_0 \rho) \right] \text{ for } \rho > a \quad (2.16b)$$

Here, and in the future, a prime affecting a Bessel function represents the derivative with respect to the argument.

Since $\mathcal{E}_{\phi}(\rho, z)$ must be continuous across the surface $\rho = a$, this condition is now applied to (2.15), resulting in

$$\begin{aligned} \frac{1}{v_0} \frac{H_m^{(1)'}(v_0 a)}{H_m^{(1)}(v_0 a)} I_z(\eta, a+) - \frac{1}{v_1} \frac{J_m'(v_1 a)}{J_m(v_1 a)} I_z(\eta, a-) \\ = \frac{m\eta}{\omega \mu a} \left(\frac{1}{v_1^2} - \frac{1}{v_0^2} \right) V_z(\eta, a) \quad (2.17) \end{aligned}$$

It is clear from the previous expressions that the fields everywhere can be expressed in terms of the three functions $V_z(\eta, a)$, $I_z(\eta, a^-)$ and $I_z(\eta, a^+)$. These are not, however, entirely suitable for the application of the Wiener-Hopf arguments. Instead, it is convenient to define

$$\mathcal{A}_\phi(\eta, a) = I_z(\eta, a^+) - I_z(\eta, a^-) , \quad (2.18a)$$

$$\mathcal{A}_z(\eta, a) = I_\phi(\eta, a^+) - I_\phi(\eta, a^-) , \quad (2.18b)$$

where $I_\phi(\eta, a^+)$ and $I_\phi(\eta, a^-)$ are defined in a manner similar to $I_z(\eta, a^+)$ and $I_z(\eta, a^-)$. \mathcal{A}_ϕ and \mathcal{A}_z will turn out to be related to the Fourier transforms of the ϕ and z components, respectively, of the surface currents on the metallic wall.

Inverting (2.3), it follows that, for $\rho = a$,

$$V_z(\eta, a) = -\frac{1}{\sqrt{2\pi}} \int_{-\infty}^{\infty} \mathcal{E}_z(a, z) e^{-i\eta z} dz . \quad (2.19)$$

Similarly, from (2.4),

$$V_\phi(\eta, a) = -\frac{a}{\sqrt{2\pi}} \int_{-\infty}^{\infty} \mathcal{E}_\phi(a, z) e^{-i\eta z} dz . \quad (2.20)$$

From (2.5), (2.6), (2.18a) and (2.18b), it follows that

$$\mathcal{A}_z(\eta, a) = \frac{a}{\sqrt{2\pi}} \int_{-\infty}^{\infty} \left[\mathcal{H}_{\phi}(a+, z) - \mathcal{H}_{\phi}(a-, z) \right] e^{-i\eta z} dz \quad , \quad (2.21)$$

$$\mathcal{A}_{\phi}(\eta, a) = \frac{1}{\sqrt{2\pi}} \int_{-\infty}^{\infty} \left[\mathcal{H}_z(a+, z) - \mathcal{H}_z(a-, z) \right] e^{-i\eta z} dz \quad . \quad (2.22)$$

It is now appropriate to use the boundary conditions at $\rho = a$. As both $\mathcal{E}_z(a, z)$ and $\mathcal{E}_{\phi}(a, z)$ are zero for $z < 0$, $V_z(\eta, a)$ and $V_{\phi}(\eta, a)$ are functions analytic in a lower half-plane of the complex variable η . Namely, \mathcal{E}_z and \mathcal{E}_{ϕ} will behave as $e^{-\delta'z}$, $\delta' > 0$, as $z \rightarrow +\infty$, where $\delta' \geq \delta = \min \{ \text{Im } k_0, \text{Im } k_1 \}$. The inverse transforms (2.3) and (2.4) can be carried out along a straight line in the η plane, parallel to the real axis, and such that $\text{Im } \eta < \delta$. Hence, $V_z(\eta, a)$ and $V_{\phi}(\eta, a)$ will be designated as $V_z^L(\eta)$ and $V_{\phi}^L(\eta)$, respectively, the index L standing for lower half-plane. Similarly, an index U will be used to denote the upper half-plane.

The integrations in (2.21) and (2.22) can be split into integrations from $-\infty$ to 0, and integrations from 0 to $+\infty$. The first integrations yield functions analytic in upper half-planes, the second integrations yield functions analytic in lower half-planes, thus (2.21) and (2.22) can be written as

$$\mathcal{A}_z(\eta, a) = \mathcal{A}_z^U(\eta) + \mathcal{A}_z^L(\eta) \quad , \quad (2.23a)$$

$$\mathcal{A}_{\phi}(\eta, a) = \mathcal{A}_{\phi}^U(\eta) + \mathcal{A}_{\phi}^L(\eta) \quad . \quad (2.23b)$$

For $z < 0$, $\mathcal{H}_\phi(a+,z) - \mathcal{H}_\phi(a-,z)$ is the z component of the surface current associated with the scattered field, $J_z(a,z)$, which is zero for $z > 0$, and whose Fourier transform is $\mathcal{A}_z^U(\eta)/a$. Similarly, $J_\phi(a,z)$ is $\mathcal{H}_z(a-,z) - \mathcal{H}_z(a+,z)$, for $z < 0$, and its Fourier transform is $-\mathcal{A}_\phi^U(\eta)$.

For $z > 0$, the discontinuity of the components of the field is due solely to the definitions (2.2), in which the incident part of the fields is identically zero for $\rho > a$, but not for $\rho < a$, $z > 0$. Hence, from (2.2), for $z > 0$, it follows that $\mathcal{H}_\phi(a+,z) - \mathcal{H}_\phi(a-,z) = H_\phi^i(a-,z)$ and $\mathcal{H}_z(a+,z) - \mathcal{H}_z(a-,z) = H_z^i(a-,z)$. Therefore, using (2.21), (2.22) and (2.23),

$$\mathcal{A}_z^L(\eta) = \frac{a}{\sqrt{2\pi}} \int_0^\infty H_\phi^i(a-,z) e^{-i\eta z} dz, \quad (2.24a)$$

$$\mathcal{A}_\phi^L(\eta) = \frac{1}{\sqrt{2\pi}} \int_0^\infty H_z^i(a-,z) e^{-i\eta z} dz. \quad (2.24b)$$

These functions can now be computed, because the incident fields are known, and given by (1.1) through (1.6).

The currents associated with the scattered field will decrease, as $z \rightarrow -\infty$, at least as fast as $e^{+\delta z}$, where

$$\delta = \min\{\text{Im}k_0, \text{Im}k_1\} \quad (2.25)$$

and hence $\mathcal{A}_Z^U(\eta)$ and $\mathcal{A}_\phi^U(\eta)$ are analytic for $\text{Im } \eta > -\delta$. Similarly, $\mathcal{A}_Z^L(\eta)$ and $\mathcal{A}_\phi^L(\eta)$ are analytic for $\text{Im } \eta < \delta$.

It is now possible to express $I_Z(\eta, a^-)$ and $I_Z(\eta, a^+)$ in terms of unknown functions which are analytic in an upper or a low half-plane, as required for the Wiener-Hopf method. $V_Z(\eta, a) = V_Z^L(\eta)$ is already in that form.

Using (2.17), (2.18a) and (2.23b), the following are obtained:

$$I_Z(\eta, a^+) = \frac{1}{M(\eta)} \left\{ v_0^2 v_1 J_m'(v_1 a) H_m^{(1)}(v_0 a) \left[\mathcal{A}_\phi^U(\eta) + \mathcal{A}_\phi^L(\eta) \right] + \frac{m\eta}{a} \omega(\epsilon_1 - \epsilon_0) J_m(v_1 a) H_m^{(1)}(v_0 a) V_Z^L(\eta) \right\}, \quad (2.26)$$

$$I_Z(\eta, a^-) = \frac{1}{M(\eta)} \left\{ v_0 v_1^2 J_m(v_1 a) H_m^{(1)'}(v_0 a) \left[\mathcal{A}_\phi^U(\eta) + \mathcal{A}_\phi^L(\eta) \right] + \frac{m\eta}{a} \omega(\epsilon_1 - \epsilon_0) J_m(v_1 a) H_m^{(1)}(v_0 a) V_Z^L(\eta) \right\}, \quad (2.27)$$

where $M(\eta)$ denotes the function

$$M(\eta) = v_0 v_1 \left[v_0 J_m'(v_1 a) H_m^{(1)}(v_0 a) - v_1 J_m(v_1 a) H_m^{(1)'}(v_0 a) \right] \quad (2.28)$$

and $\mathcal{A}_\phi^L(\eta)$ is a known function, given by (2.24b).

It is now apparent that the knowledge of $V_Z^L(\eta)$ and $\mathcal{A}_\phi^U(\eta)$ is sufficient to express the fields everywhere in space.

In order to obtain these two functions, however, it will be necessary to consider also the unknown functions $V_\phi^L(\eta)$ and $\mathcal{A}_Z^U(\eta)$.

Using (2.16) in (2.18b) and (2.23a), and using (2.26) and (2.27), it follows that

$$M(\eta)\mathcal{A}_Z^U(\eta) + N(\eta)\mathcal{A}_\phi^U(\eta) = Q(\eta)V_Z^L(\eta) + W(\eta) \quad (2.29)$$

where

$$N(\eta) = i\eta m \left[v_1 J_m'(v_1 a) H_m^{(1)}(v_0 a) - v_0 J_m(v_1 a) H_m^{(1)'}(v_0 a) \right], \quad (2.30)$$

$$Q(\eta) = -i\omega a (\epsilon_0 + \epsilon_1) v_0 v_1 J_m'(v_1 a) H_m^{(1)'}(v_0 a) + i\omega a \epsilon_1 v_0^2 \cdot \frac{[J_m'(v_1 a)]^2 H_m^{(1)}(v_0 a)}{J_m(v_1 a)} + i\omega a \epsilon_0 v_1^2 \frac{J_m(v_1 a) [H_m^{(1)'}(v_0 a)]^2}{H_m^{(1)}(v_0 a)} - \frac{i\eta^2 m^2}{\omega \mu a} \left(\frac{v_1}{v_0} - \frac{v_0}{v_1} \right)^2 J_m(v_1 a) H_m^{(1)}(v_0 a) \quad (2.31)$$

and

$$W(\eta) = -M(\eta) \cdot \mathcal{A}_Z^L(\eta) - N(\eta) \mathcal{A}_\phi^L(\eta) \quad (2.32)$$

It is now necessary to construct a second equation to complement (2.29). For that purpose, use is made of (2.15a), and the fact that $V_\phi(\eta, a) = V_\phi^L(\eta)$. Using (2.27), it is concluded that

$$P(\eta) \mathcal{A}_\phi^U(\eta) = M(\eta) V_\phi^L(\eta) - N(\eta) V_Z^L(\eta) + U(\eta) \quad (2.33)$$

where

$$P(\eta) = i\omega\mu a v_0 v_1 J_m'(v_1 a) H_m^{(1)'}(v_0 a) \quad (2.34)$$

and

$$U(\eta) = -P(\eta) \cdot \mathcal{A}_\phi^L(\eta) \quad (2.35)$$

Two coupled Wiener-Hopf equations have been derived, (2.29) and (2.33), and they can be written in matrix form as

$$\begin{bmatrix} 0 & P(\eta) \\ M(\eta) & N(\eta) \end{bmatrix} \begin{bmatrix} \mathcal{A}_Z^U(\eta) \\ \mathcal{A}_\phi^U(\eta) \end{bmatrix} = \begin{bmatrix} M(\eta) & -N(\eta) \\ 0 & Q(\eta) \end{bmatrix} \begin{bmatrix} V_\phi^L(\eta) \\ V_Z^L(\eta) \end{bmatrix} + \begin{bmatrix} U(\eta) \\ W(\eta) \end{bmatrix} \quad (2.36)$$

The functions in the square matrices have branch points for $\eta = \pm k_0$, but are analytic in the strip

$$-\delta < \text{Im } \eta < \delta \quad (2.37)$$

with δ given by (2.25). The same holds for $U(\eta)$ and $W(\eta)$, as will be seen in the following. The apparent branch points at $\eta = \pm k_1$ do not occur if m is even, and, if m is odd, are cancelled by multiplying (2.36) by v_1 , which does not change the solutions of the problem.

With the incident fields given by (1.1) through (1.6), (2.24) may be used to compute $\mathcal{A}_z^L(\eta)$ and $\mathcal{A}_\phi^L(\eta)$.

Integration yields

$$\mathcal{A}_\phi^L(\eta) = \frac{\alpha_m}{\eta - \lambda_{m11}}, \quad (2.38)$$

$$\mathcal{A}_z^L(\eta) = \frac{k_1^2}{\omega\mu} \frac{\beta_m}{\eta - \mu_{m11}} - \frac{im\lambda_{m11}a^2}{q_{m1}^2} \frac{\alpha_m}{\eta - \lambda_{m11}}, \quad (2.39)$$

where

$$\alpha_m = \frac{B^*J_m(q_{m1})}{i\sqrt{2\pi}}, \quad (2.40a)$$

$$\beta_m = \frac{A^*J'_m(p_{m1})a^2}{\sqrt{2\pi} p_{m1}}, \quad (2.40b)$$

and where p_{mn} is the n th zero of $J'_m(x)$ and q_{mn} is the n th zero of $J_m(x)$. A^* , B^* , λ_{mn1} and μ_{mn1} were defined in Chapter I, equations (1.1) through (1.7).

$U(\eta)$ and $W(\eta)$ are now calculated using (2.35) and (2.32).

2.2 Factorization of the Matrix

The Wiener-Hopf problem (2.36) must now be solved for the two unknown column matrices. Equation (2.36) is a valid relation within the strip of analyticity (2.37), and the unknown functions are analytic in one of the half-planes $\text{Im } \eta < \delta$ or $\text{Im } \eta > -\delta$, so that this is a valid coupled Wiener-Hopf problem.

The square matrix on the right-hand side of (2.36) is inverted, and (2.36) is multiplied, from the left-hand side, by the inverse matrix. The resultant equation is

$$\begin{bmatrix} \frac{N(n)}{Q(n)} & \frac{[N(n)]^2 + P(n)Q(n)}{M(n)Q(n)} \\ \frac{M(n)}{Q(n)} & \frac{N(n)}{Q(n)} \end{bmatrix} \begin{bmatrix} U_z(n) \\ U_\phi(n) \end{bmatrix} = \begin{bmatrix} V_\phi^L(n) \\ V_z^L(n) \end{bmatrix} + \begin{bmatrix} \frac{U(n)}{M(n)} + \frac{N(n)W(n)}{M(n)Q(n)} \\ \frac{W(n)}{Q(n)} \end{bmatrix} \quad (2.41)$$

The procedure to follow would be, now, to factorize the square matrix into the product of a square matrix analytic in a lower half-plane by a square matrix analytic in an upper half-plane. Equation (2.41) would then be multiplied, from the left-hand side, by the inverse of the lower half-plane square matrix, which is required to be analytic in the lower half-plane. The second column matrix on the right-hand side, which would then be obtained, would be split into the sum of a lower and an upper half-plane column matrix, and the equation would then be suitable for the application of Liouville's theorem.

The factorization of the square matrix, however, is not possible, by any known method, in the general case. Several authors have treated this factorization for matrices of special forms, but the matrix in (2.41) is not in any of those forms. The

Wiener-Hopf-Hilbert method was described by Hurd [23], and it would be applicable to (2.41) if the only singularities of the square matrix were pairs of branch points at $\eta = \pm\zeta_n$, ζ_n being arbitrary complex numbers, and if the singularities of the last column matrix of (2.41) were all in the lower half-plane. It is clear that neither of these conditions is satisfied.

In a different paper, Daniele [24] describes a factorization procedure for a square matrix of the form

$$\begin{bmatrix} 1 & A(\eta) \\ B(\eta) & 1 \end{bmatrix}, \quad (2.42)$$

but only provided that the ratio $A(\eta)/B(\eta)$ can be expressed as the ratio of two entire functions of η . This means that $A(\eta)/B(\eta)$ cannot have any branch points, only poles and zeros.

The square matrix of (2.41) can be put in the form (2.42), as follows:

The function $N(\eta)/Q(\eta)$, being analytic in the strip (2.37), can be factorized as

$$\frac{N(\eta)}{Q(\eta)} = \frac{N^U(\eta)}{Q^U(\eta)} \frac{N^L(\eta)}{Q^L(\eta)}, \quad (2.43)$$

where the split functions are analytic and nonzero in the respective half-planes.

Then, it follows that

$$\begin{bmatrix} \frac{N(n)}{Q(n)} & \frac{[N(n)]^2 + P(n)Q(n)}{M(n)Q(n)} \\ \frac{M(n)}{Q(n)} & \frac{N(n)}{Q(n)} \end{bmatrix} = \begin{bmatrix} \frac{N^L(n)}{Q^L(n)} & 0 \\ 0 & \frac{N^L(n)}{Q^L(n)} \end{bmatrix}$$

$$\cdot \begin{bmatrix} 1 & \frac{[N(n)]^2 + P(n)Q(n)}{M(n)N(n)} \\ \frac{M(n)}{N(n)} & 1 \end{bmatrix} \cdot \begin{bmatrix} \frac{N^U(n)}{Q^U(n)} & 0 \\ 0 & \frac{N^U(n)}{Q^U(n)} \end{bmatrix}, \quad (2.44)$$

and (2.41) can be rewritten as

$$\begin{bmatrix} 1 & \frac{[N(n)]^2 + P(n)Q(n)}{M(n)N(n)} \\ \frac{M(n)}{N(n)} & 1 \end{bmatrix} \begin{bmatrix} \mathcal{A}_z^{U^*}(n) \\ \mathcal{A}_\phi^{U^*}(n) \end{bmatrix} = \begin{bmatrix} V_\phi^{L^*}(n) \\ V_z^{L^*}(n) \end{bmatrix} + \begin{bmatrix} \frac{U(n)Q^L(n)}{M(n)N^L(n)} + \frac{W(n)N^U(n)}{M(n)Q^U(n)} \\ \frac{W(n)}{Q^U(n)N^L(n)} \end{bmatrix} \quad (2.45)$$

In (2.45), $\mathcal{A}_z^{U^*}(n) = N^U(n) \cdot \mathcal{A}_z^U(n)/Q^U(n)$ and $\mathcal{A}_\phi^{U^*}(n) = N^U(n) \cdot \mathcal{A}_\phi^U(n)/Q^U(n)$, which are the new unknown functions for the application of the Wiener-Hopf method, and are still analytic in an upper half-plane. Similarly, $V_\phi^{L^*}(n) = Q^L(n)V_\phi^L(n)/N^L(n)$ and

$V_Z^{L*}(\eta) = Q^L(\eta)V_Z^L(\eta)/N^L(\eta)$ are still analytic in a lower half-plane, as required.

In proceeding with the application of Daniele's method the function

$$\frac{[N(\eta)]^2 + P(\eta)Q(\eta)}{[M(\eta)]^2} \quad (2.46)$$

must be expressed as the ratio of two entire functions. However, (2.46) has branch points at $\eta = \pm k_0$, so it cannot be expressed as such a ratio.

After the failure of both Hurd's and Daniele's methods in this case, the alternative would be to find a factorization by some other method, which the author was not able to accomplish.

It is also possible that, by defining new pairs of unknown functions, as linear combinations of $\mathcal{A}_Z^U(\eta)$ and $\mathcal{A}_\phi^U(\eta)$ and of $V_\phi^L(\eta)$ and $V_Z^L(\eta)$, the ensuing square matrices would be more easily amenable to factorization by known methods. Care would have to be taken so that the linear combinations of $\mathcal{A}_Z^U(\eta)$ and $\mathcal{A}_\phi^U(\eta)$ would still be analytic in an upper half-plane, and the linear combinations of $V_\phi^L(\eta)$ and $V_Z^L(\eta)$ would still be analytic in a lower half-plane.

Unfortunately, the author was also unsuccessful in this task, except for the simpler case $\epsilon_1 = \epsilon_0$, as treated in Section 2.3, and the exact problem will, therefore, not be solved in this work. It will remain as a possible area of future research.

2.3 Simplification for the Case $\epsilon_1 = \epsilon_0$

Problem (2.36) is considerably simplified if the dielectric rod is omitted, i.e., if $\epsilon_1 = \epsilon_0$. This simpler problem has been treated before, by Weinstein [16], using a dual integral equation approach, and by Pearson [20], who considered an incident plane wave as the excitation, instead of a mode incident on the aperture from inside the guide.

The simplification of (2.36) is due to the simplification of the elements of the matrices. Using the subscript zero to denote the fact that $\epsilon_1 = \epsilon_0$, these functions become

$$P_0(\eta) = i\omega\mu a v_0^2 J_m'(v_0 a) H_m^{(1)'}(v_0 a) , \quad (2.47a)$$

$$M_0(\eta) = -\frac{2i}{\pi a} v_0^2 , \quad (2.47b)$$

$$N_0(\eta) = \frac{2m}{\pi a} \eta , \quad (2.47c)$$

$$Q_0(\eta) = -\frac{4ik_0^2}{\pi^2\omega\mu a J_m(v_0 a) H_m^{(1)'}(v_0 a)} , \quad (2.47d)$$

$$U_0(\eta) = -\frac{\alpha_m}{\eta - \lambda_{m10}} i\omega\mu a v_0^2 J_m'(v_0 a) H_m^{(1)'}(v_0 a) , \quad (2.47e)$$

$$W_0(\eta) = \frac{2}{\pi a} \left[\frac{ik_0^2 \beta_m}{\omega\mu} \frac{v_0^2}{\eta - \mu_{m10}} - \frac{m\alpha_m a^2}{q_{m1}^2} (\lambda_{m10} \eta + k_0^2) \right] . \quad (2.47f)$$

In (2.47e) and (2.47f), $\lambda_{m10} = [k_0^2 - (q_{m1}/a)^2]^{1/2}$ and $\mu_{m10} = [k_0^2 - (p_{m1}/a)^2]^{1/2}$.

The uncoupling of (2.36) is due to the following factorization of the square matrices:

$$\begin{bmatrix} 0 & P_0(\eta) \\ M_0(\eta) & N_0(\eta) \end{bmatrix} = \begin{bmatrix} i\omega\mu a v_0^2 x(\eta) & 0 \\ 0 & \frac{2i}{\pi a} \end{bmatrix} \begin{bmatrix} 0 & 1 \\ -v_0^2 & -i\eta m \end{bmatrix}, \quad (2.48)$$

and

$$\begin{bmatrix} M_0(\eta) & -N_0(\eta) \\ 0 & Q_0(\eta) \end{bmatrix} = \begin{bmatrix} \frac{2i}{\pi a} & 0 \\ 0 & -\frac{4ik_0^2}{\pi^2\omega\mu a y(\eta)} \end{bmatrix} \begin{bmatrix} -v_0^2 & i\eta m \\ 0 & 1 \end{bmatrix}, \quad (2.49)$$

where

$$x(\eta) = J_m'(v_0 a) H_m^{(1)'}(v_0 a), \quad (2.50)$$

$$y(\eta) = J_m(v_0 a) H_m^{(1)}(v_0 a). \quad (2.51)$$

Equation (2.36), thus modified, can now be written as

$$\begin{bmatrix} i\omega\mu a v_0^2 x(\eta) & 0 \\ 0 & \frac{2i}{\pi a} \end{bmatrix} \begin{bmatrix} \mathcal{A}_{10}^U(\eta) \\ \mathcal{A}_{20}^U(\eta) \end{bmatrix} = \begin{bmatrix} \frac{2i}{\pi a} & 0 \\ 0 & -\frac{4ik_0^2}{\pi^2\omega\mu a y(\eta)} \end{bmatrix} \begin{bmatrix} V_{10}^L(\eta) \\ V_{20}^L(\eta) \end{bmatrix} + \begin{bmatrix} U_0(\eta) \\ W_0(\eta) \end{bmatrix} \quad (2.52)$$

where the new unknown functions are defined by

$$\mathcal{U}_{10}^U(\eta) = \mathcal{U}_{\phi_0}^U(\eta) , \quad (2.53a)$$

$$\mathcal{U}_{20}^U(\eta) = -v_0^2 \mathcal{U}_{z_0}^U(\eta) - i\eta m \mathcal{U}_{\phi_0}^U(\eta) , \quad (2.53b)$$

$$V_{10}^L(\eta) = -v_0^2 V_{\phi_0}^L(\eta) + i\eta m V_{z_0}^L(\eta) , \quad (2.53c)$$

$$V_{20}^L(\eta) = V_{z_0}^L(\eta) . \quad (2.53d)$$

The second subscript, zero, of all the functions above, refers to the fact that $\epsilon_1 = \epsilon_0$.

Clearly, (2.52) is an uncoupled system of two Wiener-Hopf equations, so that it actually represents two parallel and independent problems. Explicitly, it may be written in the form

$$i\omega\mu a v_0^2 x(\eta) \mathcal{U}_{10}^U(\eta) = \frac{2i}{\pi a} V_{10}^L(\eta) + U_0(\eta) , \quad (2.54a)$$

$$\frac{2i}{\pi a} \mathcal{U}_{20}^U(\eta) = -\frac{4ik_0^2}{\pi^2\omega\mu a y(\eta)} V_{20}^L(\eta) + W_0(\eta) . \quad (2.54b)$$

From equations (2.53a) and (2.53b), it is clear that the newly defined unknown functions are analytic in an upper half-plane, provided that is true for $\mathcal{U}_{\phi_0}^U(\eta)$ and $\mathcal{U}_{z_0}^U(\eta)$. Similarly for (2.53c) and (2.53d), concerning analyticity in a lower half-plane.

By inverting (2.53), it follows that

$$\mathcal{L}_{z_0}^U(\eta) = -\frac{1}{v_0^2} \left[i\eta m \mathcal{L}_{10}^U(\eta) + \mathcal{L}_{20}^U(\eta) \right], \quad (2.55a)$$

and

$$V_{\phi_0}^L(\eta) = -\frac{1}{v_0^2} \left[V_{10}^L(\eta) - i\eta m V_{20}^L(\eta) \right]. \quad (2.55b)$$

Due to the factor $1/v_0^2$, equations (2.55a) and (2.55b) would seem to indicate that $\mathcal{L}_{z_0}^U(\eta)$ has a pole at $\eta = +k_0$, and $V_{\phi_0}^L(\eta)$ has a pole at $\eta = -k_0$, though that is not consistent with their assigned regions of analyticity. However, (2.53b) and (2.53c) imply that

$$\mathcal{L}_{20}^U(k_0) = -ik_0 m \mathcal{L}_{10}^U(k_0) \quad (2.56a)$$

and

$$V_{10}^L(-k_0) = -ik_0 m V_{20}^L(-k_0), \quad (2.56b)$$

showing that the aforementioned poles of (2.55) do not actually occur.

A few words are appropriate concerning the physical meaning of the unknown functions defined by (2.53), and hence of the factorizations (2.48) and (2.49).

From (2.9a) and (2.18), it follows that

$$-v_0^2 \mathcal{L}_{z_0}^U(\eta) - i\eta m \mathcal{L}_{\phi_0}^L(\eta) = i\omega \epsilon_0 a \left[\frac{\partial V_Z(\eta, \rho)}{\partial \rho} \Big|_{\rho=a+} - \frac{\partial V_Z(\eta, \rho)}{\partial \rho} \Big|_{\rho=a-} \right]. \quad (2.57)$$

Using the inverse of (2.3), (2.57) can be written as

$$-v_0^2 \mathcal{A}_{z_0}(\eta) - i\eta m \mathcal{A}_{\phi_0}(\eta) = -\frac{i\omega\epsilon_0 a}{\sqrt{2\pi}} \int_{-\infty}^{\infty} \left[\frac{\partial \mathcal{E}_z(\rho, z)}{\partial \rho} \Big|_{\rho=a+} - \frac{\partial \mathcal{E}_z(\rho, z)}{\partial \rho} \Big|_{\rho=a-} \right] e^{-i\eta z} dz, \quad (2.58)$$

and, using (2.23) and (2.53b),

$$\mathcal{A}_{z_0}^U(\eta) = -\frac{i\omega\epsilon_0 a}{\sqrt{2\pi}} \int_{-\infty}^0 \left[\frac{\partial \mathcal{E}_z(\rho, z)}{\partial \rho} \Big|_{\rho=a+} - \frac{\partial \mathcal{E}_z(\rho, z)}{\partial \rho} \Big|_{\rho=a-} \right] e^{-i\eta z} dz. \quad (2.59)$$

Then, $\mathcal{A}_{z_0}^U(\eta)$ is seen to represent the Fourier transform of the discontinuity, for $z < 0$, of $\partial \mathcal{E}_z(\rho, z)/\partial \rho$ across $\rho = a$.

In a similar fashion, using (2.9d), (2.5), (2.53c) and the fact that $V_{\phi_0}(\eta, a) = V_{\phi_0}^L(\eta)$ and $V_{z_0}(\eta, a) = V_{z_0}^L(\eta)$, it follows that

$$V_{z_0}^L(\eta) = -\frac{i\omega\mu a}{\sqrt{2\pi}} \int_0^{\infty} \frac{\partial \mathcal{H}_z(\rho, z)}{\partial \rho} \Big|_{\rho=a} e^{-i\eta z} dz. \quad (2.60)$$

From (2.60), $V_{z_0}^L(\eta)$ is seen to represent the Fourier transform of $\partial \mathcal{H}_z(\rho, z)/\partial \rho|_{\rho=a}$, which is a function that vanishes identically for $z < 0$, due to the imposed boundary conditions at the air to perfect conductor interface.

It must be noted that, due to their now-clear physical meaning, $\mathcal{U}_{20}^U(\eta)$ and $V_{10}^L(\eta)$ could have been chosen from the very beginning, instead of $\mathcal{U}_{z_0}^U(\eta)$ and $V_{\phi_0}^L(\eta)$.

The complementary integral of (2.59), i.e., from zero to $+\infty$, can be computed from the knowledge of the incident fields, and is easily seen to yield

$$\mathcal{U}_{20}^L(\eta) = -\frac{\pi a}{2i} W_0(\eta) \quad , \quad (2.61)$$

whereas the complementary integral of (2.60) vanishes. Hence, equations (2.54) could have been obtained directly, with no need to introduce $\mathcal{U}_{z_0}^U(\eta)$ and $V_{\phi_0}^L(\eta)$.

For the case $\epsilon_1 \neq \epsilon_0$, however, such a reasoning fails. In fact, across the boundary between the two dielectrics, $\rho = a$, $z > 0$, $\partial E_z / \partial \rho$ is not continuous, nor is $\partial E_z / \partial \rho$ multiplied by some function of ϵ . Hence, the complementary integral of the equivalent of (2.59) would not be a known function, and a relation corresponding to (2.61) could not be written, rather $\mathcal{U}_2^L(\eta)$ would be unknown.

Examining the problem from a more mathematical viewpoint, the factorizations (2.48) and (2.49) cannot be carried through, for the case $\epsilon_1 \neq \epsilon_0$, in such a manner that the right-hand split-matrix of (2.48) is analytic in an upper half-plane, and the right-hand split-matrix of (2.49) is analytic in a lower half-plane. Or, if such factorizations are possible, the author was not able to find them. Hence, the uncoupling of (2.36) was not achieved in this work.

2.4 Simplification for the Symmetrical Case ($m = 0$)

Another simpler version of (2.36) should be mentioned, namely the case of an excitation with no ϕ -variation, which means $m = 0$. In (2.1) and (2.2), the TE fields will have a factor $\cos \phi_0$, and the TM fields will have a factor $\sin \phi_0$. As ϕ_0 is totally arbitrary, it is seen that the TE and the TM case are independent of each other: $\phi_0 = 0$ yields a purely TE problem, $\phi_0 = \pi/2$ yields a purely TM problem, and any linear combination of these two cases is possible.

This uncoupling of the problem into two independent problems can be seen in (2.36) as well. In fact, (2.30) shows that $N(\eta) = 0$, whence (2.36) becomes a system of two uncoupled equations, namely

$$M(\eta) \mathcal{A}_Z^U(\eta) = Q(\eta) V_Z^L(\eta) + W(\eta) \quad (2.62)$$

and

$$P(\eta) \mathcal{A}_\phi^U(\eta) = M(\eta) V_\phi^L(\eta) + U(\eta) \quad , \quad (2.63)$$

with $m = 0$ in each of the functions $M(\eta)$, $Q(\eta)$, $P(\eta)$, $W(\eta)$ and $U(\eta)$. Equation (2.62) represents the TM problem, and $W(\eta)$ will only depend on $\beta_m = \beta_0$, not on $\alpha_m = \alpha_0$, once m is made to be zero. Equation (2.63) represents the TE problem, and $U(\eta)$ only depends on α_0 , not on β_0 .

CHAPTER III. TAYLOR SERIES SOLUTION FOR $\epsilon_1 - \epsilon_0 \ll \epsilon_0$

3.1 Wiener-Hopf Equations for the Zeroth- and First-Order Terms of the Series

As it was not possible to solve (2.36) exactly, an approximate solution will be sought, for the case of a relative permittivity of the dielectric which is only slightly different from one. Every function in the matrices of (2.36) is to be expanded in a Taylor series in the relative permittivity $\epsilon_r = \epsilon_1/\epsilon_0$, around the point $\epsilon_r = 1$. The notation is as follows, for a general function $F(n, k_1)$, with $\Delta k = k_1 - k_0 \ll k_0$,

$$F(n, k_1) = F_0(n, k_0) + F_1(n, k_0) \Delta k + F_2(n, k_0) (\Delta k)^2 + \dots \quad (3.1)$$

where

$$F_0(n, k_0) = F(n, k_1) \Big|_{k_1=k_0} \quad , \quad (3.2)$$

$$F_1(n, k_0) = \frac{\partial F(n, k_1)}{\partial k_1} \Big|_{k_1=k_0} \quad , \quad (3.3)$$

$$F_2(n, k_0) = \frac{1}{2} \frac{\partial^2 F(n, k_1)}{\partial k_1^2} \Big|_{k_1=k_0} \quad , \quad (3.4)$$

and so on. It is noted that the differentiations are carried out relative to k_1 , but considering ϵ_1 to be the only variable, i.e., though $k_1 = \omega\sqrt{\epsilon_1\mu}$, both ω and μ are kept constant.

Equation (2.36) can be written, in abbreviated form,

$$[A] \cdot [\mathcal{V}] = [B] [V] + [Z] \quad , \quad (3.5)$$

and each one of the matrices in (3.5) will be expanded in a series as (3.1). It follows that

$$\begin{aligned} ([A_0] + [A_1]\Delta k + \dots) \cdot ([\mathcal{V}_0] + [\mathcal{V}_1]\Delta k + \dots) &= ([B_0] + [B_1]\Delta k + \dots) \\ &\cdot ([V_0] + [V_1]\Delta k + \dots) + ([Z_0] + [Z_1]\Delta k + \dots) \quad . \quad (3.6) \end{aligned}$$

By carrying out the multiplications in (3.6), and equating the matrices multiplying equal powers of Δk on the left-hand and the right-hand sides of the equation, it is found that

$$[A_0] \cdot [\mathcal{V}_0] = [B_0][V_0] + [Z_0] \quad , \quad (3.7)$$

$$[A_0] \cdot [\mathcal{V}_1] = [B_0][V_1] + [B_1][V_0] - [A_1][\mathcal{V}_0] + [Z_1] \quad , \quad (3.8)$$

and so on.

Equation (3.7) is just the simplified version of (3.5) when $\epsilon_1 = \epsilon_0$. It can be solved exactly by the Wiener-Hopf method, and

its initial formulation was treated in Section 2.3, where the problem was shown to uncouple into two independent equations.

After (3.7) has been solved, $[\varphi_0]$ and $[V_0]$ will be known, and then the column matrix

$$[Z_1^*] = [B_1][V_0] - [A_1][\varphi_0] + [Z_1] \quad (3.9)$$

is completely known. Hence, (3.8) is seen to be almost identical to (3.7), except that the known column matrix $[Z_0]$ has been replaced by $[Z_1^*]$. The unknown matrices are now denoted by $[\varphi_1]$ and $[V_1]$, and (3.8) is solved in exactly the same manner as (3.7). The important fact is that the square matrices $[A_0]$ and $[B_0]$ are the same in both (3.7) and (3.8), so that (3.8) will uncouple in the same way as (3.7) did in Section 2.3.

The zeroth order terms of the expansions of the type (3.1) of the functions in the matrices of (2.36) are given by expressions (2.47). As for the first order terms, (3.3) must be used, yielding, after some manipulations,

$$P_1(n) = i\omega\mu \frac{k_0}{v_0} (m^2 - v_0^2 a^2) J_m(v_0 a) H_m^{(1)'}(v_0 a) , \quad (3.10a)$$

$$M_1(n) = k_0 v_0 \left[v_0 a \left(\frac{m^2}{v_0^2 a^2} - 1 \right) J_m(v_0 a) H_m^{(1)'}(v_0 a) - 2 J_m(v_0 a) H_m^{(1)'}(v_0 a) - v_0 a J_m'(v_0 a) H_m^{(1)'}(v_0 a) \right] , \quad (3.10b)$$

$$N_1(\eta) = i\eta m k_0 a \left[\left(\frac{m^2}{v_0^2 a^2} - 1 \right) J_m(v_0 a) H_m^{(1)}(v_0 a) - J_m'(v_0 a) H_m^{(1)'}(v_0 a) \right], \quad (3.10c)$$

$$Q_1(\eta) = -\frac{4k_0}{\pi v_0 \omega \mu} \left[\frac{k_0^2}{i\pi} \frac{J_m'(v_0 a)}{[J_m(v_0 a)]^2 H_m^{(1)}(v_0 a)} - (m^2 - v_0^2 a^2) \frac{k_0^2}{v_0 a} \right. \\ \left. + a k_0^2 v_0 \frac{J_m'(v_0 a) H_m^{(1)'}(v_0 a)}{J_m(v_0 a) H_m^{(1)}(v_0 a)} + (\eta^2 + k_0^2) \frac{H_m^{(1)'}(v_0 a)}{H_m^{(1)}(v_0 a)} \right. \\ \left. - \frac{2i\eta^2}{\pi v_0 a} \frac{1}{J_m(v_0 a) H_m^{(1)}(v_0 a)} \right], \quad (3.10d)$$

$$U_1(\eta) = -\frac{i\omega \mu a k_0 \alpha_m}{\eta - \lambda_{m10}} \left[v_0 a \left(\frac{m^2}{v_0^2 a^2} - 1 \right) J_m(v_0 a) H_m^{(1)'}(v_0 a) \right. \\ \left. + \frac{v_0^2}{\lambda_{m10}(\eta - \lambda_{m10})} J_m'(v_0 a) H_m^{(1)'}(v_0 a) \right], \quad (3.10e)$$

and

$$W_1(\eta) = \frac{2i\beta_m v_0^2 k_0^3}{\pi a \omega \mu} \frac{1}{\mu_{m10}(\eta - \mu_{m10})^2} - \frac{2m\alpha_m k_0 \eta a}{\pi q_{m1}^2} \frac{\eta + \lambda_{m10}}{\lambda_{m10}(\eta - \lambda_{m10})} \\ + \frac{4ik_0 \beta_m}{\pi a \omega \mu} \frac{v_0^2}{\eta - \mu_{m10}} + \left[\frac{2\beta_m k_0^3 v_0}{\omega \mu (\eta - \mu_{m10})} - \frac{2im\alpha_m k_0 v_0 \lambda_{m10} a^2}{q_{m1}^2 (\eta - \lambda_{m10})} \right] J_m(v_0 a) H_m^{(1)'}(v_0 a) \\ + \left[\frac{\beta_m v_0^2 k_0^3 a}{\omega \mu (\eta - \mu_{m10})} + \frac{im\alpha_m k_0 a^3}{q_{m1}^2} (\lambda_{m10} \eta + k_0^2) \right] \left[J_m'(v_0 a) H_m^{(1)'}(v_0 a) \right. \\ \left. - \left(\frac{m^2}{v_0^2 a^2} - 1 \right) J_m(v_0 a) H_m^{(1)}(v_0 a) \right]. \quad (3.10f)$$

As seen from (3.8) and (3.9), expressions (3.10) are important for the computation of

$$[Z_1^*] = \begin{bmatrix} U_1^*(\eta) \\ W_1^*(\eta) \end{bmatrix}, \quad (3.11)$$

but this computation can only be completed after knowing the functions $[V_0]$ and $[V_1]$, which will come from the solution of (3.7). This solution will be the subject of the next section.

Some attention will now be given to the convergence of the Taylor series expansions. From (2.28), (2.30), (2.31), (2.32), (2.34), (2.35), (2.38) and (2.39), it is easily seen that, as functions of k_1 , all these functions have branch points at $k_1 = \pm\eta$, if m is odd, but have no branch points there if m is even. These singularities are removable, however, for (3.5) may be multiplied by v_1 when m is odd, cancelling the branch points at $k_1 = \pm\eta$ in all the functions considered. It is easily shown that, when (3.5) is multiplied by v_1 , and expansions like (3.6) are carried out in the resulting equation, (3.7) and (3.8) are still valid, and the branch points have then been cancelled.

Other singularities occur, though. $Q(\eta)$ has simple poles at $k_1 = \pm\sqrt{\eta^2 + (p_{mn}/a)^2}$, for $n = 1, 2, 3, \dots$. For a TE_{m_1} exciting mode, $\alpha_m \neq 0$, $U(\eta)$ and $W(\eta)$ have branch points for $k_1 = \pm(q_{m_1}/a)$, and poles for $k_1 = \pm\sqrt{\eta^2 + (q_{m_1}/a)^2}$. For a TM_{m_1} exciting mode, $\beta_m \neq 0$, $W(\eta)$ has branch points for $k_1 = \pm(p_{m_1}/a)$, and poles for $k_1 = \pm\sqrt{\eta^2 + (p_{m_1}/a)^2}$.

In the k_1 plane, all the above-mentioned singularities are in the strip $|\text{Im } k_1| < |\text{Im } \eta|$. On the other hand, η is in the strip $|\text{Im } \eta| < \text{Im } k_0$, so that it is guaranteed that there will always exist a circle of finite radius, centered at k_0 , in the plane of k_1 , such that no singularities fall inside it. Within that circle, the series expansions performed in this section are valid. It should be recalled that the imaginary part of k_0 is being kept small but positive throughout all of the application of the Wiener-Hopf method.

3.2 Solution of the Wiener-Hopf Equations for the Zeroth-Order Terms

In this section, a solution for (3.7) will be sought. The initial steps in this solution have been carried out in Section 2.3, and the Wiener-Hopf equations which were obtained are (2.54a) and (2.54b).

The crucial step in solving (2.54) is to factorize the functions $x(\eta)$ and $y(\eta)$, which are analytic and non-vanishing in the strip

$$-\text{Im } k_0 < \text{Im } \eta < \text{Im } k_0, \quad (3.12)$$

into the product of the two functions, one analytic and non-vanishing in the upper half-plane $\text{Im } \eta > -\text{Im } k_0$, and the other analytic and non-vanishing in the lower half-plane $\text{Im } \eta < \text{Im } k_0$. These factorizations,

$$x(\eta) = x^U(\eta) \cdot x^L(\eta) \quad (3.13a)$$

and

$$y(\eta) = y^U(\eta) \cdot y^L(\eta) , \quad (3.13b)$$

were carried out by Weinstein, [16], Sections 22 and 26, and an account is given in Appendix A of this thesis.

Given (3.13), (2.54) can be written as

$$x^U(\eta) \psi_{10}^U(\eta) = \frac{2}{\pi a^2 \omega \mu} \frac{V_{10}^L(\eta)}{v_0^2 x^L(\eta)} + \frac{1}{i \omega \mu a} \frac{U_0(\eta)}{v_0^2 x^L(\eta)} \quad (3.14a)$$

$$\frac{y^U(\eta) \psi_{20}^U(\eta)}{\eta + k_0} = - \frac{2 \omega \epsilon_0}{\pi} \frac{V_{20}^L(\eta)}{(\eta + k_0) y^L(\eta)} - \frac{i \pi a}{2} \frac{y^U(\eta) W_0(\eta)}{\eta + k_0} . \quad (3.14b)$$

Equation (3.14a) will be solved first. Each one of the terms on the right-hand side is analytic in the strip (3.12), so they must be split into a sum of upper and lower half-plane functions. It follows that

$$\begin{aligned} \frac{V_{10}^L(\eta)}{v_0^2 x^L(\eta)} &= \frac{V_{10}^L(\eta)}{2k_0(k_0 - \eta)x^L(\eta)} + \frac{1}{2k_0(k_0 + \eta)} \left[\frac{V_{10}^L(\eta)}{x^L(\eta)} - \frac{V_{10}^L(-k_0)}{x^L(-k_0)} \right] \\ &\quad + \frac{V_{10}^L(-k_0)}{2k_0 x^L(-k_0)(k_0 + \eta)} , \quad (3.15) \end{aligned}$$

where the first two terms on the right-hand side are analytic in the lower half-plane, and the last term is analytic in the upper half-plane.

Similarly, denoting

$$R_0(\eta) = \frac{1}{i\omega\mu a} \frac{U_0(\eta)}{v_0^2 x^L(\eta)}, \quad (3.16)$$

and using (2.47e), the following split is found

$$R_0(\eta) = R_0^U(\eta) + R_0^L(\eta), \quad (3.17)$$

with

$$R_0^U(\eta) = -\alpha_m \frac{x^U(\eta) - x^U(\lambda_{m10})}{\eta - \lambda_{m10}}, \quad (3.18a)$$

$$R_0^L(\eta) = -\alpha_m \frac{x^U(\lambda_{m10})}{\eta - \lambda_{m10}}. \quad (3.18b)$$

Now, (3.14a) can be written as

$$\begin{aligned} & x^U(\eta) \left[U_{10}^U(\eta) - \frac{V_{10}^L(-k_0)}{\pi a^2 \omega \mu k_0 x^L(-k_0)} \frac{1}{\eta + k_0} - R_0^U(\eta) \right] \\ &= -\frac{1}{\pi a^2 \omega \mu k_0} \frac{V_{10}^L(\eta)}{x^L(\eta)(\eta - k_0)} + \frac{1}{\pi a^2 \omega \mu k_0} \left[\frac{V_{10}^L(\eta)}{x^L(\eta)} - \frac{V_{10}^L(-k_0)}{x^L(-k_0)} \right] \frac{1}{\eta + k_0} + R_0^L(\eta). \end{aligned} \quad (3.19)$$

All the left-hand side of (3.19) is analytic in the upper half-plane $\text{Im } \eta > -\text{Im } k_0$, and all the right-hand side is analytic in the lower half-plane $\text{Im } \eta < \text{Im } k_0$. Since the two sides are equal over the strip (3.12), and are analytic there, they actually represent analytic continuations of each other over the whole finite complex η -plane, i.e., they are representations, in their respective half-planes, of the same entire function $e(\eta)$.

It is now necessary to analyze the behavior of the several terms of (3.19) as $\eta \rightarrow \infty$. It is known (Meixner, [27]) that, as $z \rightarrow 0$, i.e., at the metal edge, the following order behavior is physically required.

$$J_z(z) = o(z^0) \quad , \quad (3.20a)$$

$$J_\phi(z) = o(z^{-1}) \quad , \quad (3.20b)$$

$$\mathcal{E}_z(a,z) = o(z^{-1}) \quad , \quad (3.20c)$$

$$\mathcal{E}_\phi(a,z) = o(z^0) \quad . \quad (3.20d)$$

These expressions are also valid for the zeroth order functions $J_{z0}(z)$, $J_{\phi0}(z)$, $\mathcal{E}_{z0}(a,z)$ and $\mathcal{E}_{\phi0}(a,z)$, though they do not represent the strictest behavior which can be imposed, i.e., $J_{z0}(z) = o(z^{1/2})$, $J_{\phi0}(z) = o(z^{-1/2})$, $\mathcal{E}_{z0}(a,z) = o(z^{-1/2})$, $\mathcal{E}_{\phi0}(a,z) = o(z^{1/2})$. For the present purpose, however, imposing (3.20) is sufficient, and that is the behavior which will be considered.

This behavior at the origin translates into the following behavior, as $\eta \rightarrow \infty$ in the respective half-planes of analyticity, of the one-sided Fourier transforms (see, for example, Mitra and Lee, [11]):

$$\mathcal{Q}_{z_0}^U(\eta) = o(\eta^{-1}) \quad , \quad (3.21a)$$

$$\mathcal{Q}_{\phi_0}^U(\eta) = o(\eta^0) \quad , \quad (3.21b)$$

$$V_{z_0}^L(\eta) = o(\eta^0) \quad , \quad (3.21c)$$

and

$$V_{\phi_0}^L(\eta) = o(\eta^{-1}) \quad . \quad (3.21d)$$

Using (3.21) in (2.53), it follows that, as $\eta \rightarrow \infty$,

$$\mathcal{Q}_{1_0}^U(\eta) = o(\eta^0) \quad , \quad (3.22a)$$

$$\mathcal{Q}_{2_0}^U(\eta) = o(\eta^1) \quad , \quad (3.22b)$$

$$V_{1_0}^L(\eta) = o(\eta^1) \quad , \quad (3.22c)$$

and

$$V_{2_0}^L(\eta) = o(\eta^0) \quad (3.22d)$$

Also, from Appendix A, it is known that all of the functions $x^U(\eta)$, $x^L(\eta)$, $y^U(\eta)$, $y^L(\eta)$ have behavior $O(\eta^{-1/2})$ as $\eta \rightarrow \infty$ in the respective half-planes of analyticity. Hence, $R_0^U(\eta) = O(\eta^{-3/2})$ and $R_0^L(\eta) = O(\eta^{-1})$.

It is now clear that the left-hand side of (3.19) has behavior $o(\eta^{-1/2})$ as $\eta \rightarrow \infty$. As for the right-hand side, it may be rewritten as

$$\frac{2}{\pi a^2 \omega \mu} \frac{v_{10}^L(\eta)}{v_0^2 x^L(\eta)} - \frac{v_{10}^L(-k_0)}{\pi a^2 \omega \mu k_0 x^L(-k_0)} \frac{1}{\eta + k_0} + R_0^L(\eta) \quad , \quad (3.23)$$

whence it is clear that its behavior as $\eta \rightarrow \infty$ is $o(\eta^{-1/2})$.

Then, the sides of equation (3.19) represent an entire function $e(\eta)$, and their behavior at infinity is $o(\eta^{-1/2})$, i.e., $e(\eta)$ is an entire function which vanishes at infinity. By using Liouville's theorem, it follows that

$$e(\eta) = 0 \quad (3.24)$$

over the entire complex η plane. By equating to zero both sides of (3.19), it follows that

$$\psi_{10}^U(\eta) = \frac{v_{10}^L(-k_0)}{\pi a^2 \omega \mu k_0 x^L(-k_0)} \frac{1}{(\eta + k_0) x^U(\eta)} + \frac{R_0^U(\eta)}{x^U(\eta)} \quad (3.25a)$$

and

$$v_{10}^L(\eta) = - \frac{v_{10}^L(-k_0)}{2k_0 x^L(-k_0)} (\eta - k_0) x^L(\eta) - \frac{\pi a^2 \omega \mu}{2} v_0^2 x^L(\eta) R_0^L(\eta) \quad , \quad (3.25b)$$

which constitute the solution to (3.14a).

Equation (3.14b) will now be solved in a similar fashion. The terms on the right-hand side must be additively split into lower and upper half-plane functions, as follows:

$$\frac{V_{20}^L(\eta)}{(\eta + k_0)y^L(\eta)} = \left[\frac{V_{20}^L(\eta)}{y^L(\eta)} - \frac{V_{20}^L(-k_0)}{y^L(-k_0)} \right] \frac{1}{\eta + k_0} + \frac{V_{20}^L(-k_0)}{y^L(-k_0)} \frac{1}{\eta + k_0} , \quad (3.26)$$

where the first term on the right-hand side is analytic in the lower half-plane, and the second term is analytic in the upper half-plane. Defining

$$S_0(\eta) = \frac{i\pi a}{2} \frac{y^U(\eta)W_0(\eta)}{\eta + k_0} , \quad (3.27)$$

and using (2.47f), it follows that

$$S_0(\eta) = S_0^U(\eta) + S_0^L(\eta) , \quad (3.28)$$

with

$$S_0^U(\eta) = - \frac{ima^2\alpha_m}{q_{m1}^2} \frac{\lambda_{m10}\eta + k_0^2}{\eta + k_0} y^U(\eta) + \frac{k_0^2\beta_m}{\omega\mu} \cdot \left[(\eta - k_0)y^U(\eta) - (\mu_{m10} - k_0)y^U(\mu_{m10}) \right] \frac{1}{\eta - \mu_{m10}} \quad (3.29a)$$

and

$$S_0^L(\eta) = \frac{k_0^2\beta_m(\mu_{m10} - k_0)y^U(\mu_{m10})}{\omega\mu} \frac{1}{\eta - \mu_{m10}} . \quad (3.29b)$$

Now, (3.14b) can be written as

$$\begin{aligned} \frac{y^U(\eta) Q_{20}^U(\eta)}{\eta + k_0} + \frac{2\omega\epsilon_0 V_{20}^L(-k_0)}{\pi y^L(-k_0)} \frac{1}{\eta + k_0} + S_0^U(\eta) \\ = -\frac{2\omega\epsilon_0}{\pi} \left[\frac{V_{20}^L(\eta)}{y^L(\eta)} - \frac{V_{20}^L(-k_0)}{y^L(-k_0)} \right] \frac{1}{\eta + k_0} - S_0^L(\eta) . \end{aligned} \quad (3.30)$$

The left-hand side of (3.30) is analytic in the upper half-plane $\text{Im } \eta > -\text{Im } k_0$, and the right-hand side is analytic in the lower half-plane $\text{Im } \eta < \text{Im } k_0$. By analytic continuation, each side is equal to an entire function $f(\eta)$ in its respective half-plane of analyticity.

From (3.29), it follows that, as $\eta \rightarrow \infty$, $S_0^U(\eta) = O(\eta^{-1/2})$ in the upper half-plane, and $S_0^L(\eta) = O(\eta^{-1})$ in the lower half-plane. Using also (3.22), it is concluded that the left-hand side of (3.30) has behavior $O(\eta^{-1/2})$, and the right-hand side has behavior $o(\eta^{-1/2})$, i.e., both sides vanish at infinity in their respective half-planes of analyticity.

Hence, application of Liouville's theorem yields $f(\eta) = 0$, and each side of (3.30) may be equated to zero identically, whence it follows that

$$Q_{20}^U(\eta) = -\frac{2\omega\epsilon_0 V_{20}^L(-k_0)}{\pi y^L(-k_0)} \frac{1}{y^U(\eta)} - \frac{(\eta + k_0) S_0^U(\eta)}{y^U(\eta)} \quad (3.31a)$$

and

$$V_{20}^L(\eta) = \frac{V_{20}^L(-k_0)}{y^L(-k_0)} y^L(\eta) - \frac{\pi}{2\omega\epsilon_0} (\eta + k_0) y^L(\eta) S_0^L(\eta) \quad . \quad (3.31b)$$

This is the solution to (3.14b), completing the zeroth-order solution of the problem.

A final detail will be to express $V_{10}^L(-k_0)$ and $V_{20}^L(-k_0)$ in terms of more suitable quantities. Using equations (2.56) in (3.25a) and (3.31a), it follows that

$$V_{20}^L(-k_0) = \frac{\frac{ik_0 m \alpha_m x^U(\lambda_{m10})}{(k_0 - \lambda_{m10}) x^U(k_0)} - \frac{2k_0^3 \beta_m y^U(\mu_{m10})}{\omega \mu y^U(k_0)}}{\frac{2\omega\epsilon_0}{\pi [y^U(k_0)]^2} - \frac{m^2}{2\pi a^2 \omega \mu [x^U(k_0)]^2}}, \quad (3.32)$$

and $V_{10}^L(-k_0)$ is now obtained by using (2.56b).

Equations (2.53a) and (2.53d) will yield $\mathcal{A}_{\phi_0}^U(\eta)$ and $V_{z_0}^L(\eta)$ immediately. As to $\mathcal{A}_{z_0}^U(\eta)$ and $V_{\phi_0}^L(\eta)$, equations (2.55) are used, together with (3.25) and (3.31), resulting in

$$\begin{aligned}
 \mathcal{U}_{z_0}^U(\eta) &= - \frac{m^2 v_{20}^L(-k_0)}{\pi a^2 \omega \mu x^U(k_0)} \frac{\eta}{v_0^2(\eta + k_0) x^U(\eta)} - im \alpha_m x^U(\lambda_{m10}) \\
 &\cdot \frac{\eta}{v_0^2(\eta - \lambda_{m10}) x^U(\eta)} + \frac{2\omega \epsilon_0 v_{20}^L(-k_0)}{\pi y^U(k_0)} \\
 &\cdot \frac{1}{v_0^2 y^U(\eta)} + \frac{im \alpha_m a^2}{q_{m1}^2} \frac{\lambda_{m10}}{\eta - \lambda_{m10}} - \omega \epsilon_0 \beta_m \frac{1}{\eta - \mu_{m10}} \\
 &\quad + \omega \epsilon_0 \beta_m (\mu_{m10} - k_0) y^U(\mu_{m10}) \frac{1}{(\eta - \mu_{m10})(\eta - k_0) y^U(\eta)} \quad (3.33a)
 \end{aligned}$$

and

$$\begin{aligned}
 V_{\phi_0}^L(\eta) &= \frac{im v_{20}^L(-k_0)}{2x^U(k_0)} \frac{x^L(\eta)}{\eta + k_0} - \frac{\pi}{2} \alpha_m \omega \mu a^2 x^U(\lambda_{m10}) \frac{x^L(\eta)}{\eta - \lambda_{m10}} \\
 &+ \frac{im v_{20}^L(-k_0)}{y^U(k_0)} \frac{\eta y^L(\eta)}{v_0^2} + \frac{\pi}{2} \beta_m im (\mu_{m10} - k_0) y^U(\mu_{m10}) \frac{\eta y^L(\eta)}{(\eta - \mu_{m10})(\eta - k_0)} \cdot \\
 &\hspace{20em} (3.33b)
 \end{aligned}$$

It must be recalled that, due to (2.56), the apparent poles at $\eta = k_0$, for $\mathcal{U}_{z_0}^U(\eta)$, and $\eta = -k_0$, for $V_{\phi_0}^L(\eta)$, are actually points of analyticity, as may be verified by taking the limits as $\eta \rightarrow k_0$ in (3.33a) and $\eta \rightarrow -k_0$ in (3.33b).

3.3 Solution of the Wiener-Hopf Equations for the First-Order Terms

This section will deal with the solution of (3.8), in a manner similar to the solution of (3.7), treated in the previous section. The difference between the two problems is that $[Z_0]$ is replaced by $[Z_1^*]$, i.e., $U_0(\eta)$ is replaced by $U_1^*(\eta)$ and $W_0(\eta)$ by $W_1^*(\eta)$. The \mathcal{U} and V functions will also be different, and that fact will be indicated by replacing the second subscript, zero, by one.

With those modifications, equations (3.14) are valid, and so are (3.19) and (3.30). $R_0(\eta)$ and $S_0(\eta)$ are replaced by $R_1(\eta)$ and $S_1(\eta)$, defined as

$$R_1(\eta) = \frac{1}{i\omega\mu a} \frac{U_1^*(\eta)}{v_0^2 x^L(\eta)}, \quad (3.34a)$$

and

$$S_1(\eta) = \frac{i\pi a}{2} \frac{y^U(\eta)W_1^*(\eta)}{\eta + k_0}. \quad (3.34b)$$

The following splits must be performed,

$$R_1(\eta) = R_1^U(\eta) + R_1^L(\eta), \quad (3.35a)$$

$$S_1(\eta) = S_1^U(\eta) + S_1^L(\eta). \quad (3.35b)$$

Since it can be shown (Appendix B) that the split functions in the right-hand sides of (3.35) have a similar behavior, as $\eta \rightarrow \infty$, as their zeroth order counterparts, and since (3.20) also imposes the behavior (3.21) on the corresponding first order unknown functions, the solution of (3.8) will be analogous to (3.25) and (3.31), namely

$$\mathcal{A}_{11}^U(\eta) = \frac{V_{11}^L(-k_0)}{\pi a^2 \omega \mu k_0 x^L(-k_0)} \frac{1}{(\eta + k_0) x^U(\eta)} + \frac{R_1^U(\eta)}{x^U(\eta)} , \quad (3.36a)$$

$$\mathcal{A}_{21}^U(\eta) = - \frac{2\omega \epsilon_0 V_{21}^L(-k_0)}{\pi y^L(-k_0)} \frac{1}{y^U(\eta)} - \frac{(\eta + k_0) S_1^U(\eta)}{y^U(\eta)} , \quad (3.36b)$$

$$V_{11}^L(\eta) = - \frac{V_{11}^L(-k_0)}{2k_0 x^L(-k_0)} (\eta - k_0) x^L(\eta) - \frac{\pi a^2 \omega \mu}{2} v_0^2 x^L(\eta) R_1^L(\eta) , \quad (3.36c)$$

$$V_{21}^L(\eta) = \frac{V_{21}^L(-k_0)}{y^L(-k_0)} y^L(\eta) - \frac{\pi}{2\omega \epsilon_0} (\eta + k_0) y^L(\eta) S_1^L(\eta) . \quad (3.36d)$$

Equations corresponding to (2.53) and (2.56) are still valid for the first order functions. This leads to

$$V_{21}^L(-k_0) = \frac{ik_0 m \frac{R_1^U(k_0)}{x^U(k_0)} - 2k_0 \frac{S_1^U(k_0)}{y^U(k_0)}}{\frac{2\omega\epsilon_0}{\pi[y^U(k_0)]^2} - \frac{m^2}{2\pi\omega\mu a^2[x^U(k_0)]^2}} \quad (3.37a)$$

and

$$V_{11}^L(-k_0) = -ik_0 m V_{21}^L(-k_0) . \quad (3.37b)$$

From (3.9), after some manipulations, it follows that

$$U_I^*(n) = -\frac{M_1(n)}{v_0^2} V_{10}^L(n) - \frac{2nmP_1(n)}{\omega\mu(m^2 - v_0^2 a^2)} V_{20}^L(n) - P_1(n) \mathcal{U}_{10}^U(n) + U_1(n) \quad (3.38a)$$

and

$$W_1^*(n) = Q_1(n) V_{20}^L(n) - \frac{2nmP_1(n)}{\omega\mu(m^2 - v_0^2 a^2)} \mathcal{U}_{10}^U(n) + \frac{M_1(n)}{v_0^2} \mathcal{U}_{20}^U(n) + W_1(n) , \quad (3.38b)$$

where the first order functions are given in (3.10), and the solution functions of the previous section are used.

Use of (3.38) and (3.34) leads to

$$\begin{aligned}
 R_1(\eta) &= \left(\frac{A}{\eta + k_0} + \frac{B}{\eta - \lambda_{m10}} \right) f_1(\eta) + C \frac{x^U(\eta)}{(\eta - \lambda_{m10})^2} \\
 &+ \left(\frac{D}{\eta + k_0} + \frac{F}{\eta - \mu_{m10}} \right) \frac{\eta y^L(\eta)}{(\eta - k_0) v_0 x^L(\eta)} J_m(v_0 a) H_m^{(1)'}(v_0 a) \quad (3.39a)
 \end{aligned}$$

and

$$\begin{aligned}
 S_1(\eta) &= -\frac{k_0^2 a^2}{\pi m} \left(\frac{D}{\eta + k_0} + \frac{F}{\eta - \mu_{m10}} \right) f_2(\eta) \\
 &+ \frac{2m}{ia} \left(\frac{A}{\eta + k_0} + \frac{B}{\eta - \lambda_{m10}} \right) \frac{\eta y^U(\eta)}{(\eta + k_0) v_0 x^U(\eta)} J_m(v_0 a) H_m^{(1)'}(v_0 a) \\
 &+ \left[G \frac{\eta(\eta + \lambda_{m10})}{(\eta - \lambda_{m10})(\eta + k_0)} + L \frac{\eta - k_0}{\eta - \mu_{m10}} + T \frac{\eta - k_0}{(\eta - \mu_{m10})^2} \right] y^U(\eta) \quad , \quad (3.39b)
 \end{aligned}$$

for η in the strip of analyticity, (3.12), and with the definitions:

$$\begin{aligned}
 f_1(\eta) &= \frac{m^2 - v_0^2 a^2}{v_0^2 a^2} \left[\frac{2i}{\pi a v_0} \frac{J_m(v_0 a)}{J_m'(v_0 a)} + J_m(v_0 a) H_m^{(1)'}(v_0 a) \right] \\
 &- \frac{2}{a v_0} J_m(v_0 a) H_m^{(1)'}(v_0 a) - J_m'(v_0 a) H_m^{(1)'}(v_0 a) \quad , \quad (3.40a)
 \end{aligned}$$

$$f_2'(\eta) = \frac{2\eta^2}{k_0^2 a v_0^2} + \frac{1}{v_0} \frac{J_m'(v_0 a)}{J_m(v_0 a)} + \frac{\pi a}{2i} \frac{m^2 - v_0^2 a^2}{v_0^2 a^2} J_m(v_0 a) H_m^{(1)}(v_0 a) \\ + \frac{i\pi}{k_0^2} \frac{\eta^2}{v_0} J_m(v_0 a) H_m^{(1)'}(v_0 a) + \frac{i\pi a}{2} J_m'(v_0 a) H_m^{(1)'}(v_0 a) , \quad (3.40b)$$

and

$$A = \frac{k_0 m V_{20}^L(-k_0)}{2\omega \mu x^L(-k_0)} , \quad (3.41a)$$

$$B = \frac{i\pi \alpha_m k_0 a^2 x^U(\lambda_{m10})}{2} , \quad (3.41b)$$

$$C = -\frac{k_0}{\lambda_{m10}} \alpha_m , \quad (3.41c)$$

$$D = \frac{2mk_0 V_{20}^L(-k_0)}{\omega \mu y^L(-k_0)} , \quad (3.41d)$$

$$F = \frac{\pi m \beta_m k_0}{\omega \mu a} (k_0 - \mu_{m10}) y^U(\mu_{m10}) , \quad (3.41e)$$

$$G = -\frac{imk_0 \alpha_m a^2}{\lambda_{m10} q_{m1}^2} , \quad (3.41f)$$

$$L = \frac{2k_o \beta_m}{\omega \mu} , \quad (3.41g)$$

and

$$T = \frac{\omega \epsilon_o k_o \beta_m}{\mu_{m1o}} . \quad (3.41h)$$

Expressions (3.39) must now be split according to (3.35), and that task is carried out in Appendix B. By using (B.34) and (B.35) in (3.36a) and (3.36b), together with the first order versions of (2.53a) and (2.55a), the following expressions result:

$$\begin{aligned} \psi_{\phi 1}^U(\eta) &= \frac{K_o}{(\eta + k_o)x^U(\eta)} + \sum_{n=1}^{\infty} \frac{K_n}{(\eta + \lambda_{mn})x^U(\eta)} \\ &+ C \frac{x^U(\eta) - x^U(\lambda_{m1o}) - (\eta - \lambda_{m1o})x^{U'}(\lambda_{m1o})}{(\eta - \lambda_{m1o})^2 x^U(\eta)} \\ &+ \frac{2x^U(k_o)}{\pi a} A \frac{u_1(\eta)}{x^U(\eta)} + \frac{iB}{\pi} \frac{u_2(\eta)}{x^U(\eta)} - \frac{iF}{\pi} \frac{u_3(\eta)}{x^U(\eta)} \end{aligned} \quad (3.42a)$$

and

$$\begin{aligned}
 \mathcal{L} U_{z_1}^U(\eta) &= \frac{K_0}{v_0^2} \left[\frac{2ik_0^2 a^2 x^U(k_0)}{m y^U(k_0)} \frac{1}{y^U(\eta)} - im \frac{\eta}{(\eta + k_0) x^U(\eta)} \right] \\
 &- \pi m \sum_{n=1}^{\infty} K_n \left[\lambda_{mn} h_{mn} \frac{1}{(\eta - k_0) y^U(\eta)} + \frac{i}{\pi} \frac{\eta}{v_0^2 x^U(\eta)} \right] \frac{1}{\eta + \lambda_{mn}} \\
 &+ \sum_{n=1}^{\infty} \frac{K'_n}{(\eta - k_0)(\eta + \mu_{mn}) y^U(\eta)} + \frac{q_{m_1}^2}{a^2} \\
 &\cdot G \left[- \frac{2\lambda_{m_1 0}^2 a^2 y^U(\lambda_{m_1 0})}{q_{m_1}^2 (k_0 + \lambda_{m_1 0})} \frac{\eta + k_0}{y^U(\eta)} + x^{U'}(\lambda_{m_1 0}) \frac{\eta}{x^U(\eta)} \right. \\
 &+ \left. x^U(\lambda_{m_1 0}) \frac{\eta}{(\eta - \lambda_{m_1 0}) x^U(\eta)} - \frac{a^2 \eta v_0^2}{q_{m_1}^2 (\eta - \lambda_{m_1 0})} \right] \frac{1}{v_0^2 (\eta - \lambda_{m_1 0})} \\
 &+ \frac{\mu_{m_1 0}}{k_0} T \left\{ - \frac{2}{k_0} + \frac{2(\mu_{m_1 0} - k_0) y^U(\mu_{m_1 0})}{k_0} \frac{1}{(\eta - k_0) y^U(\eta)} \right. \\
 &- \frac{k_0}{\mu_{m_1 0}} \frac{1}{\eta - \mu_{m_1 0}} + \frac{k_0 (\mu_{m_1 0} - k_0) y^U(\mu_{m_1 0})}{\mu_{m_1 0}} \frac{1}{(\eta - \mu_{m_1 0})(\eta - k_0) y^U(\eta)} \\
 &+ \left. \frac{k_0}{\mu_{m_1 0}} \left[y^U(\mu_{m_1 0}) + (\mu_{m_1 0} - k_0) y^{U'}(\mu_{m_1 0}) \right] \frac{1}{(\eta - k_0) y^U(\eta)} \right\} \frac{1}{\eta - \mu_{m_1 0}} \\
 &- \frac{2im x^U(k_0)}{\pi a} A \frac{\eta u_1(\eta)}{v_0^2 x^U(\eta)} + \frac{m}{\pi} B \frac{\eta u_2(\eta)}{v_0^2 x^U(\eta)} - \frac{m}{\pi} F \frac{\eta u_3(\eta)}{v_0^2 x^U(\eta)} \\
 &+ \frac{k_0 a y^U(k_0)}{2m\pi} D \frac{u_4(\eta)}{(\eta - k_0) y^U(\eta)} + \frac{2m}{\pi a} B \frac{u_5(\eta)}{(\eta - k_0) y^U(\eta)} \\
 &+ \frac{k_0^2 a^3}{2\pi m} F \frac{u_6(\eta)}{(\eta - k_0) y^U(\eta)} \quad . \quad (3.42b)
 \end{aligned}$$

In these expressions, $\mu_{mn} = \sqrt{k_0^2 - (p_{mn}/a)^2}$, $\lambda_{mn} = \sqrt{k_0^2 - (q_{mn}/a)^2}$, and the functions $u_1(\eta)$, $u_2(\eta)$, $u_3(\eta)$, $u_4(\eta)$, $u_5(\eta)$ and $u_6(\eta)$ are defined by equations (B.17) and (B.18). The constants h_{mn} , K_n and K'_n are given by (B.26) and (B.28), and K_0 is

$$K_0 = K^* - \frac{\text{im}V_{21}^L(-k_0)}{\pi\omega\mu a^2 x^U(k_0)}, \quad (3.43)$$

where K^* is defined by (B.22), and $V_{21}^L(-k_0)$ by (3.37a).

The functions $u_n(\eta)$ are analytic everywhere except for branch points at $\eta = -k_0$. The branch cuts were taken to be the straight line from $-k_0$ to $-k_0 i^\infty$, but they can be deformed as mentioned on pages 124 through 125. At infinity, $u_n(\eta) = O(\eta^{-1})$, away from the branch cut.

CHAPTER IV. REFLECTION COEFFICIENTS INSIDE THE METALLIC GUIDE

4.1 Inverse Fourier Transformation of $\mathcal{A}_{\phi 0}^U(\eta)$ and $\mathcal{A}_{z 0}^U(\eta)$

The ϕ and z components of the surface currents, associated with the scattered fields, will be represented by $J_{\phi}(z)$ and $J_z(z)$, respectively. They will be the inverse Fourier transforms of $-\mathcal{A}_{\phi}^U(\eta)$ and $\mathcal{A}_z^U(\eta)/a$, i.e.,

$$J_{\phi}(z) = -\frac{1}{\sqrt{2\pi}} \int_{-\infty}^{\infty} \mathcal{A}_{\phi}^U(\eta) e^{iz\eta} d\eta \quad (4.1a)$$

and

$$J_z(z) = \frac{1}{a\sqrt{2\pi}} \int_{-\infty}^{\infty} \mathcal{A}_z^U(\eta) e^{iz\eta} d\eta. \quad (4.1b)$$

When $J_{\phi}(z)$ and $J_z(z)$ are represented as series of type (3.1), the zeroth order terms are obtained from (4.1) by using $\mathcal{A}_{\phi 0}^U(\eta)$ and $\mathcal{A}_{z 0}^U(\eta)$ in the integrands, the first order terms are obtained by using $\mathcal{A}_{\phi 1}^U(\eta)$ and $\mathcal{A}_{z 1}^U(\eta)$ in the integrands, and so on.

$\mathcal{A}_{\phi 0}^U(\eta)$ is given by (3.25a), (3.18a) and (2.53a). It is seen that, as $\eta \rightarrow \infty$ (away from the negative side of the lower half-plane hyperbolic branch cuts of Fig. 2.1), $\mathcal{A}_{\phi 0}^U(\eta) = O(\eta^{-1/2})$. $\mathcal{A}_{z 0}^U(\eta)$ is given by (3.33a), and it has $O(\eta^{-1})$ behavior as $\eta \rightarrow \infty$ in the same region. Hence, when $z > 0$, the path of integration can be

closed by a semicircle at infinity in the upper half-plane, and the result is zero for both (4.1a) and (4.1b), because the integrands are analytic in the upper half-plane. This simply means that the surface currents vanish for $z > 0$, i.e., outside the metal. When $z < 0$, the paths of integration may be deformed to run along both sides of the branch cut, (which will be considered to be a straight line from $-k_0$ to $-k_0 - i\infty$), capturing, along the way, any poles of the integrand. This is similar to the procedure used in Appendix B, and to Fig. B.2a. When the path is thus deformed, the functions $x^U(\eta)$ and $y^U(\eta)$ must be represented by their analytic continuations into the lower half-plane, i.e.,

$$x^U(\eta) = \frac{J'_m(\nu_0 a) H_m^{(1)'}(\nu_0 a)}{x^L(\eta)}, \quad y^U(\eta) = \frac{J_m(\nu_0 a) H_m^{(1)}(\nu_0 a)}{y^L(\eta)}. \quad (4.2)$$

$\mathcal{L}_{\phi_0}^U(\eta)$ can be rewritten as

$$\mathcal{L}_{\phi_0}^U(\eta) = \frac{-2i}{\pi a^2 k_0} \left(\frac{A}{\eta + k_0} + \frac{B}{\eta - \lambda_{m10}} \right) \frac{x^L(\eta)}{J'_m(\nu_0 a) H_m^{(1)'}(\nu_0 a)} - \frac{\alpha_m}{\eta - \lambda_{m10}} \quad (4.3)$$

where A and B are defined in (3.41).

The integration (4.1a) around $-k_0$ does not contribute anything, because the integrand is of $O(|\eta + k_0|)$ as $\eta \rightarrow -k_0$. Along the branch cut, from $-k_0$ to $-\infty$, the integrand will be $[\mathcal{U}_{\phi_0+}^U(\eta) - \mathcal{U}_{\phi_0-}^U(\eta)]e^{iz\eta}$. Using (B.10), the contribution of this integral to $J_{\phi_0}(z)$ will be

$$s_1(z) = \sqrt{\frac{2}{\pi}} \frac{2i}{\pi a^2 k_0} \int_{-k_0}^{-i\infty} \left(\frac{A}{\eta + k_0} + \frac{B}{\eta - \lambda_{m10}} \right) \cdot \frac{x^L(\eta) e^{iz\eta}}{[J'_m(\nu_0 a)]^2 + [Y'_m(\nu_0 a)]^2} d\eta \quad (4.4)$$

$\mathcal{U}_{\phi_0}^U(\eta)$ has simple poles at $-\lambda_{mn}$, $n = 1, 2, 3, \dots$, so their residues will be captured by the deformation of the path, affected by a negative sign because the path circles them clockwise. The result is

$$J_{\phi_0}(z) = \frac{\sqrt{2\pi} i}{k_0 a^4} \sum_{n=1}^{\infty} \frac{q_{mn}^4 x^L(-\lambda_{mn})}{\lambda_{mn} (m^2 - q_{mn}^2)} \left(\frac{A}{\lambda_{mn} - k_0} + \frac{B}{\lambda_{mn} + \lambda_{m10}} \right) e^{-i\lambda_{mn} z} + s_1(z) \quad (4.5)$$

The same process is to be carried out for (3.33a), with $x^U(\eta)$ and $y^U(\eta)$ replaced by expressions (4.2), i.e., for

$$\begin{aligned}
 \mathcal{L}_{z_0}^U(\eta) \frac{1}{a} = & - \frac{2m}{\pi k_0 a^3} \left(\frac{A}{\eta + k_0} + \frac{B}{\eta - \lambda_{m10}} \right) \frac{\eta x^L(\eta)}{v_0^2 J_m'(v_0 a) H_m^{(1)'}(v_0 a)} \\
 & - \frac{k_0}{m\pi} \left(\frac{D}{\eta + k_0} + \frac{F}{\eta - \mu_{m10}} \right) \frac{y^L(\eta)}{(\eta - k_0) J_m(v_0 a) H_m^{(1)}(v_0 a)} \\
 & - \frac{\lambda_{m10}^2 G}{k_0 a} \frac{1}{\eta - \lambda_{m10}} - \frac{\mu_{m10} T}{k_0 a} \frac{1}{\eta - \mu_{m10}} \quad , \quad (4.6)
 \end{aligned}$$

where the constants A, B, D, F, G and T are defined in (3.41). It must be remarked that the apparent poles at $\eta = \mu_{m10}$ and $\eta = \lambda_{m10}$ are actually cancelled by combining the term in F with the term in T and the term in B with the term in G. Also, (4.6) remains finite as $\eta \rightarrow -k_0$, because the apparent infinities of the A and the D terms cancel each other. Hence, the integration around $-k_0$ vanishes, and all that is left is the integration, along the branch cut, of the discontinuity of (4.6), and the residue contributions from the poles at $-\lambda_{mn}$ (terms A and B) and at $-\mu_{mn}$ (terms D and F). The integration along the branch cut yields $s_2(z) + s_3(z)$, where

$$\begin{aligned}
 s_2(z) = & -\sqrt{\frac{2}{\pi}} \frac{2m}{\pi k_0 a^3} \int_{-k_0}^{-i\infty} \left(\frac{A}{\eta + k_0} + \frac{B}{\eta - \lambda_{m10}} \right) \eta \frac{x^L(\eta)}{v_0^2} \\
 & \cdot \frac{e^{iz\eta}}{[J_m'(v_0 a)]^2 + [Y_m'(v_0 a)]^2} d\eta \quad (4.7a)
 \end{aligned}$$

and

$$s_3(z) = -\sqrt{\frac{2}{\pi}} \frac{k_0}{m\pi} \int_{-k_0}^{-j\infty} \left(\frac{D}{\eta + k_0} + \frac{F}{\eta - \lambda_{m10}} \right) \frac{y^L(\eta)}{\eta - k_0} \cdot \frac{e^{iz\eta}}{[J_m(v_0 a)]^2 + [Y_m(v_0 a)]^2} d\eta \quad (4.7b)$$

By including the pole contributions, it follows that

$$J_{z0}(z) = \frac{\sqrt{2\pi} m}{k_0 a^3} \sum_{n=1}^{\infty} \frac{q_{mn}^2 x^L(-\lambda_{mn})}{(m^2 - q_{mn}^2)} \left(\frac{A}{\lambda_{mn} - k_0} + \frac{B}{\lambda_{mn} + \lambda_{m10}} \right) e^{-i\lambda_{mn} z}$$

$$- \sqrt{\frac{\pi}{2}} \frac{k_0}{ma^2} \sum_{n=1}^{\infty} \frac{p_{mn}^2 y^L(-\mu_{mn})}{(k_0 + \mu_{mn}) \mu_{mn}} \left(\frac{D}{\mu_{mn} - k_0} + \frac{F}{\mu_{mn} + \mu_{m10}} \right) e^{-i\mu_{mn} z}$$

$$+ s_2(z) + s_3(z) \quad (4.8)$$

It must be noted that all the integrals $s_1(\eta)$, $s_2(\eta)$ and $s_3(\eta)$ are convergent, and this can be verified by analyzing the behavior of the integrands as $\eta \rightarrow -k_0$ and as $\eta \rightarrow -k_0 - i\infty$.

The different terms in the expressions for the components of the surface current density, (4.5) and (4.8), must now be given some physical interpretation.

In Appendix C it is shown that the Fourier transforms of the field components, for $\rho < a$, have no branch points in the lower half-plane, only poles. In Appendix D, it is shown that, for $\rho > a$, they have no poles, only branch points at $\eta = -k_0$, in the lower half-plane. Consider the current densities $J_{\phi 0}(z)$ and $J_{\phi 1}(z)$ as being the sum of the densities on the inside ($\rho = a^-$) and the outside ($\rho = a^+$) of the metallic cylindrical shell. The inside current densities will be the limit values of the tangential magnetic field components as $\rho \rightarrow a^-$ from values $\rho < a$, and the outside current densities will be the limit values of the tangential magnetic field components as $\rho \rightarrow a^+$ from values $\rho > a$.

Hence, the parts of (4.5) and (4.8) which resulted from integration around poles, in the lower half-plane, are seen to correspond to the fields inside the metallic waveguide, and represent, therefore, the current densities on the inside wall of the metallic cylinder. Thus, the terms in the summation of (4.5) and in the first summation of (4.8) represent reflected TE_{mn} modes inside the guide, propagating or evanescent, in the negative z -direction. Similarly, each term in the second summation of (4.8) represents a reflected TM_{mn} mode inside the guide.

The $s_n(z)$ terms in (4.5) and (4.8), on the other hand, result from integrations along the branch cut in the lower half-plane, and hence correspond to the fields outside the metallic guide, for $z < 0$. They represent the current densities on the outside wall of the metallic cylinder, and they are not expressed

as a summation of modes, i.e., they represent a continuous, not discrete, spectrum.

4.2 Inverse Fourier Transformation of $\mathcal{A}_{\phi_1}^U(\eta)$ and $\mathcal{A}_{z_1}^U(\eta)$

Expressions (3.42a) and (3.42b) will now be inverse Fourier transformed, by using (4.1) and path deformations similar to the ones used in Section 4.1. In an analogous manner, (4.2) will be used to continue $x^U(\eta)$ and $y^U(\eta)$ into the lower half-plane, when the path of integration is deformed, for $z < 0$. For $z > 0$, the inverse Fourier transforms are zero, as in the previous section.

From (B.17) and (B.18) it is seen that all the $u_n(\eta)$ are of the form

$$u_n(\eta) = \int_{-k_0}^{-i\infty} \frac{\kappa_n(\xi)}{\xi - \eta} d\xi, \quad (4.9)$$

where the only singularities of $\kappa_n(\xi)$ are on the branches of hyperbola of Fig. B.1. The $u_n(\eta)$ have branch points at $\eta = -k_0$, and are of $O(\ln(\eta + k_0))$ behavior when $\eta \rightarrow -k_0$, because $\kappa_n(\xi)$ are bounded at $-k_0$, as seen in Appendix B. The branch cuts can be taken anywhere in the third quadrant of the η plane, connecting $-k_0$ to $-i\infty$; here, they will be taken as the straight dashed lines of Fig. B.1. The limit values of $u_n(\eta)$ for the positive side and the negative side of the branch cut are given by Plemelj formulas (Pogorzelski [28]), and are

$$u_{n+}(\eta) = i\pi\kappa_n(\eta) + \mathcal{P}_\eta[u_n(\eta)] \quad (4.10a)$$

and

$$u_{n-}(\eta) = -i\pi\kappa_n(\eta) + \mathcal{P}_\eta[u_n(\eta)] \quad , \quad (4.10b)$$

where the operator \mathcal{P}_η means the principal value at η .

In (3.42), $u_n(\eta)$ appears divided by $x^U(\eta)$ or $y^U(\eta)$, and, using (4.2), the following discontinuities will occur across the branch cut:

$$\frac{u_n(\eta)}{x^U(\eta)} \Big|_+ - \frac{u_n(\eta)}{x^U(\eta)} \Big|_- = \frac{2x^L(\eta)\{\pi\kappa_n(\eta)Y'_m(\nu_0 a) + \mathcal{P}_\eta[u_n(\eta)] \cdot J'_m(\nu_0 a)\}}{J'_m(\nu_0 a) \{[J'_m(\nu_0 a)]^2 + [Y'_m(\nu_0 a)]^2\}} \quad (4.11a)$$

and

$$\frac{u_n(\eta)}{y^U(\eta)} \Big|_+ - \frac{u_n(\eta)}{y^U(\eta)} \Big|_- = \frac{2y^L(\eta)\{\pi\kappa_n(\eta)Y_m(\nu_0 a) + \mathcal{P}_\eta[u_n(\eta)] \cdot J_m(\nu_0 a)\}}{J_m(\nu_0 a) \{[J_m(\nu_0 a)]^2 + [Y_m(\nu_0 a)]^2\}} \quad (4.11b)$$

The deformation of the original path, to the path of Fig. B.2b, is possible because the right-hand sides of (3.42) vanish at infinity, away from the branch cut. In fact, noting that $u_n(\eta) = O(\eta^{-1})$ as $\eta \rightarrow \infty$, the conclusion follows.

As $\eta \rightarrow -k_0$, the right-hand side of (3.42a) remains bounded, and the same holds for the terms on the right-hand side of (3.42b),

with the exception of the six last terms, the ones including the $u_n(\eta)$, which behave as $\ln(\eta + k_0)$. In any case, the integration around $-k_0$, along a small circle with vanishing radius, is zero. The only contributions to the inverse Fourier transforms will come from the integration of the discontinuity along the branch cut and the residues of the poles captured in the path deformation.

The branch cut integrations for $J_{\phi_1}(z)$ are

$$\bar{s}_1(z) = -\sqrt{\frac{2}{\pi}} K_0 \int_{-k_0}^{-i\infty} \frac{\bar{f}(\eta)}{\eta + k_0} e^{iz\eta} d\eta, \quad (4.12a)$$

$$\bar{s}_2(z) = -\sqrt{\frac{2}{\pi}} \sum_{n=1}^{\infty} K_n \int_{-k_0}^{-i\infty} \frac{\bar{f}(\eta)}{\eta + \lambda_{mn}} e^{iz\eta} d\eta, \quad (4.12b)$$

$$\bar{s}_3(z) = \sqrt{\frac{2}{\pi}} C \int_{-k_0}^{-i\infty} \left[\frac{x^U(\lambda_{m10})}{(\eta - \lambda_{m10})^2} + \frac{x^{U'}(\lambda_{m10})}{\eta - \lambda_{m10}} \right] \bar{f}(\eta) e^{iz\eta} d\eta, \quad (4.12c)$$

$$\bar{s}_4(z) = -\sqrt{\frac{2}{\pi}} \frac{2x^U(k_0)A}{\pi a} \int_{-k_0}^{-i\infty} \bar{f}(\eta) \bar{g}_1(\eta) e^{iz\eta} d\eta, \quad (4.12d)$$

$$\bar{s}_5(z) = -\sqrt{\frac{2}{\pi}} \frac{iB}{\pi} \int_{-k_0}^{-i\infty} \bar{f}(\eta) \bar{g}_2(\eta) e^{iz\eta} d\eta, \quad (4.12e)$$

and

$$\bar{s}_6(z) = \sqrt{\frac{2}{\pi}} \frac{iF}{\pi} \int_{-k_0}^{-i\infty} \bar{f}(\eta) \bar{g}_3(\eta) e^{iz\eta} d\eta, \quad (4.12f)$$

where

$$\bar{f}(\eta) = \frac{x^L(\eta)}{[J'_m(v_0 a)]^2 + [Y'_m(v_0 a)]^2}, \quad (4.13a)$$

and, for n in $\{1,2,3\}$,

$$\bar{g}_n(\eta) = \pi \kappa_n(\eta) \frac{Y'_m(v_0 a)}{J'_m(v_0 a)} + \mathcal{P}_\eta[u_n(\eta)] \quad (4.13b)$$

and the $\kappa_n(\eta)$ are given by (4.9).

Similarly, for $J_{z_1}(z)$,

$$\bar{s}_1(z) = \sqrt{\frac{2}{\pi}} \frac{K_0}{a} \int_{-k_0}^{-i\infty} \left[\frac{2ik_0^2 a^2 x^U(k_0)}{my^U(k_0)} \bar{f}(\eta) - im \frac{\eta \bar{f}(\eta)}{\eta + k_0} \right] e^{iz\eta} d\eta, \quad (4.14a)$$

$$\bar{s}_2(z) = -\frac{m\sqrt{2\pi}}{a} \sum_{n=1}^{\infty} K_n \int_{-k_0}^{-i\infty} \left[\lambda_{mn} h_{mn} \frac{\bar{f}(\eta)}{\eta - k_0} + \frac{i}{\pi} \frac{\eta \bar{f}(\eta)}{v_0^2} \right] e^{iz\eta} d\eta, \quad (4.14b)$$

$$\bar{s}_3(z) = \sqrt{\frac{2}{\pi}} \sum_{n=1}^{\infty} \frac{K'_n}{a} \int_{-k_0}^{-i\infty} \frac{\bar{f}(\eta) e^{iz\eta}}{(\eta - k_0)(\eta + \mu_{mn})} d\eta, \quad (4.14c)$$

$$\begin{aligned} \bar{s}_4(z) = \sqrt{\frac{2}{\pi}} \frac{q_{m1}^2 G}{a^3} \int_{-k_0}^{-i\infty} \left\{ -\frac{2\lambda_{m10}^2 a^2 y^U(\lambda_{m10})}{q_{m1}^2 (k_0 + \lambda_{m10})} (\eta + k_0) \bar{f}(\eta) \right. \\ \left. + \left[x^{U'}(\lambda_{m10}) + \frac{x^U(\lambda_{m10})}{\eta - \lambda_{m10}} \right] \eta \bar{f}(\eta) \right\} \frac{e^{iz\eta}}{v_0^2 (\eta - \lambda_{m10})} d\eta, \quad (4.14d) \end{aligned}$$

$$\begin{aligned}
 \bar{s}_5(z) &= \sqrt{\frac{2}{\pi}} \frac{\mu_{m10} T}{k_0 a} \int_{-k_0}^{-i\infty} \left\{ \frac{2}{k_0} (\mu_{m10} - k_0) y^U(\mu_{m10}) \right. \\
 &+ \frac{k_0}{\mu_{m10}} [y^U(\mu_{m10}) + (\mu_{m10} - k_0) y^{U'}(\mu_{m10})] \\
 &+ \left. \frac{k_0}{\mu_{m10}} (\mu_{m10} - k_0) y^U(\mu_{m10}) \frac{1}{\eta - \mu_{m10}} \right\} \frac{\bar{f}(\eta) e^{iz\eta}}{(\eta - k_0)(\eta - \mu_{m10})} d\eta, \quad (4.14e)
 \end{aligned}$$

$$\bar{s}_6(z) = \sqrt{\frac{2}{\pi}} \frac{2m x^U(k_0) A}{i\pi a^2} \int_{-k_0}^{-i\infty} \frac{\eta \bar{f}(\eta) \bar{g}_1(\eta)}{v_0^2} e^{iz\eta} d\eta, \quad (4.14f)$$

$$\bar{s}_7(z) = \sqrt{\frac{2}{\pi}} \frac{mB}{\pi a} \int_{-k_0}^{-i\infty} \frac{\eta \bar{f}(\eta) \bar{g}_2(\eta)}{v_0^2} e^{iz\eta} d\eta, \quad (4.14g)$$

$$\bar{s}_8(z) = -\sqrt{\frac{2}{\pi}} \frac{mF}{\pi a} \int_{-k_0}^{-i\infty} \frac{\eta \bar{f}(\eta) \bar{g}_3(\eta)}{v_0^2} e^{iz\eta} d\eta, \quad (4.14h)$$

$$\bar{s}_9(z) = \frac{k_0 y^U(k_0) D}{\sqrt{2\pi} \pi m} \int_{-k_0}^{-i\infty} \frac{\bar{f}(\eta) \bar{g}_4(\eta)}{\eta - k_0} e^{iz\eta} d\eta, \quad (4.14i)$$

$$\bar{s}_{10}(z) = \sqrt{\frac{2}{\pi}} \frac{2mB}{\pi a^2} \int_{-k_0}^{-i\infty} \frac{\bar{f}(\eta) \bar{g}_5(\eta)}{\eta - k_0} e^{iz\eta} d\eta, \quad (4.14j)$$

and

$$\bar{s}_{11}(z) = \frac{k_0^2 a^2 F}{\sqrt{2\pi} \pi m} \int_{-k_0}^{-i\infty} \frac{\bar{f}(\eta) \bar{g}_6(\eta)}{\eta - k_0} e^{iz\eta} d\eta, \quad (4.14k)$$

where

$$\bar{f}(\eta) = \frac{y^L(\eta)}{[J_m(\nu_0 a)]^2 + [Y_m(\nu_0 a)]^2} \quad (4.15a)$$

and

$$\bar{g}_n(\eta) = \pi \kappa_n(\eta) \frac{Y_m(\nu_0 a)}{J_m(\nu_0 a)} + \mathcal{P}_\eta [u_n(\eta)] \quad (4.15b)$$

for n in $\{4,5,6\}$.

Next, the contribution from the poles will be calculated.

$\mathcal{L}_{\phi_1}^U(\eta)$ has double poles for $\eta = -\lambda_{mn}$, $n = 1,2,3,\dots$, and a residue calculation yields

$$J_{\phi_1}(z) = \sum_{n=1}^{\infty} (\bar{K}_n + \bar{K}_n z) e^{-i\lambda_{mn} z} + \sum_{\ell=1}^6 \bar{s}_\ell(z) \quad (4.16)$$

where the $\bar{s}_\ell(z)$ are given by (4.12), and where

$$\begin{aligned}
 \bar{K}_n = & \sqrt{\frac{\pi}{2}} \frac{\pi q_{mn}^4 x^L(-\lambda_{mn})}{a^2 \lambda_{mn} (m^2 - q_{mn}^2)} \left\{ \frac{K_0}{k_0 - \lambda_{mn}} - \frac{Cx^U(\lambda_{m10})}{(\lambda_{m10} + \lambda_{mn})^2} + \frac{Cx^{U'}(\lambda_{m10})}{\lambda_{m10} + \lambda_{mn}} \right. \\
 & + \sum_{\substack{n'=1 \\ n' \neq n}}^{\infty} \frac{K_{n'}}{\lambda_{mn'} - \lambda_{mn}} + K_n \left[\frac{3a^2 \lambda_{mn}}{q_{mn}^2} + \frac{x^{L'}(-\lambda_{mn})}{x^L(-\lambda_{mn})} + \frac{1}{2\lambda_{mn}} + \frac{a^2 \lambda_{mn}}{m^2 - q_{mn}^2} \right. \\
 & \left. \left. + \frac{ia^2 \lambda_{mn} (m^2 - q_{mn}^2) H_m^{(1)}(q_{mn})}{q_{mn}^3 Y'_m(q_{mn})} \right] + \frac{2x^U(k_0)}{\pi a} Au_1(-\lambda_{mn}) + \frac{iB}{\pi} u_2(-\lambda_{mn}) \right. \\
 & \left. - \frac{iF}{\pi} u_3(-\lambda_{mn}) \right\} \quad (4.17a)
 \end{aligned}$$

and

$$\bar{K}_n = i \sqrt{\frac{\pi}{2}} \frac{\pi q_{mn}^4 x^L(-\lambda_{mn})}{a^2 \lambda_{mn} (m^2 - q_{mn}^2)} K_n \quad (4.17b)$$

From (3.42b), it is seen that $\mathcal{D}_{z_1}^U(\eta)$ has double poles for $\eta = -\lambda_{mn}$ and for $\eta = -\mu_{mn}$, $n = 1, 2, 3, \dots$. A calculation of residues yields

$$\begin{aligned}
 J_{z_1}(z) = & \sum_{n=1}^{\infty} \left[\bar{C}_n + \bar{C}_n \left(\frac{i}{\lambda_{mn}} + z \right) \right] e^{-i\lambda_{mn}z} \\
 & + \sum_{n=1}^{\infty} [\bar{D}_n + \bar{D}_n z] e^{-i\mu_{mn}z} + \sum_{\ell=1}^{11} \bar{S}_{\ell}(z) \quad , \quad (4.18)
 \end{aligned}$$

where the $\bar{s}_\rho(z)$ are given by (4.14), and where

$$\begin{aligned} \bar{c}_n = & -\sqrt{\frac{\pi}{2}} \frac{\pi q_{mn}^2 x^L(-\lambda_{mn})}{a(m^2 - q_{mn}^2)} \left\{ \frac{imK_0}{k_0 - \lambda_{mn}} + im \sum_{\substack{n'=1 \\ n' \neq n}}^{\infty} \frac{K_{n'}}{\lambda_{mn'} - \lambda_{mn}} \right. \\ & + mK_n \left[\frac{ia^2 m^2 \lambda_{mn}}{q_{mn}^2 (m^2 - q_{mn}^2)} + i \frac{x^{L'}(-\lambda_{mn})}{x^L(-\lambda_{mn})} - \frac{a^2 \lambda_{mn} (m^2 - q_{mn}^2) H_m^{(1)}(q_{mn})}{q_{mn}^3 Y'_m(q_{mn})} \right. \\ & \left. \left. + \frac{i}{2\lambda_{mn}} \right] + \frac{q_{m1}^2 G}{a^2 (\lambda_{m10} + \lambda_{mn})} \left[x^{U'}(\lambda_{m10}) - \frac{x^U(\lambda_{m10})}{\lambda_{m10} + \lambda_{mn}} \right] \right. \\ & \left. + \frac{2imx^U(k_0)}{\pi a} Au_1(-\lambda_{mn}) - \frac{m}{\pi} Bu_2(-\lambda_{mn}) + \frac{m}{\pi} Fu_3(-\lambda_{mn}) \right\} , \quad (4.19a) \end{aligned}$$

$$\bar{c}_n = \sqrt{\frac{\pi}{2}} \frac{\pi m q_{mn}^2 x^L(-\lambda_{mn})}{a(m^2 - q_{mn}^2)} K_n , \quad (4.19b)$$

$$\begin{aligned}
 \bar{D}_n &= \sqrt{\frac{\pi}{2}} \frac{\pi p_{mn}^2 y^L(-\mu_{mn})}{a^3 \mu_{mn} (k_0 + \mu_{mn})} \left\{ \frac{2ik_0^2 a^4 x^U(k_0)}{mp_{mn}^2 y^U(k_0)} K_0(k_0 + \mu_{mn}) \right. \\
 &+ \pi m \sum_{n'=1}^{\infty} \frac{K_{n'} \lambda_{mn'} h_{mn'}}{\lambda_{mn'} - \mu_{mn}} - \sum_{\substack{n'=1 \\ n' \neq n}}^{\infty} \frac{K_{n'}}{\mu_{mn'} - \mu_{mn}} \\
 &- K_n' \left[\frac{a^2 \mu_{mn}}{p_{mn}^2} + \frac{1}{2\mu_{mn}} + \frac{y^{L'}(-\mu_{mn})}{y^L(-\mu_{mn})} + \frac{1}{k_0 + \mu_{mn}} + \frac{ia^2 \mu_{mn} H_m^{(1)'}(p_{mn})}{p_{mn} Y_m(p_{mn})} \right] \\
 &+ \frac{2G\lambda_{m10}^2 y^U(\lambda_{m10})}{(k_0 + \lambda_{m10})(\lambda_{m10} + \mu_{mn})} + \frac{\mu_{m10} T}{k_0} \left[2 \frac{y^U(\mu_{m10})}{k_0} - \frac{k_0 y^U(\mu_{m10})}{\mu_{m10}(\mu_{m10} + \mu_{mn})} \right. \\
 &+ \left. \frac{k_0 y^U(\mu_{m10})}{\mu_{m10}(\mu_{m10} - k_0)} + \frac{k_0 y^{U'}(\mu_{m10})}{\mu_{m10}} \right] \frac{\mu_{m10} - k_0}{\mu_{m10} + \mu_{mn}} \\
 &- \left. \frac{k_0 a y^U(k_0)}{2m\pi} Du_4(-\mu_{mn}) - \frac{2m}{\pi a} Bu_5(-\mu_{mn}) - \frac{k_0^2 a^3}{2\pi m} Fu_6(-\mu_{mn}) \right\} \quad (4.19c)
 \end{aligned}$$

and

$$\bar{D}_n = -i \sqrt{\frac{\pi}{2}} \frac{\pi p_{mn}^2 y^L(-\mu_{mn})}{a^3 \mu_{mn} (k_0 + \mu_{mn})} K_n' \quad (4.19d)$$

The physical interpretation of the different terms of (4.16) and (4.18) is analogous to the analysis of (4.5) and (4.8), done at the end of Section 4.1. The results of Appendices C and D are, again, used, with the conclusion that the infinite summation of (4.16) and the first summation of (4.18) correspond to the reflected TE_{mn} modes inside the metallic waveguide; the second infinite summation of (4.18) corresponds to the reflected TM_{mn} modes inside the metallic waveguide. All the mentioned terms represent current densities on the inside wall of the metallic shell.

The $\bar{s}_\ell(z)$ of (4.16) and the $\bar{\bar{s}}_\ell(z)$ of (4.18) result from the branch cut integrations, and correspond to the fields outside the metallic cylinder, for $z < 0$. They represent the current densities on the outside wall of the metallic shell.

4.3 Reflection Coefficients: Zeroth and First Order Terms

A reflected TM_{mn} mode inside the metallic guide will have a z-directed surface current density, of the general form (the ϕ variation is factored out)

$$J_z^{TM}(z) = A_n(k_1) e^{-i\mu_{mn1}z}, \quad (4.20)$$

where

$$\mu_{mn1} = \sqrt{k_1^2 - (p_{mn}/a)^2}.$$

A reflected TE_{mn} mode will have both components of the current, of general form

$$J_{\phi}^{TE}(z) = B_n(k_1) e^{-i\lambda_{mn} z} \quad (4.21a)$$

and

$$J_z^{TE}(z) = -\frac{im\lambda_{mn} a}{q_{mn}^2} B_n(k_1) e^{-i\lambda_{mn} z}, \quad (4.21b)$$

where

$$\lambda_{mn} = \sqrt{k_1^2 - (q_{mn}/a)^2}.$$

Equations (4.20) and (4.21) must be expanded in series such as (3.1). Using $\mu_{mn} = \sqrt{k_0^2 - (p_{mn}/a)^2}$ and $\lambda_{mn} = \sqrt{k_0^2 - (q_{mn}/a)^2}$,

$$J_{z0}^{TM}(z) = A_n(k_0) e^{-i\mu_{mn} z}, \quad (4.22a)$$

$$J_{z1}^{TM}(z) = \left[A'_n(k_0) - \frac{ik_0}{\mu_{mn}} A_n(k_0) z \right] e^{-i\mu_{mn} z}, \quad (4.22b)$$

$$J_{\phi 0}^{TE}(z) = B_n(k_0) e^{-i\lambda_{mn} z}, \quad (4.22c)$$

$$J_{\phi 1}^{TE}(z) = \left[B'_n(k_0) - \frac{ik_0}{\lambda_{mn}} B_n(k_0) z \right] e^{-i\lambda_{mn} z}, \quad (4.22d)$$

$$J_{z0}^{TE}(z) = -\frac{im\lambda_{mn} a}{q_{mn}^2} B_n(k_0) e^{-i\lambda_{mn} z}, \quad (4.22e)$$

$$J_z^{TE}(z) = -\frac{mk_0 a}{q_{mn}^2} \left[i \frac{\lambda_{mn}}{k_0} B'_n(k_0) + \left(\frac{i}{\lambda_{mn}} + z \right) B_n(k_0) \right] e^{-i\lambda_{mn} z}. \quad (4.22f)$$

If only a TE_{m1} mode is incident as the excitation, i.e., if $\alpha_m \neq 0$ but $\beta_m = 0$, the incident surface current densities will be (1.10a) and (1.10b), i.e.,

$$J_{\phi}^{iTE}(z) = i\sqrt{2\pi} \alpha_m e^{i\lambda_{m1}z} \quad (4.23a)$$

and

$$J_z^{iTE}(z) = \frac{im\lambda_{m1}a}{q_{m1}^2} i\sqrt{2\pi} \alpha_m e^{i\lambda_{m1}z} . \quad (4.23b)$$

By comparing to (4.20) and (4.21), the following reflection coefficients are defined

$$\Gamma_n^{TE} = \frac{[B_n(k_1)]_{\beta_m=0}}{i\sqrt{2\pi} \alpha_m} \quad (4.24a)$$

and

$$\Gamma_n'^{TE} = \frac{[A_n(k_1)]_{\beta_m=0}}{i\sqrt{2\pi} \alpha_m} . \quad (4.24b)$$

The unprimed coefficients account for the generation of reflected TE modes from a TE incident mode, whereas the primed coefficients account for the generation of TM reflected modes from a TE incident mode. These latter coefficients are also referred to, in the literature, as conversion coefficients.

Series expansions of (4.24) yield

$$\Gamma_{n0}^{TE} = \frac{[B_n(k_0)]_{\beta_m=0}}{i\sqrt{2\pi} \alpha_m}, \quad (4.25a)$$

$$\Gamma_{n1}^{TE} = \frac{[B'_n(k_0)]_{\beta_m=0}}{i\sqrt{2\pi} \alpha_m}, \quad (4.25b)$$

$$\Gamma_{n0}'^{TE} = \frac{[A_n(k_0)]_{\beta_m=0}}{i\sqrt{2\pi} \alpha_m} \quad (4.25c)$$

and

$$\Gamma_{n1}'^{TE} = \frac{[A'_n(k_0)]_{\beta_m=0}}{i\sqrt{2\pi} \alpha_m}. \quad (4.25d)$$

Similarly, if only a TM_{m1} mode is incident, i.e., if $\beta_m \neq 0$ but $\alpha_m = 0$, the incident surface current density will be (1.10b), i.e.,

$$J_z^{iTM}(z) = \frac{\sqrt{2\pi}\beta_m k_1^2}{i\omega\mu a} e^{i\mu_{m1}z}. \quad (4.26)$$

By comparing with (4.20) and (4.21) the following reflection coefficients are defined

$$\Gamma_n^{TM} = \frac{i\omega\mu a}{\sqrt{2\pi} \beta_m} \frac{[A_n(k_1)]_{\alpha_m=0}}{k_1^2} \quad (4.27a)$$

and

$$\Gamma_n^{\prime TM} = \frac{i\omega\mu a}{\sqrt{2\pi} \beta_m} \frac{[B_n(k_1)]_{\alpha_m=0}}{k_1^2}, \quad (4.27b)$$

where the unprimed coefficient denotes the generation of a TM reflected mode by a TM incident mode, and the primed coefficient (also called a conversion coefficient) denotes the generation of a TE reflected mode from a TM incident mode. Series expansions of (4.27) yield:

$$\Gamma_{n0}^{TM} = \frac{i\omega\mu a}{\sqrt{2\pi} \beta_m k_0^2} [A_n(k_0)]_{\alpha_m=0}, \quad (4.28a)$$

$$\Gamma_{n1}^{TM} = \frac{i\omega\mu a}{\sqrt{2\pi} \beta_m k_0^2} \left\{ [A_n'(k_0)]_{\alpha_m=0} - \frac{2}{k_0} [A_n(k_0)]_{\alpha_m=0} \right\}, \quad (4.28b)$$

$$\Gamma_{n0}^{\prime TM} = \frac{i\omega\mu a}{\sqrt{2\pi} \beta_m k_0^2} [B_n(k_0)]_{\alpha_m=0} \quad (4.28c)$$

and

$$\Gamma_{n1}^{\prime TM} = \frac{i\omega\mu a}{\sqrt{2\pi} \beta_m k_0^2} \left\{ [B_n'(k_0)]_{\alpha_m=0} - \frac{2}{k_0} [B_n(k_0)]_{\alpha_m=0} \right\}. \quad (4.28d)$$

Expressions (4.25) and (4.28) completely determine the zeroth and first order terms of the series expansions of the different reflection coefficients, as defined by (4.24) and (4.27),

provided that $A_n(k_0)$, $A'_n(k_0)$, $B_n(k_0)$ and $B'_n(k_0)$ are known. The determination of these functions will be the task of the remaining part of this section.

To determine $A_n(k_0)$, (4.22a) is compared to (4.8), to yield

$$A_n(k_0) = -\sqrt{\frac{\pi}{2}} \frac{k_0}{ma^2} \frac{p_{mn}^2 y^L(-\mu_{mn})}{(k_0 + \mu_{mn})\mu_{mn}} \left(\frac{D}{\mu_{mn} - k_0} + \frac{F}{\mu_{mn} + \mu_{m10}} \right). \quad (4.29)$$

As a further check on the validity of (4.29), (4.22b) is compared to (4.18), with exactly the same result. From this last comparison, it follows also that

$$A'_n(k_0) = \bar{D}_n, \quad (4.30)$$

which is given explicitly by (4.19c).

To obtain $B_n(k_0)$, (4.22c) is compared to (4.5), with the result

$$B_n(k_0) = \frac{i\sqrt{2\pi}}{k_0 a^4} \frac{q_{mn}^4 x^L(-\lambda_{mn})}{\lambda_{mn}(m^2 - q_{mn}^2)} \left(\frac{A}{\lambda_{mn} - k_0} + \frac{B}{\lambda_{mn} + \lambda_{m10}} \right). \quad (4.31)$$

This result must also be obtained if, instead, (4.22d) is compared to (4.16), (4.22e) to (4.8), or (4.22f) to (4.18), and it is indeed obtained, proving the consistency of the expressions previously reached for the current densities.

From the comparison of (4.22f) to (4.18), it also ensues that

$$B'_n(k_0) = i \frac{q_{mn}^2}{m\lambda_{mn} a} \bar{C}_n, \quad (4.32)$$

where \bar{C}_n is given by (4.19a).

When using (4.29) through (4.32) in (4.25) and (4.28), either $\beta_m = 0$ or $\alpha_m = 0$, which cause considerable simplification. Among the constants defined by (3.41), for example, F, L and T vanish if $\beta_m = 0$, and B, C and G vanish if $\alpha_m = 0$. In either case, A and D will simplify, because $V_{20}^L(-k_0)$ simplifies, as expressed by (3.32). No one of expressions (4.25) and (4.28) is identically zero, however, which shows that an incident mode with an m th order variation in ϕ originates both TE and TM reflected modes when $m \geq 1$. The simpler case of $m = 0$ only admits TE reflected modes when the incident mode is TE, and similarly for TM modes, as was pointed out in Section 2.4.

The zeroth order terms for the several reflection coefficients, (4.25a), (4.25c), (4.28a) and (4.28c) must agree with the results arrived at by Weinstein, [16], Section 27. After some laborious conversion of notation between Weinstein [16] and this work, this agreement can be proved.

4.4 Some Numerical Computations for the TE_{11} Mode

It is assumed, in this section, that $\text{Im } k_0$ and $\text{Im } k_1$ are zero, and that the structure was dimensioned in such a manner that the only propagating mode inside the metallic waveguide is the dominant TE_{11} mode, all the others being evanescent. The cutoff for this mode occurs for $k_1 a = q_{11} = 1.84118$. Considering only modes with the same ϕ -variation, $m = 1$, the next lowest cutoff corresponds to the TM_{11} mode, and occurs when $k_1 a = p_{11} = 3.83171$. Therefore, it is assumed that

$$1.84118 < k_1 a < 3.83171 \quad . \quad (4.33)$$

If all possible ϕ -variations were allowed, TE_{11} would still be dominant, but the right-hand bound of (4.33) would be replaced with $p_{01} = 2.40483$, the cutoff of the TM_{01} mode.

The exciting mode is an incident TE_{11} mode and, since all other modes are evanescent, the only reflected field inside the waveguide, far enough away from the open end, will be a reflected TE_{11} mode. Therefore, the reflection coefficient of interest is Γ_1^{TE} , with the zeroth and first-order terms given by (4.25a) and (4.25b), for $n = 1$, i.e.,

$$\Gamma_{10}^{TE} = \frac{i\pi q_{11}^4 [x_1^U(\lambda_{11})]^2}{2\lambda_{11} a(1 - q_{11}^2)} \left\{ \frac{1}{2\lambda_{11} a} - \frac{2k_0 a [y_1^U(k_0)]^2}{(\lambda_{11} a - k_0 a)^2 [4(k_0 a)^2 [x_1^U(k_0)]^2 - [y_1^U(k_0)]^2]} \right\}, \quad (4.34)$$

and

$$\frac{\Gamma_{11}^{TE}}{a} = \frac{q_{11}^2}{\sqrt{2\pi} \alpha_{11} \lambda_{11} a^2} \left[\bar{C}_1 \right]_{\substack{m=1 \\ \beta_{m=0}}} . \quad (4.35)$$

In these expressions, the subscript in $x_1^U(n)$ and $y_1^U(n)$ means that $m = 1$ in the functions $x^U(n)$ and $y^U(n)$, which were defined in Appendix A. \bar{C}_n is given by (4.19a).

For a given $k_0 a$, and for a given relative permittivity of the dielectric, $\epsilon_r = \epsilon_1 / \epsilon_0$, which is sufficiently close to unity, the reflection coefficient for the TE_{11} mode is

$$\Gamma_1^{TE}(k_0 a, \epsilon_r) \approx \Gamma_{10}^{TE}(k_0 a) + \frac{1}{a} \Gamma_{11}^{TE}(k_0 a) \cdot k_0 a (\sqrt{\epsilon_r} - 1), \quad (4.36)$$

where the only variation with ϵ_r is shown explicitly by the factor $(\sqrt{\epsilon_r} - 1)$.

Numerical computations of expressions (4.34) and (4.35) were carried out on the University of Michigan's Amdahl 470/V8 computer, and the results are displayed in Table 4.1 and Fig. 4.1.

Table 4.1
 Numerical Values for $\Gamma_1^{\text{TE}} = \Gamma_{10}^{\text{TE}} + \Gamma_{11}^{\text{TE}} \Delta k + \dots$

$k_0 a$	Γ_{10}^{TE}	$\frac{1}{a} \Gamma_{11}^{\text{TE}}$	Coarse upper bound for ϵ_r
1.842	-0.9125 - i0.0040	15.4501 + i14.1663	1.0009
1.85	-0.7436 - i0.0120	6.0213 + i1.1114	1.0096
1.9	-0.4634 - i0.0216	3.6548 - i0.4324	1.0629
2.0	-0.2811 - i0.0129	2.3994 - i0.1441	1.1651
2.2	-0.1491 + i0.0041	1.4726 + i0.1639	1.3528
2.5	-0.0739 + i0.0179	0.8425 + i0.2625	1.5965
3.0	-0.0258 + i0.0206	0.3944 + i0.1724	1.6313
3.4	-0.0073 + i0.0199	0.2616 + i0.0901	1.2701

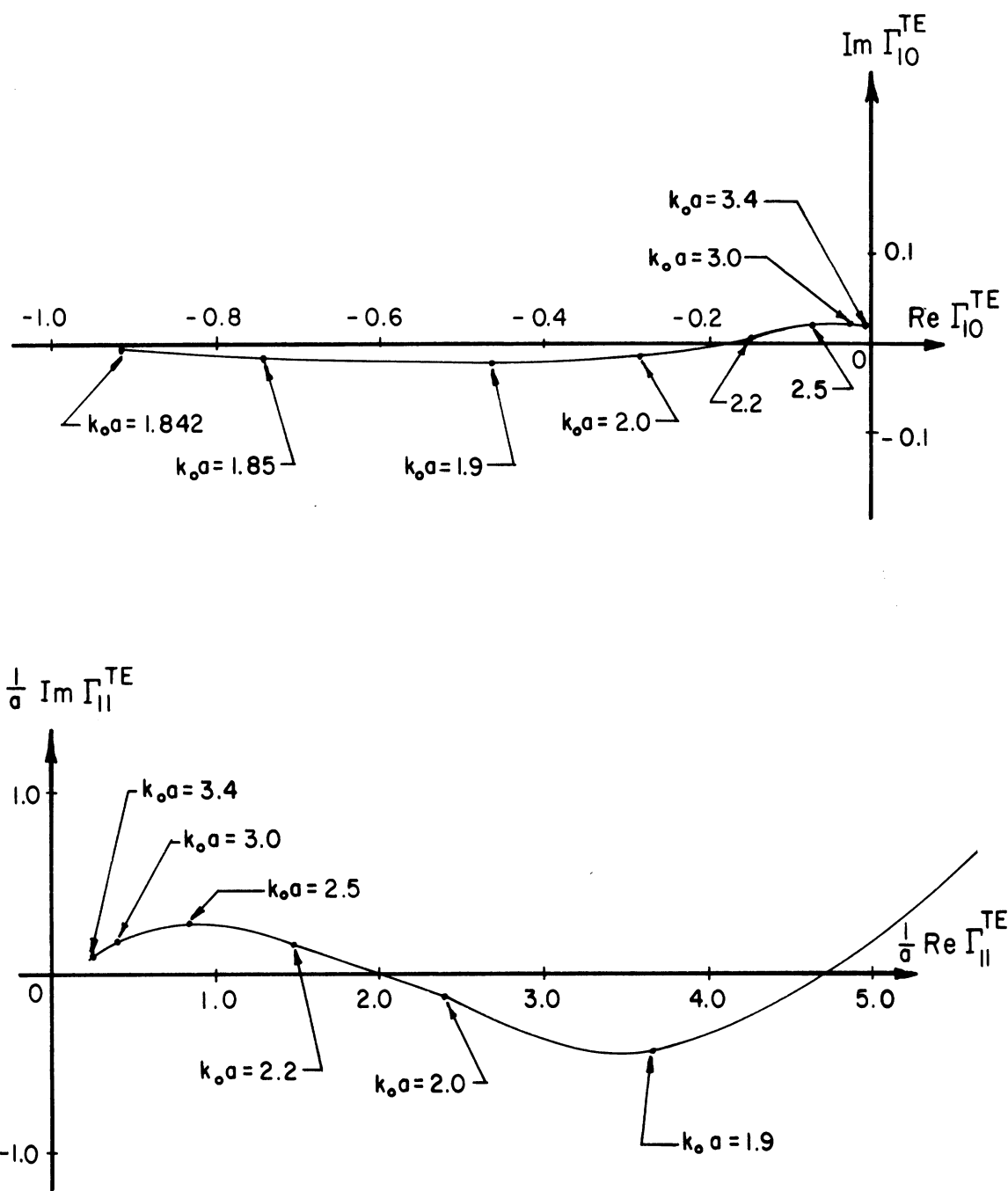


Fig. 4.1: Variation with $k_0 a$ of the complex functions Γ_{10}^{TE} and $\frac{1}{a} \Gamma_{11}^{TE}$.

These results show that, for $k_0 a$ close to q_{11} , i.e., near the cutoff of the TE_{11} mode, Γ_{10}^{TE} is close to -1, and Γ_{11}^{TE} is quite large. This means an almost total reflection of the mode for $\epsilon_r \approx 1$, and a very large sensitivity of Γ_1^{TE} , (4.36), to a small increase in ϵ_r (which leads to a decrease in $|\Gamma_1^{TE}|$). However, as discussed later on in this section and as displayed in the last column of Table 4.1, even a small increase in ϵ_r would invalidate (4.36).

As $k_0 a$ is increased $|\Gamma_{10}^{TE}|$ decreases rather fast, indicating that increasingly more of the incident power will leave the waveguide through the open end, and progressively less of it will be reflected back into the guide. An increase in ϵ_r will still lead to a decrease in $|\Gamma_1^{TE}|$. The sensitivity of (4.36) to that increase in ϵ_r , however, becomes progressively less, while at the same time larger values of ϵ_r are allowed before the validity of (4.36) is jeopardized.

Therefore, when the structure is to be used as an antenna, the farther the frequency is from cutoff, the more power is available outside of the guide. This power will be radiated in a real antenna, for which the dielectric rod is terminated at a finite distance from the open end. Another important factor is the radiation pattern, which will be discussed in Chapter V.

If $k_0 a$ were to be increased beyond $p_{11} = 3.83171$, the TM_{11} mode would also propagate back into the guide. The derivative of $\Gamma_1^{TE}(k_0 a)$ with respect to $k_0 a$, as $k_0 a$ crossed the value p_{11} , would change abruptly, as was concluded by Weinstein [16], Section 26, about the zeroth order term Γ_{10}^{TE} . This reflects the fact that $\Gamma_1^{TE}(k_0 a, \epsilon_r)$ is a function of the propagation constants of the guided modes, λ_{1n} and μ_{1n} , $n = 1, 2, 3, \dots$. Therefore, as a function of $k_1 a$, it has branch points at $k_1 a = p_{1n}$ and $k_1 a = q_{1n}$, $n = 1, 2, 3, \dots$.

This fact establishes the radius of convergence of the Taylor series for Γ_1^{TE} around $k_1 a = k_0 a$, which is the smallest of the quantities $k_0 a - 1.84118$ and $3.83171 - k_0 a$. As k_1 will be real, positive, and larger than k_0 , this means that $k_1 a < \min \{(2k_0 a - 1.84118), 3.83171\}$ is the condition for the convergence of the Taylor series expansion. This imposes an upper bound on ϵ_r in expression (4.36), namely

$$\epsilon_r < \min \left\{ \left(2 - \frac{1.84118}{k_0 a} \right)^2, \left(\frac{3.83171}{k_0 a} \right)^2 \right\}. \quad (4.37)$$

This bound for ϵ_r has the numerical values displayed in the last column of Table 4.1, and should be understood only as a coarse restriction on the choice of ϵ_r . Clearly, (4.36) will always be in error, and it will be more accurate the closer ϵ_r is to unity. For ϵ_r close to the maximum allowable value of (4.37), the convergence of the Taylor series for Γ_1^{TE} will be quite slow, and the two terms of (4.36) probably will not be sufficient to describe the whole series with reasonable accuracy.

The upper bound on the allowable value of ε_r is one of the most serious limitations of the perturbation approach undertaken in this work.

CHAPTER V. FIELDS OUTSIDE THE METALLIC GUIDE

5.1 Some Properties of the Field Components for $z > 0$

In Appendices C and D, the transforms of the field components were analyzed for their behavior in the lower half-plane, which is relevant to the behavior of the fields for $z < 0$. In Chapter IV, it was then concluded that, for $z < 0$, the fields inside the guide are completely described by an infinite summation of reflected modes. Outside the guide, for $z < 0$, the fields are described by integrals along the branch cut in the lower half-plane, representing a continuous spectrum.

The same transformed functions should now be analyzed in the upper half-plane, so that conclusions may be reached about the behavior of the field components for $z > 0$.

Hence, for $\rho < a$, and in the upper half-plane (C.2) and (C.3) may be written as follows. Using (3.31b), (C.2a) becomes

$$V_{z0}(\eta, \rho) = \frac{\omega \mu a}{2mk_0} \left(\frac{D}{\eta + k_0} + \frac{F}{\eta - \mu_{m10}} \right) \frac{\eta + k_0}{y^U(\eta)} H_m^{(1)}(\nu_0 a) J_m(\nu_0 \rho) \quad (5.1)$$

From (3.36d), (C.2b) yields

$$V_{z1}(\eta, \rho) = \left\{ \left[\frac{V_{z1}^L(-k_0)}{y^L(-k_0)(\eta + k_0)} - \frac{\pi}{2\omega \epsilon_0} S_1^L(\eta) \right] J_m(\nu_0 \rho) + \frac{\omega \mu a}{2mk_0} \cdot \left(\frac{D}{\eta + k_0} + \frac{F}{\eta - \mu_{m10}} \right) J_m(\nu_0 a) w(\eta, \rho) \right\} \frac{\eta + k_0}{y^U(\eta)} H_m^{(1)}(\nu_0 a) \quad (5.2)$$

where $S_1^L(\eta)$ is given by (B.37), and $w(\eta, \rho)$ is given by (C.4).

Using (C.5a), (C.3a) may be written as

$$I_{Z_0}(\eta, \rho) = \frac{i\pi a}{2} \left[\mathcal{U}_{\phi_0}^U(\eta) + \frac{\alpha_m}{\eta - \lambda_{m10}} \right] v_0 H_m^{(1)'}(v_0 a) J_m(v_0 \rho) \quad (5.3)$$

Expression (C.3b) is also valid in the upper half-plane, with $I_{Z_0}(\eta, a^-)$ and $I_{Z_1}(\eta, a^-)$ given by (C.5a) and (C.5b).

The zeroth order terms, (5.1) and (5.3), represent physically the case of having no dielectric rod, i.e., $\epsilon_1 = \epsilon_0$. In agreement with that, it is easily seen that the singularities of $V_{Z_0}(\eta, \rho)$ and $I_{Z_0}(\eta, \rho)$ in the upper half-plane are a branch point at $\eta = +k_0$ and a single pole at $\eta = \mu_{m10}$ or $\eta = \lambda_{m10}$, respectively. It is straightforward to verify that these poles yield contributions to $\mathcal{E}_{Z_0}(\rho, z)$ and to $\mathcal{H}_{Z_0}(\rho, z)$ which exactly cancel the zeroth order fields due to the incident modes, $E_{Z_0}^i$ and $H_{Z_0}^i$. The total fields for $z > 0$, as given by (2.1) and (2.2), do not have any modal components in the zeroth order terms, as physically expected.

For the first order terms, these conclusions are not as easily reached. From (5.2) and (C.3b), it is seen that $V_{Z_1}(\eta, \rho)$ and $I_{Z_1}(\eta, \rho)$ have a branch point at $\eta = +k_0$.

For a TM_{m1} incident mode, the first order term of the series expansion of the z-component of E^i is, (1.1),

$$E_{z1}^i = \frac{\sqrt{2\pi} k_0 \beta_m p_{mi}}{a^2 \mu_{m10} J_m'(p_{m1})} J_m(p_{m1} \frac{\rho}{a}) z \exp(i\mu_{m10} z) \quad (5.4)$$

In (5.2), it is noted that $V_{z1}(\eta, \rho)$ has a double pole at μ_{m10} , which is in the term multiplied by the constant F . As in Section 4.2, the double pole will yield for $\mathcal{E}_{z1}(\rho, z)$ among others, a term with $z \exp(i\mu_{m10} z)$ variation in the variable z , and it is relatively easy to show that, in this case, that term will exactly cancel (5.4), so that it does not appear in the total field E_{z1} , (2.1c).

It is also straightforward, though laborious, to show that the apparent poles at μ_{mn} are actually cancelled among the several terms of (5.2), and that the residues at μ_{m10} of the different terms cancel each other exactly, except for the part that varies with z as $z \exp(i\mu_{m10} z)$, which was mentioned before, and which accounts for the incident field. Hence, the first order term for the z -component of the total electric field, E_{z1} , has no modal parts for $z > 0$, $\rho < a$, being given by a branch cut integration alone.

When a TE_{m1} mode is incident, the first order term for the z -component of the incident magnetic field is derived from (1.2), and is

$$H_{z1}^i = - \frac{\sqrt{2\pi} k_0 \alpha_m}{\lambda_{m10} J_m'(q_{m1})} J_m(q_{m1} \frac{\rho}{a}) z \exp(i\lambda_{m10} z) \quad (5.5)$$

The study of (C.3b) in the upper half-plane is simplified by the fact that (C.5a) and (C.5b) include $\mathcal{A}_{\phi_0}^U(\eta)$ and $\mathcal{A}_{\phi_1}^U(\eta)$, which, being analytic in the region of interest, require no further analysis.

It seems that $I_{z_1}(\eta, \rho)$ has poles at $\eta = \mu_{mn}$, $n = 1, 2, 3, \dots$, but these poles are cancelled among the several terms, and hence removed. There is a double pole at $\eta = \lambda_{m10}$ but, upon inverse transforming in accordance with (2.5), it is seen that its contribution to $\mathcal{K}_{z_1}(\rho, z)$ exactly cancels (5.5). Thus, the first order term of the total field, H_{z_1} , (as given by (2.2)), has no modal type contributions either, and is expressed as a branch cut integration, for $\rho < a$, $z > 0$. These arguments can be extended to the ρ -derivatives of (5.1), (5.2), (5.3) and C.3b), whence these results also apply to expressions (C.8). Thus, it is concluded that the zeroth and first order terms of the total field components for $\rho < a$, $z > 0$, are given by branch cut integrations. The mode contribution of the scattered field components is exactly cancelled by the zeroth and first order terms of the incident fields, and does not appear in the total fields.

A similar analysis must be done for $\rho > a$, $z > 0$, which means analyzing the functions (D.1) in the upper half-plane.

Using (3.31b), (D.1a) is, in the upper half plane,

$$V_{z_0}(\eta, \rho) = \frac{\omega \mu a}{2mk_0} \left(\frac{D}{\eta + k_0} + \frac{F}{\eta - \mu_{m10}} \right) \frac{\eta + k_0}{y^U(\eta)} J_m(\nu_0 a) H_m^{(1)}(\nu_0 \rho) \quad (5.6)$$

From (3.36d) and (D.1b),

$$V_{z_1}(\eta, \rho) = \left\{ \frac{V_{z_1}^L(-k_0)}{y^L(-k_0)} \frac{1}{\eta + k_0} - \frac{\pi}{2\omega \epsilon_0} S_1^L(\eta) \right\} \frac{\eta + k_0}{y^U(\eta)} J_m(\nu_0 a) H_m^{(1)}(\nu_0 \rho) \quad (5.7)$$

with $S_1^L(\eta)$ given by (B.37). From (D.2) and (D.1c), get

$$I_{z0}(\eta, \rho) = \frac{1}{k_0 a} \left(\frac{A}{\eta + k_0} + \frac{B}{\eta - \lambda_{m10}} \right) \frac{v_0 J'_m(v_0 a)}{x'(\eta)} H_m^{(1)}(v_0 \rho) \quad . \quad (5.8)$$

Expressions (D.1d) and (D.3) remain valid for $I_{z1}(\eta, \rho)$, with $V_{z0}^L(\eta)$ in (D.3) given by (3.31b).

It is clear that none of the functions (5.6), (5.7) or (5.8) has poles in the upper half-plane, and the respective field components are represented by integrals along the branch cut from k_0 to $+i\infty$. The same conclusion is reached concerning $I_{z1}(\eta, \rho)$, because the poles at λ_{m10} of two of its terms actually cancel each other.

From (D.1), it is clear that differentiation with respect to ρ does not change the aforementioned properties. Then, using the corresponding forms of (C.8) for $\rho > a$, and similarly for the ρ -components, it follows that all the field components are represented by branch cut integrations, with no mode-like parts.

It should be remarked here that, inasmuch as the total field inside the metallic waveguide is completely described by a summation of TE and TM reflected modes in addition to the incident modes, the total fields outside the metallic waveguide display no modal components. This fact must perforce be attributed to the nature of the mathematical approach undertaken, namely to the expansion of all quantities in Taylor series about the permittivity of free space.

The exact solution of this problem must display modal components of the fields, along the dielectric rod outside the metallic cylinder (see Kiely [1] and Andersen [5]). If the complete Taylor series were used (clearly, impossible in practice), the poles of the Fourier transformed functions would be reconstituted at the propagation constants of the modes of the dielectric rod. Since only the first two terms of the series are used, however, these modes do not appear explicitly. Rather, they show themselves in the form of a first order perturbation of the fields of the zeroth order case. The latter case represents the physical case $\epsilon_1 = \epsilon_0$, which admits no modal components for $z > 0$.

5.2 Zeroth Order Asymptotic Far Field

It is now convenient to express the fields in a spherical coordinate system, (r, θ, ϕ) , such that ϕ is the same as for the cylindrical system, and where

$$\rho = r \sin \theta \quad , \quad z = r \cos \theta \quad . \quad (5.9)$$

A vector field, for example (E_ρ, E_ϕ, E_z) , will now be represented as (E_r, E_θ, E_ϕ) , where E_ϕ remains unchanged, but

$$E_r = E_\rho \sin \theta + E_z \cos \theta \quad , \quad E_\theta = E_\rho \cos \theta - E_z \sin \theta \quad . \quad (5.10)$$

As in Section 2.1, the Fourier transform integrals are defined:

$$\mathcal{E}_r(\rho, z) = -\frac{1}{\sqrt{2\pi}} \int_{-\infty}^{\infty} V_r(\eta, \rho) e^{i\eta z} d\eta, \quad (5.11a)$$

$$\mathcal{E}_\theta(\rho, z) = -\frac{1}{\sqrt{2\pi}} \int_{-\infty}^{\infty} V_\theta(\eta, \rho) e^{i\eta z} d\eta, \quad (5.11b)$$

$$\mathcal{H}_r(\rho, z) = \frac{1}{\sqrt{2\pi}} \int_{-\infty}^{\infty} I_r(\eta, \rho) e^{i\eta z} d\eta \quad (5.11c)$$

and

$$\mathcal{H}_\theta(\rho, z) = \frac{1}{\sqrt{2\pi}} \int_{-\infty}^{\infty} I_\theta(\eta, \rho) e^{i\eta z} d\eta. \quad (5.11d)$$

Then, (2.9a), (2.9d), (2.7), (2.8) and (5.10) give

$$V_\phi(\eta, \rho) = \frac{i}{v^2} \left\{ \omega\mu\rho \frac{\partial I_z(\eta, \rho)}{\partial \rho} + \eta m V_z(\eta, \rho) \right\}, \quad (5.12a)$$

$$I_\phi(\eta, \rho) = -\frac{i}{v^2} \left\{ \omega\varepsilon\rho \frac{\partial V_z(\eta, \rho)}{\partial \rho} + \eta m I_z(\eta, \rho) \right\}, \quad (5.12b)$$

$$V_r(\eta, \rho) = \frac{i m \omega \mu}{v^2 r} I_z(\eta, \rho) + \left(\frac{i \eta}{v^2} \sin \theta \frac{\partial}{\partial \rho} + \cos \theta \right) V_z(\eta, \rho), \quad (5.12c)$$

$$I_r(\eta, \rho) = \frac{i m \omega \varepsilon}{v^2 r} V_z(\eta, \rho) + \left(\frac{i \eta}{v^2} \sin \theta \frac{\partial}{\partial \rho} + \cos \theta \right) I_z(\eta, \rho), \quad (5.12d)$$

$$V_{\theta}(\eta, \rho) = \frac{i m \omega \mu}{v^2 r \tan \theta} I_Z(\eta, \rho) + \left(\frac{i \eta}{v^2} \cos \theta \frac{\partial}{\partial \rho} - \sin \theta \right) V_Z(\eta, \rho) \quad (5.12e)$$

and

$$I_{\theta}(\eta, \rho) = \frac{i m \omega \epsilon}{v^2 r \tan \theta} V_Z(\eta, \rho) + \left(\frac{i \eta}{v^2} \cos \theta \frac{\partial}{\partial \rho} - \sin \theta \right) I_Z(\eta, \rho) \quad (5.12f)$$

where (ϵ, v) are (ϵ_0, v_0) for $\rho > a$ and (ϵ_1, v_1) for $\rho < a$.

Expressions (5.12) will now be expanded in series like (3.1).

The zeroth order terms are obtained from expressions (5.12) by simply replacing v with v_0 , ϵ with ϵ_0 , $I_Z(\eta, \rho)$ with $I_{Z0}(\eta, \rho)$ and $V_Z(\eta, \rho)$ with $V_{Z0}(\eta, \rho)$. The correct expressions for $I_{Z0}(\eta, \rho)$ and $V_{Z0}(\eta, \rho)$ must be chosen according to whether $\rho < a$ or $\rho > a$ (Appendices C and D, respectively, or Section 5.1).

In this section, it is assumed that $\text{Im } k_0$ is made to vanish. With k_0 real and positive, the path of integration for the inverse Fourier transform integrals will have to be indented to avoid the branch points, but that does not affect any of the analysis.

The inverse Fourier transformation of the zeroth order terms of (5.12), for $\rho > a$, will now be carried out, asymptotically for large $k_0 r$, with θ away from 0 or π , i.e., with

$$\sin \theta > \delta > 0, \quad \delta \ll 1. \quad (5.13)$$

This restriction means that the axial directions of the structure are avoided, and only the region $\rho > a$ is considered. The first component to be treated will be

$$\xi_{\phi_0}(\rho, z) = -\frac{1}{\sqrt{2\pi}} \int_{-\infty}^{\infty} \frac{V_{\phi_0}(\eta, \rho)}{\rho} e^{i\eta z} d\eta . \quad (5.14)$$

$V_{\phi_0}(\eta, \rho)$ is derived from (5.12a), with $V_{z_0}(\eta, \rho)$ and $I_{z_0}(\eta, \rho)$ given by (5.6) and (5.8), and hence

$$\begin{aligned} \frac{V_{\phi_0}(\eta, \rho)}{\rho} &= \frac{i\omega\mu}{k_0 a} \left(\frac{A}{\eta + k_0} + \frac{B}{\eta - \lambda_{m10}} \right) \frac{J'_m(\nu_0 a)}{x^U(\eta)} H_m^{(1)'}(\nu_0 r \sin \theta) \\ &- \frac{i\omega\mu a}{2k_0} \left(\frac{D}{\eta + k_0} + \frac{F}{\eta - \mu_{m10}} \right) \frac{\eta J_m(\nu_0 a)}{(\eta - k_0)y^U(\eta)} \frac{H_m^{(1)}(\nu_0 r \sin \theta)}{r \sin \theta} . \end{aligned} \quad (5.15)$$

The following asymptotic expressions for large $k_0 r$ will be useful (see Watson, [29], Chapter VII):

$$\begin{aligned} H_m^{(1)}(\nu_0 r \sin \theta) &\sim \left(\frac{2}{\pi \nu_0 r \sin \theta} \right)^{1/2} e^{i\nu_0 r \sin \theta} \exp[-i(2m+1)/(4)\pi] \\ &\cdot (1 + O(r^{-1})) \end{aligned} \quad (5.16a)$$

and

$$\begin{aligned} H_m^{(1)'}(\nu_0 r \sin \theta) &\sim \left(\frac{2}{\pi \nu_0 r \sin \theta} \right)^{1/2} e^{i\nu_0 r \sin \theta} \exp[-i(2m-1)/(4)\pi] \\ &\cdot (1 + O(r^{-1})) , \end{aligned} \quad (5.16b)$$

both valid in region (5.13).

Using (5.16) in (5.15), it is seen that, for large enough $k_0 r$, the second half of the right-hand side of (5.15) is negligible, when compared to the first half, and then

$$\frac{V_{\phi 0}(\eta, \rho)}{\rho} \sim \sqrt{\frac{2}{\pi}} \frac{i\omega\mu \exp[-i(2m-1)/(4)\pi]}{k_0 a} \left(\frac{A}{\eta + k_0} + \frac{B}{\eta - \frac{\lambda}{m} k_0} \right) \cdot \frac{J'_m(v_0 a)}{x^U(\eta)} \frac{e^{i v_0 r \sin \theta}}{\sqrt{v_0 r \sin \theta}} (1 + O(r^{-1})) \quad (5.17)$$

Expression (5.17) is now used in (5.14), but first it is convenient to perform a change of variables, as follows

$$\eta = k_0 \cos \alpha, \quad v_0 = k_0 \sin \alpha, \quad d\eta = -k_0 \sin \alpha \, d\alpha \quad (5.18)$$

The asymptotic version of (5.14) can then be written,

$$\mathcal{E}_{\phi 0}(r, \theta) \sim \frac{i\omega\mu \exp[-i(2m-1)/(4)\pi]}{\pi k_0 a \sqrt{k_0 r \sin \theta}} \int_c \left(\frac{A}{\cos \alpha + 1} + \frac{B}{\cos \alpha - \frac{\lambda}{m} \frac{k_0}{k_0}} \right) \cdot \frac{J'_m(k_0 a \sin \alpha)}{x^U(k_0 \cos \alpha)} \sqrt{\sin \alpha} e^{i k_0 r \cos(\alpha - \theta)} d\alpha, \quad (5.19)$$

where c is the path of integration in the α -plane, as shown in Fig. 5.1.

It must be noted that $J'_m(k_0 a \sin \alpha)/x^U(k_0 \cos \alpha)$ is an appropriate expression in Regions I and II of Fig. 5.1, but it may be convenient to replace it by $x^L(k_0 \cos \alpha)/H_m^{(1)'}(k_0 a \sin \alpha)$ for Regions III and IV. It is seen that the only singularities of the integrand of (5.19) are branch points at $\alpha = n\pi$, $n = 0, \pm 1, \pm 2, \dots$

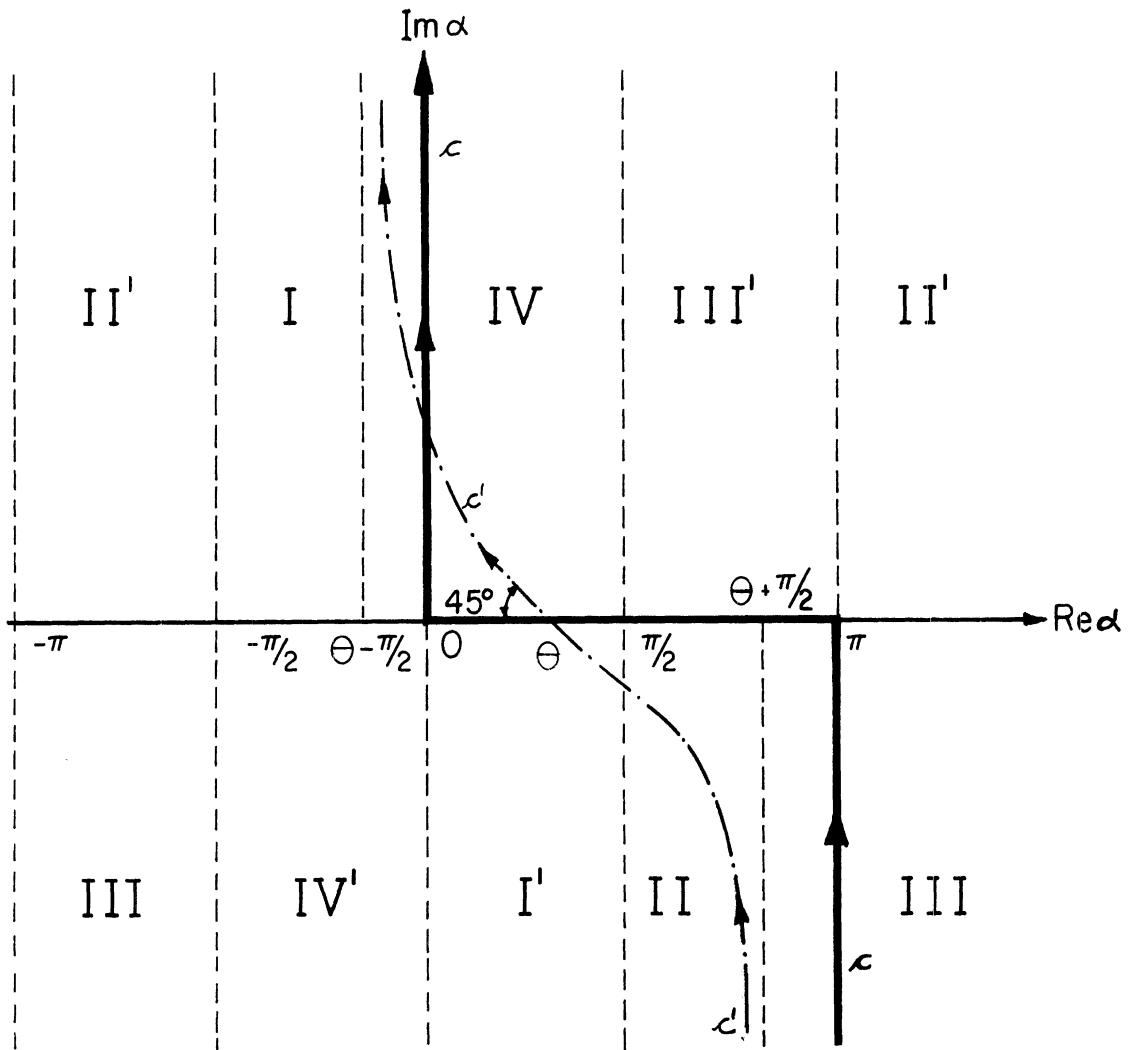


Fig. 5.1: Paths of integration in the α -plane. The regions numbered I, II, III, and IV are the images of the first, second, third and fourth quadrants of the n -plane through $n = k_0 \cos \alpha$, with k_0 real. The primed regions are such that $v_0 = k_0 \sin \alpha$ has negative imaginary part, with $\text{Im } v_0$ positive in the unprimed regions.

Integral (5.19) is in a form convenient for evaluation by the method of steepest descents, for large $k_0 r$, and that will now be carried out. The function $\cos(\alpha - \theta)$ has a stationary point at $\alpha = \theta$, and the path of steepest descents passes through θ and is such that $\cos[\text{Re}(\alpha - \theta)] \cdot \cosh[\text{Im}(\alpha - \theta)] = 1$. This path will be denoted c' , and is also depicted in Fig. 5.1, for a given θ in $(0, \pi)$. The asymptotic expression for (5.19) is thus

$$\mathcal{E}_{\phi_0}(r, \theta) \sim \sqrt{\frac{2}{\pi}} \frac{\omega \mu \exp[i(3-m)/(2)\pi]}{k_0 a} R_{\phi_0}^E(\theta) \frac{e^{ik_0 r}}{k_0 r}, \quad (5.20a)$$

where

$$R_{\phi_0}^E(\theta) = \left(\frac{A}{\cos \theta + 1} + \frac{B}{\cos \theta - \frac{\lambda_{m10}}{k_0}} \right) \frac{J'_m(k_0 a \sin \theta)}{x^U(k_0 \cos \theta)}. \quad (5.20b)$$

Next, attention will be given to the zeroth order version of (5.11b). Similarly, the use of (5.6) and (5.8) in (5.12e) yields

$$\begin{aligned} V_{\theta_0}(\eta, \rho) &= \frac{i m \omega \mu}{k_0 a} \left(\frac{A}{\eta + k_0} + \frac{B}{\eta - \lambda_{m10}} \right) \frac{J'_m(\nu_0 a)}{\nu_0 x^U(\eta)} \frac{H_m^{(1)}(\nu_0 r \sin \theta)}{r \tan \theta} \\ &+ \frac{\omega \mu a}{2 m k_0} \left(\frac{D}{\eta + k_0} + \frac{F}{\eta - \mu_{m10}} \right) \frac{(\eta + k_0) J_m(\nu_0 a)}{y^U(\eta)} \\ &\cdot \left\{ \frac{i \eta}{\nu_0} \cos \theta H_m^{(1)'}(\nu_0 r \sin \theta) - \sin \theta H_m^{(1)}(\nu_0 r \sin \theta) \right\}. \quad (5.21) \end{aligned}$$

Using (5.16), the following is valid for large r :

$$V_{\phi 0}(n, \rho) \sim - \frac{\omega \mu a \exp[-i(2m+1)/(4)\pi]}{\sqrt{2\pi} m k_0} \left(\frac{D}{n + k_0} + \frac{F}{n - \mu_{m10}} \right) \cdot \frac{(\eta + k_0) J_m(\nu_0 a)}{y^U(\eta)} \left(\frac{\eta}{\nu_0} \cos \theta + \sin \theta \right) \frac{e^{i\nu_0 r \sin \theta}}{\sqrt{\nu_0} r \sin \theta} (1 + O(r^{-1})) \quad (5.22)$$

Using (5.18) in (5.22) and (5.11b) gives

$$\mathcal{E}_{\theta 0}(r, \theta) \sim - \frac{\omega \mu a \exp[i(2m+1)/(4)\pi]}{2\pi m k_0 \sqrt{k_0} r \sin \theta} \int_c \left(\frac{D}{\cos \alpha + 1} + \frac{F}{\cos \alpha - \frac{\mu_{m10}}{k_0}} \right) \cdot \frac{(\cos \alpha + 1) J_m(k_0 a \sin \alpha)}{y^U(k_0 \cos \alpha)} \frac{\cos(\alpha - \theta)}{\sqrt{\sin \alpha}} e^{ik_0 r \cos(\alpha - \theta)} d\alpha \quad (5.23)$$

The only singularities of this integrand are branch points at $\alpha = n\pi$, $n = 0, \pm 1, \pm 2, \dots$. The steepest descent evaluation, by integrating along c' , yields

$$\mathcal{E}_{\theta 0}(r, \theta) \sim \frac{\omega \mu a \exp[i(3-m)/(2)\pi]}{\sqrt{2\pi} m k_0} R_{\theta 0}^E(\theta) \frac{e^{ik_0 r}}{k_0 r}, \quad (5.24a)$$

where

$$R_{\theta 0}^E(\theta) = \left(\frac{D}{\cos \theta + 1} + \frac{F}{\cos \theta - \frac{\mu_{m10}}{k_0}} \right) \frac{\cos \theta + 1}{\sin \theta} \frac{J_m(k_0 a \sin \theta)}{y^U(k_0 \cos \theta)} \quad (5.24b)$$

Using (5.6) and (5.8) in (5.12c), the expression obtained for $V_{r0}(\eta, \rho)$ is very similar to (5.21). The only differences are that $(\tan \theta)^{-1}$ does not appear in the first half of the right-hand side of (5.21) and, inside the brackets, $\cos \theta$ is replaced with $\sin \theta$, and $-\sin \theta$ with $\cos \theta$. Then, (5.22) is valid for $V_{r0}(\eta, \rho)$, if $[(\eta/v_0)\cos \theta + \sin \theta]$ is replaced by $[(\eta/v_0)\sin \theta - \cos \theta]$. Thus, in (5.23), the factor $\cos(\alpha - \theta)$, which appears in the integrand multiplying the exponential, must be replaced with $\sin(\theta - \alpha)$. This factor causes the first term of the asymptotic expansion, of $O[(e^{ik_0 r})/(k_0 r)]$ behavior, to vanish. As a consequence,

$$\mathcal{E}_{r0}(r, \theta) = O\left(\frac{e^{ik_0 r}}{(k_0 r)^2}\right) \quad (5.25)$$

as $k_0 r$ increases without bound, and is, therefore, negligible when compared with (5.20a) and (5.24a). This fact was obviously expected for the zeroth order radiation field, which corresponds physically to the case $\epsilon_1 = \epsilon_0$.

The magnetic field components will now be analyzed. Using (5.6) and (5.8) in (5.12b), and using the asymptotic expressions (5.16), it follows that, for large $k_0 r$,

$$\frac{I_{\phi 0}(\eta, \rho)}{\rho} \sim \frac{k_0 a \exp[-i(2m+1)/(4)\pi]}{\sqrt{2\pi m}} \left(\frac{D}{\eta + k_0} + \frac{F}{\eta - \mu_{m10}} \right) \cdot \frac{(\eta + k_0) J_m(v_0 a)}{v_0 y^U(\eta)} \frac{e^{i v_0 r \sin \theta}}{\sqrt{v_0 r \sin \theta}} (1 + O(r^{-1})) \quad (5.26)$$

Following the same procedure that was used for the zeroth order components of the electric field, the following asymptotic expression is obtained

$$\mathcal{H}_{\phi_0}(r, \theta) \sim \frac{a \exp[i(3-m)/(2)\pi]}{\sqrt{2\pi m}} R_{\theta_0}^E(\theta) \frac{e^{ik_0 r}}{k_0 r}, \quad (5.27)$$

where $R_{\theta_0}^E(\theta)$ is given by (5.24b). Comparing (5.24) and (5.27), it follows that, asymptotically for large $k_0 r$,

$$\frac{\mathcal{E}_{\theta_0}(r, \theta)}{\mathcal{H}_{\phi_0}(r, \theta)} \sim \sqrt{\frac{\mu}{\epsilon_0}} \approx 120 \pi \text{ (ohms)}, \quad (5.28)$$

which is an expected result.

In a similar manner, inverse transforming the asymptotic version of (5.12f), it is concluded that

$$\frac{\mathcal{E}_{\phi_0}(r, \theta)}{\mathcal{H}_{\theta_0}(r, \theta)} \sim -\sqrt{\frac{\mu}{\epsilon_0}}, \quad (5.29)$$

as was also expected for large $k_0 r$.

Following the same procedure for (5.12d), it is concluded that (5.25) also holds for $\mathcal{H}_{r_0}(r, \theta)$. Thus, the radial component of the zeroth order magnetic field is negligible in the far zone, when compared with the transverse components, again an expected result.

5.3 First Order Asymptotic Far Field Outside the Dielectric

For $\rho > a$, expressions (5.12) are taken with $\epsilon = \epsilon_0$, $\nu = \nu_0$. The first order terms are simply (5.12) with $\epsilon = \epsilon_0$, $\nu = \nu_0$, and with $I_z(\eta, \rho)$ and $V_z(\eta, \rho)$ replaced with $I_{z1}(\eta, \rho)$ and $V_{z1}(\eta, \rho)$. These first order functions are given in Appendix D and in Section 5.1 (in the lower and the upper half-planes, respectively).

The inverse Fourier transformation of the first order terms will now be carried out, asymptotically for large $k_0 r$, in a manner similar to Section 5.2. Restriction (5.13) will hold in this case as well, and k_0 is supposed to be real and positive.

It must be remarked that, as was concluded in Appendix D and in Section 5.1, the Fourier transforms of the zeroth and first order terms of the components of the fields for $\rho > a$ have no poles in the complex η -plane, their only singularities being branch points for $\eta = \pm k_0$. This property is not changed by the change of variable (5.18), and is thus extended to the α -plane. Hence, no poles are ever captured when the path of integration c (Fig.5.1) is deformed into the path of steepest descents, c' .

Expressions (5.7) or (D.1b) will be used for $V_{z1}(\eta, \rho)$, and expressions (D.1d) and (D.3) for $I_{z1}(\eta, \rho)$. It is seen that the ρ -variation of either of these functions is given by a factor $H_m^{(1)}(\nu_0 \rho)$, similarly to what happens with the zeroth order functions.

Using (2.4), (5.12a), (5.16) and (5.18), it follows that

$$\mathcal{E}_{\phi_1}(r, \theta) \sim \frac{\omega\mu}{\pi k_0} \frac{\exp[i(3-2m)/(4)\pi]}{\sqrt{k_0 r \sin \theta}} \int_c \left[\frac{I_{Z_1}(\eta, a^+)}{H_m^{(1)}(\nu_0 a)} \right]_{\substack{\eta=k_0 \cos \alpha \\ \nu_0=k_0 \sin \alpha}} \cdot \frac{e^{ik_0 r \cos(\alpha-\theta)}}{\sqrt{\sin \alpha}} d\alpha, \quad (5.30)$$

where $I_{Z_1}(\eta, a^+)$ is given by (D.3).

A steepest descent evaluation, along the path c' of Fig. 5.1, yields

$$\mathcal{E}_{\phi_1}(r, \theta) \sim \sqrt{\frac{2}{\pi}} \frac{\omega\mu}{k_0} \exp[i(3-m)/(2)\pi] R_{\phi_1}^E(\theta) \frac{e^{ik_0 r}}{k_0 r}, \quad (5.31a)$$

where

$$R_{\phi_1}^E(\theta) = \frac{1}{\sin \theta} \left[\frac{I_{Z_1}(\eta, a^+)}{H_m^{(1)}(\nu_0 a)} \right]_{\substack{\eta=k_0 \cos \theta \\ \nu_0=k_0 \sin \theta}}. \quad (5.31b)$$

Similarly, from (5.11b), (5.12e), (5.16), (5.18) and a steepest descent evaluation, it follows that

$$\mathcal{E}_{\theta_1}(r, \theta) \sim \sqrt{\frac{2}{\pi}} \exp[i(3-m)/(2)\pi] R_{\theta_1}^E(\theta) \frac{e^{ik_0 r}}{k_0 r}, \quad (5.32a)$$

where

$$R_{\theta_1}^E(\theta) = \frac{1}{\sin \theta} \left[\frac{V_{z_1}^L(n)}{H_m^{(1)}(\nu_0 a)} \right]_{\substack{\eta = k_0 \cos \theta \\ \nu_0 = k_0 \sin \theta}}, \quad (5.32b)$$

and $V_{z_1}^L(n)$ is given by (3.36d), i.e.,

$$\frac{V_{z_1}^L(n)}{H_m^{(1)}(\nu_0 a)} = \left\{ \frac{V_{z_1}^L(-k_0)}{y^L(-k_0)} - \frac{\pi}{2\omega\epsilon_0} (n + k_0) S_1^L(n) \right\} \frac{J_m(\nu_0 a)}{y^U(n)} \quad (5.33)$$

with $S_1^L(n)$ as in (B.37).

Conclusion (5.25) is easily reached concerning $\mathcal{E}_{r_1}(r, \theta)$, so that this component is negligible in the far field, when compared with (5.31a) and (5.32a).

Using the same procedure for the first order terms of the components of the magnetic field, the following conclusions are reached:

$$\frac{\mathcal{E}_{\theta_1}(r, \theta)}{\mathcal{H}_{\phi_1}(r, \theta)} \sim \sqrt{\frac{\mu}{\epsilon_0}}, \quad (5.34)$$

$$\frac{\mathcal{E}_{\phi_1}(r, \theta)}{\mathcal{H}_{\theta_1}(r, \theta)} \sim -\sqrt{\frac{\mu}{\epsilon_0}}, \quad (5.35)$$

and $\mathcal{H}_{r_1}(r, \theta)$ behaves as (5.25), hence it is negligible in the far field.

CHAPTER VI. COMMENTS AND CONCLUSIONS

The problem introduced in Section 1.2 has been discussed. The method of Wiener-Hopf was used and, upon its failure for the general case, the problem was reformulated for a dielectric rod with relative permittivity slightly greater than unity. A perturbation analysis was used, and the zeroth-order (unperturbed) and first-order problems were treated. Each one of these was solved by the Wiener-Hopf method. The zeroth and first order terms were found for the surface current density, the reflection and conversion coefficients inside the metallic guide, and the off-axis far electromagnetic field.

As was mentioned in Chapter V, the perturbation approach undertaken does not bring out explicitly any of the dielectric-rod modes which are known to be excited by the incident fields. The HE_{11} surface wave mode is the most important constituent of the near-field of a dielectric-rod antenna. In fact, a cross-section of the field distribution of that mode shows that this field extends much beyond the radius of the rod, forming a large equivalent aperture to account for the forward lobe. The field outside the dielectric decreases exponentially in the radial direction, without changing its phase, when the HE_{11} mode is the only contribution to it. Near the junction with the metallic waveguide, however, the field along the dielectric rod is not well described by the HE_{11} mode, and the contribution from the space wave ([5], Chapter III) is a major part of the total field.

For progressively greater distances from the junction, along the rod, the HE_{11} mode will become the major part of the field. Only then does the cross-section field distribution constitute an enlarged equiphase aperture, smoothly tapered off at the edges, which will produce a strong forward lobe and ideally no sidelobes. The least distance from the junction at which this occurs, will represent the smallest desirable length for a dielectric rod antenna. The optimum length for the antenna will be determined by studying the phase differences of the surface wave and the space wave along the rod. A reinforcing interference of these two contributions is desirable (see [5]). Therefore, a study of the relative magnitudes of the field constituents along the rod is of great importance for the design of practical antennas. It was left out in this work because the perturbation approach undertaken did not bring out explicitly the modal contribution. Hence, further work in that direction will be necessary.

APPENDIX A. FACTORIZATION OF $x(\eta)$ AND $y(\eta)$

The factorizations (3.13) are to be performed to the functions (2.50) and (2.51). This has been done, for instance, by Weinstein [16], Sections 22 and 26, and the results will be summarized here.

For the function

$$y(\eta) = J_m(\nu_0 a) H_m^{(1)}(\nu_0 a) , \quad (\text{A.1})$$

the factorization $y(\eta) = y^L(\eta) \cdot y^U(\eta)$ is given by

$$y^L(\eta) = [J_m(\nu_0 a) H_m^{(1)}(\nu_0 a)]^{1/2} e^{-(1/2)\psi_m(\eta)} \quad (\text{A.2a})$$

and

$$y^U(\eta) = [J_m(\nu_0 a) H_m^{(1)}(\nu_0 a)]^{1/2} e^{(1/2)\psi_m(\eta)} , \quad (\text{A.2b})$$

where

$$\psi_m(\eta) = -\frac{2\eta}{\pi} \sum_{n=1}^{\infty} \int_{\mu_{m(n-1)}}^{\mu_{mn}} \frac{\Lambda_m(\xi)}{\xi^2 - \eta^2} d\xi . \quad (\text{A.3})$$

In (A.3), $\mu_{mn} = \sqrt{k_0^2 - (p_{mn}/a)^2}$, $n = 1, 2, 3, \dots$, and $\mu_{m0} = k_0$.

The integration is carried out along the branch cut, which is the

line $\text{Im} \sqrt{k_0^2 - \xi^2} = 0$, and the function $\Lambda_m(\xi)$ is given by

$$\Lambda_m(\xi) = \arctan \left[-\frac{J_m(\tau_0 a)}{Y_m(\tau_0 a)} \right], \quad 0 \leq \Lambda_m(\xi) < \pi, \quad (\text{A.4})$$

with $\tau_0 = \sqrt{k_0^2 - \xi^2}$. $\Lambda_m(\xi)$ is continuous for every arc $(\mu_{m(n-1)}, \mu_n)$, increasing there from zero to π , and has a discontinuity of $-\pi$ at every point μ_{mn} , $n = 1, 2, 3, \dots$

In a similar fashion, the function

$$x(\eta) = J_m'(v_0 a) H_m^{(1)'}(v_0 a) \quad (\text{A.5})$$

has the factorization

$$x^L(\eta) = [J_m'(v_0 a) H_m^{(1)'}(v_0 a)]^{1/2} e^{-(1/2)\chi_m(\eta)} \quad (\text{A.6a})$$

and

$$x^U(\eta) = [J_m'(v_0 a) H_m^{(1)'}(v_0 a)]^{1/2} e^{(1/2)\chi_m(\eta)}, \quad (\text{A.6b})$$

where

$$\chi_m(\eta) = -\frac{2\eta}{\pi} \sum_{n=1}^{\infty} \int_{\lambda_{m(n-1)}}^{\lambda_{mn}} \frac{\Omega_m(\xi)}{\xi^2 - \eta^2} d\xi. \quad (\text{A.7})$$

In (A.7), $\lambda_{mn} = \sqrt{k_0^2 - (q_{mn}/a)^2}$, $n = 1, 2, 3, \dots$, and $\lambda_{m0} = k_0$.

The integration is carried out along the same line, $\text{Im } \tau_0 = 0$, and

$$\Omega_m(\xi) = \arctan \left[-\frac{J'_m(\tau_0 a)}{Y'_m(\tau_0 a)} \right], \quad 0 \leq \Omega_m(\xi) < \pi \quad . \quad (\text{A.8})$$

$\Omega_m(\xi)$ has a discontinuity of $-\pi$ at every point λ_{mn} , $n = 1, 2, 3, \dots$, and is continuous otherwise, increasing from zero to π when ξ goes from $\lambda_{m(n-1)}$ to λ_{mn} , $n = 2, 3, \dots$. At $\xi = k_0$, $\Omega_m(\xi)$ is π , then it decreases, has a relative minimum, and increases back to π for $\xi = \lambda_{m1}$.

Both $y^L(\eta)$ and $x^L(\eta)$ have a branch point for $\eta = k_0$, and both $y^U(\eta)$ and $x^U(\eta)$ have a branch point for $\eta = -k_0$. The following properties hold:

$$y^L(\eta) = y^U(-\eta) \quad (\text{A.9a})$$

and

$$x^L(\eta) = x^U(-\eta) \quad . \quad (\text{A.9b})$$

As $|\eta| \rightarrow \infty$, away from the negative sides of the respective hyperbolic branch cuts (as in Fig. 2.1), the four split functions (A.2) and (A.6) have $O(\eta^{-1/2})$ behavior.

APPENDIX B. ADDITIVE DECOMPOSITION OF $R_1(\eta)$ AND $S_1(\eta)$

Expressions (3.39) must be split according to (3.35). Some of the terms in (3.39) are split by simple extraction of a pole. Namely,

$$R_C(\eta) = C \frac{x^U(\eta)}{(\eta - \lambda_{m10})^2} = R_C^U(\eta) + R_C^L(\eta) \quad , \quad (B.1a)$$

where

$$R_C^U(\eta) = C \frac{x^U(\eta) - x^U(\lambda_{m10}) - (\eta - \lambda_{m10})x^{U'}(\lambda_{m10})}{(\eta - \lambda_{m10})^2} \quad (B.1b)$$

is analytic in the upper half-plane $\text{Im } \eta > -\text{Im } k_0$, because the pole at λ_{m10} has been cancelled, and where

$$R_C^L(\eta) = C \frac{x^U(\lambda_{m10}) + (\eta - \lambda_{m10})x^{U'}(\lambda_{m10})}{(\eta - \lambda_{m10})^2} \quad (B.1c)$$

is analytic in the lower half-plane $\text{Im } \eta < \text{Im } k_0$.

Hence, it is only necessary to split the function

$$R_1^*(\eta) = R_1(\eta) - R_C(\eta) = R_1^{*U}(\eta) + R_1^{*L}(\eta) \quad , \quad (B.2a)$$

for then

$$R_1^U(\eta) = R_1^{*U}(\eta) + R_C^U(\eta) \text{ and } R_1^L(\eta) = R_1^{*L}(\eta) + R_C^L(\eta) \quad . \quad (B.2b)$$

In a similar manner,

$$S_G(n) = G \frac{n(n + \lambda_{m10})y^U(n)}{(n - \lambda_{m10})(n + k_0)} = S_G^U(n) + S_G^L(n) \quad , \quad (B.3a)$$

where

$$S_G^U(n) = Gn \frac{(n + \lambda_{m10})y^U(n)}{(n + k_0)(n - \lambda_{m10})} - G \frac{2\lambda_{m10}^2 y^U(\lambda_{m10})}{k_0 + \lambda_{m10}} \frac{1}{n - \lambda_{m10}} \quad (B.3b)$$

and

$$S_G^L(n) = G \frac{2\lambda_{m10}^2 y^U(\lambda_{m10})}{k_0 + \lambda_{m10}} \frac{1}{n - \lambda_{m10}} \quad . \quad (B.3c)$$

Also,

$$S_L(n) = L \frac{(n - k_0)y^U(n)}{n - \mu_{m10}} = S_L^U(n) + S_L^L(n) \quad , \quad (B.4a)$$

where

$$S_L^U(n) = L \frac{(n - k_0)y^U(n) - (\mu_{m10} - k_0)y^U(\mu_{m10})}{n - \mu_{m10}} \quad (B.4b)$$

and

$$S_L^L(n) = L \frac{(\mu_{m10} - k_0)y^U(\mu_{m10})}{n - \mu_{m10}} \quad . \quad (B.4c)$$

Finally,

$$S_T(n) = T \frac{(n - k_0)y^U(n)}{(n - \mu_{m10})^2} = S_T^U(n) + S_T^L(n) , \quad (B.5a)$$

where

$$S_T^U(n) = T \frac{(n - k_0)y^U(n) - (\mu_{m10} - k_0)y^U(\mu_{m10}) - (n - \mu_{m10}) \cdot [y^U(\mu_{m10}) + (\mu_{m10} - k_0)y^{U'}(\mu_{m10})]}{(n - \mu_{m10})^2} \quad (B.5b)$$

and

$$S_T^L(n) = T \frac{(\mu_{m10} - k_0)y^U(\mu_{m10}) + (n - \mu_{m10}) \cdot [y^U(\mu_{m10}) + (\mu_{m10} - k_0)y^{U'}(\mu_{m10})]}{(n - \mu_{m10})^2} . \quad (B.5c)$$

Hence, all that is left is splitting the function

$$S_1^*(n) = S_1(n) - S_G(n) - S_L(n) - S_T(n) = S_1^{*U}(n) + S_1^{*L}(n) , \quad (B.6a)$$

and then

$$S_1^U(n) = S_1^{*U}(n) + S_G^U(n) + S_L^U(n) + S_T^U(n) \quad (B.6b)$$

and

$$S_1^L(n) = S_1^{*L}(n) + S_G^L(n) + S_L^L(n) + S_T^L(n) . \quad (B.6c)$$

Clearly, both $R_1^*(\eta)$ and $S_1^*(\eta)$ are analytic in the strip

$$-\text{Im } k_0 < \text{Im } \eta < \text{Im } k_0 \quad , \quad (\text{B.7})$$

and it is relatively easy to show that they both vanish at infinity within that strip. Then, the following decomposition expressions are valid (see, for example, Noble [8], Section 1.3, Theorem B)

$$R_1^{*U}(\eta) = \frac{1}{2\pi i} \int_{\gamma_1} \frac{R^*(\xi)}{\xi - \eta} d\xi \quad , \quad \text{for any } \eta \text{ above } \gamma_1 \quad , \quad (\text{B.8a})$$

$$R_1^{*L}(\eta) = \frac{1}{2\pi i} \int_{\gamma_2} \frac{R^*(\xi)}{\xi - \eta} d\xi \quad , \quad \text{for any } \eta \text{ below } \gamma_2 \quad , \quad (\text{B.8b})$$

and similarly for $S_1^{*U}(\eta)$ and $S_1^{*L}(\eta)$, with $S^*(\eta)$ replacing $R^*(\xi)$.

Figure B.1 shows the paths of integration γ_1 and γ_2 .

It is necessary to analyze the singularities of $R_1^*(\xi)$ and $S_1^*(\xi)$ in both the upper and lower half-planes. Either of these two functions has branch points at $\xi = k_0$ and $\xi = -k_0$, and the branch cuts will be taken to be the dashed lines of Fig. B.1. Note that, here and in the future, when ξ is taken as the variable instead of η , $v_0 = (k_0^2 - \eta^2)^{1/2}$ is replaced by $\tau_0 = (k_0^2 - \xi^2)^{1/2}$.

By starting with ξ on the positive side of one of the branch cuts, describing a curve in the ξ plane around the respective branch point, and returning to the initial point ξ , but this time on the negative side of the branch cut, τ_0 will have the initial value

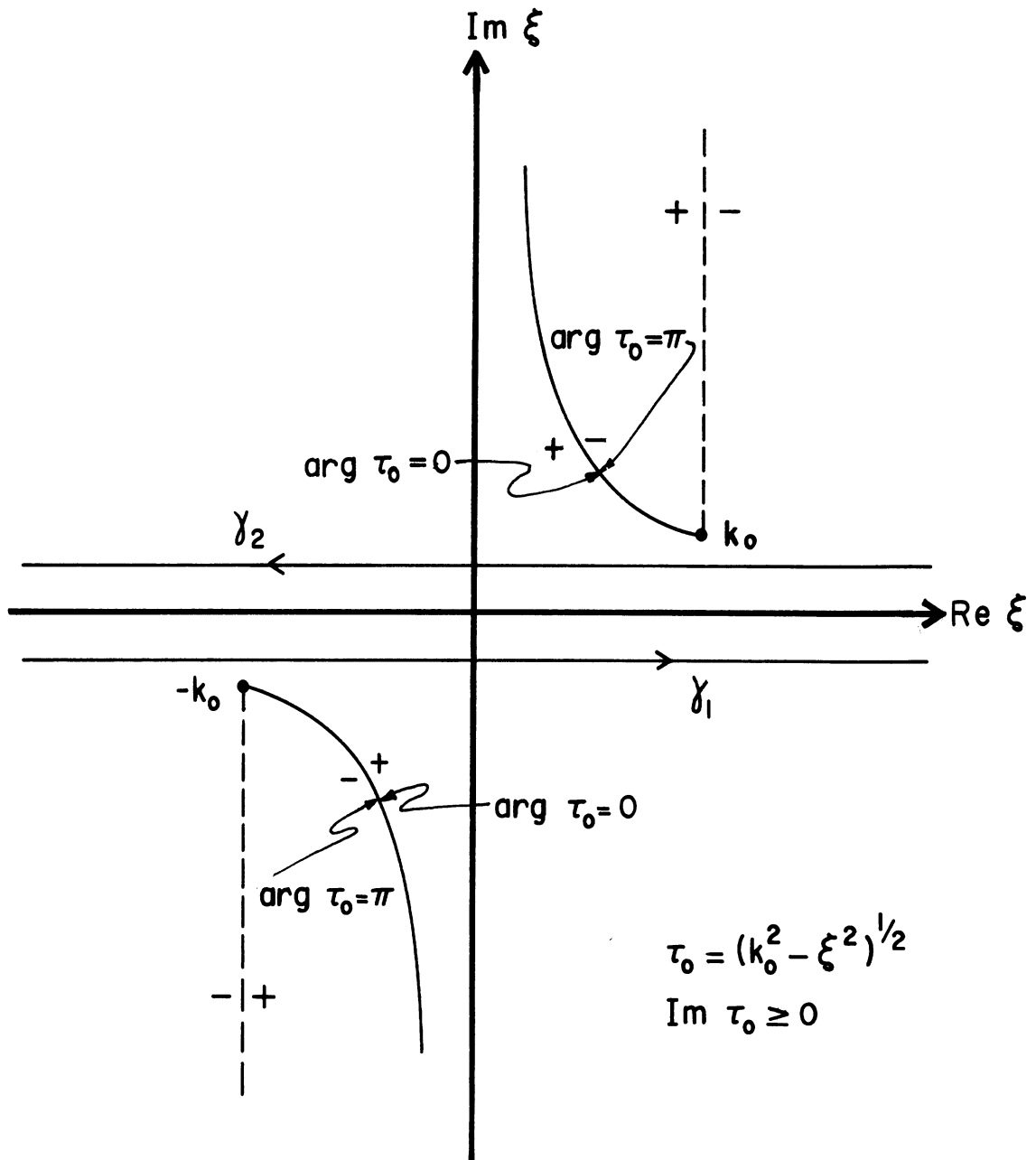


Fig. B.1: Branch cuts and paths of integration for the additive decomposition of $R_1(\eta)$ and $S_1(\eta)$. The dashed lines represent alternative branch cuts, which are used in Appendix B.

multiplied by $e^{i\pi}$. By using subscripts + and -, this can be represented by

$$\tau_{0-} = \tau_{0+} e^{i\pi} , \quad (\text{B.9})$$

where it is understood that both τ_{0-} and τ_{0+} are evaluated at the same value of ξ on the branch cut. The Bessel and Hankel functions will also have a discontinuity across the branch cuts (see Watson [29], Section 3.62), as follows:

$$J_m(\tau_{0-}a) = (-1)^m J_m(\tau_{0+}a) , \quad (\text{B.10a})$$

$$J'_m(\tau_{0-}a) = (-1)^{m+1} J'_m(\tau_{0+}a) , \quad (\text{B.10b})$$

$$H_m^{(1)}(\tau_{0-}a) = (-1)^{m+1} H_m^{(2)}(\tau_{0+}a) , \quad (\text{B.10c})$$

and

$$H_m^{(1)'}(\tau_{0-}a) = (-1)^m H_m^{(2)'}(\tau_{0+}a) . \quad (\text{B.10d})$$

Using (B.9) and (B.10), $f_1(\xi)$ and $f_2(\xi)$, given by (3.40), are seen to have the following discontinuities, for ξ on the branch cuts,

$$f_{1+}(\xi) - f_{1-}(\xi) = -2g(\xi) , \quad (\text{B.11a})$$

$$f_{2+}(\xi) - f_{2-}(\xi) = i\pi a \left[g(\xi) - \frac{2}{k_0^2 a} \tau_{0+} J_m(\tau_{0+}a) J'_m(\tau_{0+}a) \right] , \quad (\text{B.11b})$$

where the subscripts + and - were used to specify the two sides of the branch cuts, and where $g(\xi)$ is defined as

$$g(\xi) = \frac{\tau_0^2 a^2 - m^2}{\tau_0^2 a^2} \left[J_m(\tau_0 a) \right]^2 + \frac{2}{\tau_0 a} J_m(\tau_0 a) J'_m(\tau_0 a) + [J'_m(\tau_0 a)]^2 . \quad (B.12)$$

It should be noted that $g(\xi)$ has no branch points, neither does the right-hand side of (B.11b).

Equations (3.39) are written in the strip of analyticity (3.12) and, in that strip, according to Appendix A, it is true that

$$x^U(\xi) = \frac{J'_m(\tau_0 a) H_m^{(1)'}(\tau_0 a)}{x^L(\xi)} , \quad (B.13a)$$

$$y^U(\xi) = \frac{J_m(\tau_0 a) H_m^{(1)}(\tau_0 a)}{y^L(\xi)} , \quad (B.13b)$$

and similarly for $x^L(\xi)$ and $y^L(\xi)$ written in terms of $x^U(\xi)$ and $y^U(\xi)$. When $R_1^*(\xi)$ and $S_1^*(\xi)$ are considered outside of the strip (3.12), (B.13) must be used for analytic continuation into the lower half-plane, and similarly $x^L(\xi)$ and $y^L(\xi)$ must be written in terms of $x^U(\xi)$ and $y^U(\xi)$ for analytic continuation into the upper half-plane.

Keeping that in mind, the discontinuity of $R_1^*(\xi)$ across the branch cut is, in the upper half-plane,

$$R_{1+}^*(\xi) - R_{1-}^*(\xi) = -2 \left(\frac{A}{\xi + k_0} + \frac{B}{\xi - \lambda_{m10}} \right) g(\xi) + \left(2 \frac{D}{\xi + k_0} + \frac{F}{\xi - \mu_{m10}} \right) \frac{\xi x^U(\xi)}{(\xi - k_0) y^U(\xi)} \frac{[J_m(\tau_0 a)]^3}{\tau_0 J'_m(\tau_0 a)}, \quad (\text{B.14a})$$

and, for ξ on the lower half-plane branch cut,

$$R_{1+}^*(\xi) - R_{1-}^*(\xi) = -2 \left(\frac{A}{\xi + k_0} + \frac{B}{\xi - \lambda_{m10}} \right) g(\xi) + 2 \left(\frac{D}{\xi + k_0} + \frac{F}{\xi - \mu_{m10}} \right) \frac{\xi y^L(\xi)}{(\xi - k_0) x^L(\xi)} \frac{J_m(\tau_0 a) J'_m(\tau_0 a)}{\tau_0}. \quad (\text{B.14b})$$

Similarly, for $S_1^*(\xi)$ across the upper half-plane branch cut,

$$S_{1+}^*(\xi) - S_{1-}^*(\xi) = - \frac{ik_0^2 a^3}{m} \left(\frac{D}{\xi + k_0} + \frac{F}{\xi - \mu_{m10}} \right) \cdot \left[g(\xi) - \frac{2\tau_0}{k_0^2 a} J_m(\tau_0 a) J'_m(\tau_0 a) \right] + \frac{4m}{ia} \left(\frac{A}{\xi + k_0} + \frac{B}{\xi - \lambda_{m10}} \right) \frac{\xi y^U(\xi)}{(\xi + k_0) x^U(\xi)} \frac{J_m(\tau_0 a) J'_m(\tau_0 a)}{\tau_0} \quad (\text{B.14c})$$

and, for the lower half-plane branch cut,

$$S_{1+}^*(\xi) - S_{1-}^*(\xi) = - \frac{ik_0^2 a^3}{m} \left(\frac{D}{\xi + k_0} + \frac{F}{\xi - \mu_{m10}} \right) \cdot \left[g(\xi) - \frac{2\tau_0}{k_0^2 a} J_m(\tau_0 a) J'_m(\tau_0 a) \right] + \frac{4m}{ia} \left(\frac{A}{\xi + k_0} + \frac{B}{\xi - \lambda_{m10}} \right) \frac{\xi x^L(\xi)}{(\xi + k_0) y^L(\xi)} \frac{[J_m(\tau_0 a)]^3}{\tau_0 J'_m(\tau_0 a)}. \quad (\text{B.14d})$$

None of the right-hand sides of equations (B.14) has branch points in the respective half-planes, so that it does not make any difference whether τ_0 is taken to be τ_{0+} or τ_{0-} .

In addition to having branch points at $\xi = \pm k_0$, $R_1^*(\xi)$ and $S_1^*(\xi)$ also have poles outside the strip of analyticity, and it will be seen that they all fall on the branches of hyperbola shown in Fig. B.1. $R_1^*(\xi)$ has simple poles for $\xi = \pm \lambda_{mn} = \pm \sqrt{k_0^2 - (q_{mn}/a)^2}$, except for $\xi = \lambda_{m1} = \lambda_{m10}$, where it has a double pole. $S_1^*(\xi)$ has simple poles for $\xi = \pm \mu_{mn} = \pm \sqrt{k_0^2 - (p_{mn}/a)^2}$ and for $\xi = -\lambda_{mn}$, except for $\xi = \mu_{m1} = \mu_{m10}$, where it has a double pole; it also has a simple pole for $\xi = \lambda_{m10}$.

In order to carry out integrations (B.8), the paths of integration γ_1 and γ_2 will be deformed into the paths γ_1' and γ_2' , respectively, as depicted in Fig. B.2. These paths have clearly distinct parts: the integration along γ_1' can be separated into a sum of residue contributions from the poles, computed on the positive side of the hyperbolic branch cut, plus an integration around $-k_0$ along a circle of vanishing radius, plus an integration along the branch cut, from $-k_0$ to $-i\infty$, of the discontinuity of the integrand across that branch cut. The separation of γ_2' into different parts is analogous to the separation of γ_1' .

It must be noted that these deformations of γ_1 and γ_2 are valid because both $R_1^*(\xi)$ and $S_1^*(\xi)$ vanish as $\xi \rightarrow \infty$, away from the negative sides of the hyperbolic branch cuts of Fig. B.1. In fact, using the asymptotic expansions for Bessel and Hankel functions,

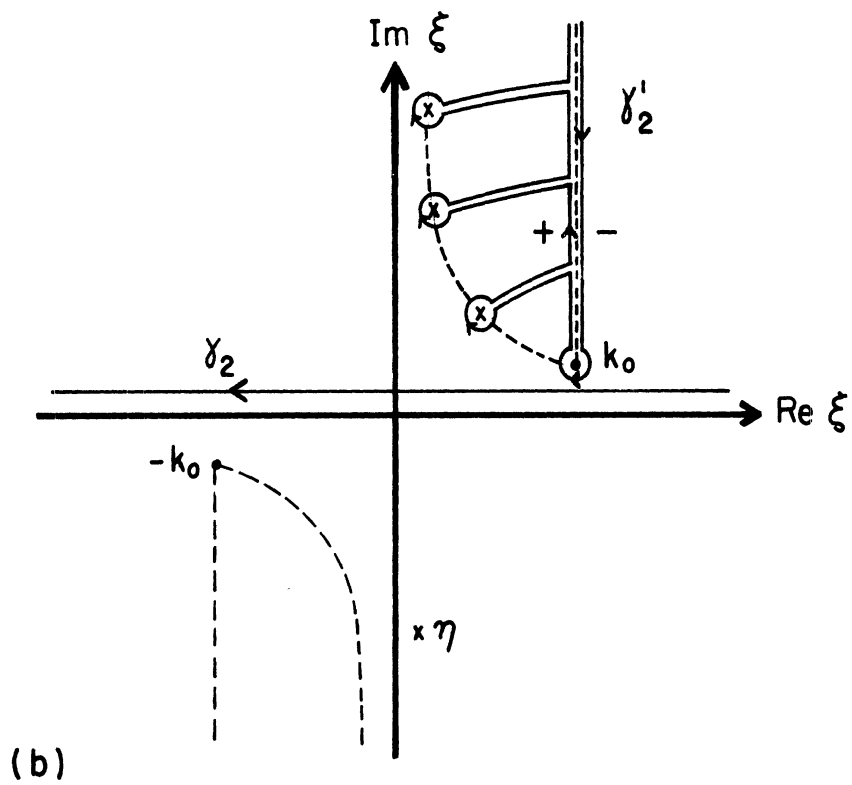
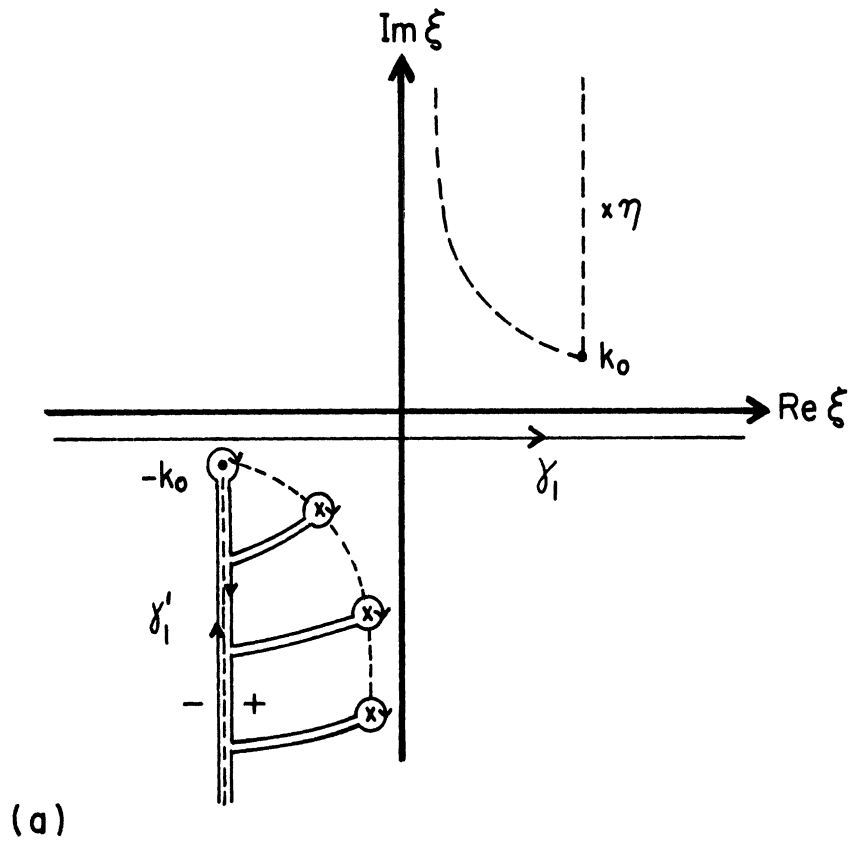


Fig. B.2: Deformation of the paths of integration γ_1 and γ_2 into γ'_1 and γ'_2 , respectively, showing the capture of the residues of the poles on the branches of the hyperbola.

given by Watson [29], Section 7.2, it follows that, as $\xi \rightarrow \infty$, $f_1(\xi) = O(\xi^{-2})$ and $f_2(\xi) = O(\xi^0)$, whence $R_1^*(\xi) = O(\xi^{-3})$ and $S_1^*(\xi) = O(\xi^{-1})$. As a consequence, the integrations (B.8) along the quarter-circles at infinity in each of the quadrants of the ξ -plane are zero.

Considering the parts of γ_1' and γ_2' which are the integrations along the branch cuts, it is seen that, for $R_1^U(\eta)$ and $S_1^U(\eta)$, the integrations will be from $\xi = -k_0$ to $\xi = -i\infty$, and the integrands will be (B.14b) and (B.14d), respectively, divided by $(\xi - \eta)$. For $R_1^L(\eta)$ and $S_1^L(\eta)$, the integrations will be from $\xi = k_0$ to $\xi = i\infty$, and the integrands will be (B.14a) and (B.14c), respectively, divided by $(\xi - \eta)$.

Using the asymptotic expansions for Bessel functions of large argument, it is concluded that, as $\xi \rightarrow \pm i\infty$,

$$g(\xi) = \pm \frac{2i}{\pi a \xi} + O(\xi^{-2}) \quad , \quad (B.15)$$

and that each separate term on the right-hand sides of (B.14) goes to zero at least as fast as ξ^{-1} , hence ensuring the convergence of the integrals, as long as the behavior of the integrands at $\pm k_0$ is appropriate. To verify that that is the case, use must be made of the expansion of Bessel functions in ascending powers of the argument, (as given by Watson [29], Section 3.1), because $\tau_0 a \rightarrow 0$ as $\xi \rightarrow \pm k_0$. It is concluded that, as $\tau_0 a \rightarrow 0$,

$$g(\xi) = \frac{2m}{4^m(m!)^2} (\tau_0 a)^{2m-2} + o(\tau_0^{2m}) \quad , \quad (B.16a)$$

$$J_m(\tau_0 a) J'_m(\tau_0 a) = \frac{m}{4^m(m!)^2} (\tau_0 a)^{2m-1} + o(\tau_0^{2m+1}) \quad (B.16b)$$

and

$$\frac{[J_m(\tau_0 a)]^3}{J'_m(\tau_0 a)} = \frac{1}{m4^m(m!)^2} (\tau_0 a)^{2m+1} + o(\tau_0^{2m+3}) \quad . \quad (B.16c)$$

Since $m \geq 1$, it is seen that, as $\xi \rightarrow k_0$, each one of the terms on the right-hand sides of (B.14a) and (B.14c) either vanishes or remains finite. The same can be stated about (B.14b) and (B.14d), as $\xi \rightarrow -k_0$, but with the following exceptions: when $m = 1$, the terms corresponding to the constants A and D in (B.14b) go to infinity as $\xi \rightarrow -k_0$, but the problem is overcome if they are considered together, because the leading terms cancel each other, and all that is left is a zero limit value. Also for $m = 1$, the terms corresponding to the constants D and A in (B.14d) go to infinity as $\xi \rightarrow -k_0$, but again they must be taken together, cancelling the singularities, and leaving a zero limit value.

Using (B.14b) in (B.8a), and considering only the branch cut integration, the contribution to $R_1^{*U}(\eta)$ is

$$\frac{2x^U(k_0)}{\pi a} A u_1(\eta) - \frac{B}{\pi i} u_2(\eta) + \frac{F}{\pi i} u_3(\eta) \quad , \quad (B.17a)$$

where

$$u_1(\eta) = \int_{-k_0}^{-i\infty} \left[\frac{ia}{2x^U(k_0)} \frac{g(\xi)}{\xi + k_0} + \frac{2i}{y^U(k_0)} \frac{y^L(\xi)}{x^L(\xi)} \frac{\xi}{\tau_0^3} J_m(\tau_0 a) J'_m(\tau_0 a) \right] \cdot \frac{d\xi}{\xi - \eta} , \quad (B.17b)$$

$$u_2(\eta) = \int_{-k_0}^{-i\infty} \frac{g(\xi)}{\xi - \lambda_{m10}} \frac{d\xi}{\xi - \eta} \quad (B.17c)$$

and

$$u_3(\eta) = \int_{-k_0}^{-i\infty} \frac{y^L(\xi)}{x^L(\xi)} \frac{\xi J_m(\tau_0 a) J'_m(\tau_0 a)}{\tau_0 (\xi - k_0) (\xi - \mu_{m10})} \frac{d\xi}{\xi - \eta} . \quad (B.17d)$$

Similarly, from (B.14d) and (B.8a), the contribution to $S_1^{*U}(\eta)$ of the branch cut integrations is

$$- \frac{4ik_0}{m} x^U(k_0) Au_4(\eta) + \frac{4m}{ia} Bu_5(\eta) - \frac{ik_0^2 a^3}{m} Fu_6(\eta) , \quad (B.18a)$$

where

$$u_4(\eta) = \int_{-k_0}^{-i\infty} \left\{ \frac{k_0 a^2}{y^U(k_0)} \frac{g(\xi) - \frac{2\tau_0}{k_0 a} J_m(\tau_0 a) J'_m(\tau_0 a)}{\xi + k_0} + \frac{m^2}{k_0 a x^U(k_0)} \cdot \frac{x^L(\xi)}{y^L(\xi)} \frac{\xi}{\tau_0 (\xi + k_0)^2} \frac{[J_m(\tau_0 a)]^3}{J'_m(\tau_0 a)} \right\} \frac{d\xi}{\xi - \eta} , \quad (B.18b)$$

$$u_5(\eta) = \int_{-k_0}^{-i\infty} \frac{x^L(\xi)}{y^L(\xi)} \frac{\xi [J_m(\tau_0 a)]^3}{J_m'(\tau_0 a) \tau_0 (\xi + k_0) (\xi - \lambda_{m10})} \frac{d\xi}{\xi - \eta} \quad (\text{B.18c})$$

and

$$u_6(\eta) = \int_{-k_0}^{-i\infty} \frac{g(\xi) - \frac{2\tau_0}{k_0^2 a} J_m(\tau_0 a) J_m'(\tau_0 a)}{\xi - \mu_{m10}} \frac{d\xi}{\xi - \eta} \quad (\text{B.18d})$$

Using (B.14a) in (B.8b), the contribution of the branch cut integration to $R_1^{*L}(\eta)$ is

$$-2Av_1(\eta) - 2Bv_2(\eta) - 2Dv_3(\eta) + 2Fv_4(\eta) \quad , \quad (\text{B.19a})$$

where

$$v_1(\eta) = \int_{k_0}^{i\infty} \frac{g(\xi)}{\xi + k_0} \frac{d\xi}{\xi - \eta} \quad , \quad v_2(\eta) = \int_{k_0}^{i\infty} \frac{g(\xi)}{\xi - \lambda_{m10}} \frac{d\xi}{\xi - \eta} \quad , \quad (\text{B.19b})$$

$$v_3(\eta) = \int_{k_0}^{i\infty} \frac{x^U(\xi)}{y^U(\xi)} \frac{\xi [J_m(\tau_0 a)]^3}{\tau_0^3 J_m'(\tau_0 a)} \frac{d\xi}{\xi - \eta} \quad (\text{B.19c})$$

and

$$v_4(\eta) = \int_{k_0}^{i\infty} \frac{x^U(\xi)}{y^U(\xi)} \frac{\xi [J_m(\tau_0 a)]^3}{\tau_0 (\xi - k_0) (\xi - \mu_{m10}) J_m'(\tau_0 a)} \frac{d\xi}{\xi - \eta} \quad (\text{B.19d})$$

Finally, from (B.14c) and (B.8b), the contribution to $S_1^{*L}(\eta)$ of the branch cut integration is

$$-\frac{ik_0^2 a^3}{m} Dv_5(\eta) - \frac{ik_0^2 a^3}{m} Fv_6(\eta) + \frac{4m}{ia} Av_7(\eta) + \frac{4m}{ia} Bv_8(\eta) \quad , \quad (B.20a)$$

where

$$v_5(\eta) = \int_{k_0}^{i\infty} \frac{g(\xi) - \frac{2\tau_0}{k_0^2 a} J_m(\tau_0 a) J'_m(\tau_0 a)}{\xi + k_0} \frac{d\xi}{\xi - \eta} \quad , \quad (B.20b)$$

$$v_6(\eta) = \int_{k_0}^{i\infty} \frac{g(\xi) - \frac{2\tau_0}{k_0^2 a} J_m(\tau_0 a) J'_m(\tau_0 a)}{\xi - \mu_{m10}} \frac{d\xi}{\xi - \eta} \quad , \quad (B.20c)$$

$$v_7(\eta) = \int_{k_0}^{i\infty} \frac{y U(\xi)}{x U(\xi)} \frac{\xi J_m(\tau_0 a) J'_m(\tau_0 a)}{\tau_0 (\xi + k_0)^2} \frac{d\xi}{\xi - \eta} \quad (B.20d)$$

and

$$v_8(\eta) = \int_{k_0}^{i\infty} \frac{y U(\xi)}{x U(\xi)} \frac{\xi J_m(\tau_0 a) J'_m(\tau_0 a)}{\tau_0 (\xi + k_0) (\xi - \lambda_{m10})} \frac{d\xi}{\xi - \eta} \quad . \quad (B.20e)$$

It must be noted that all the functions $u_n(\eta)$ and $v_n(\eta)$ are Cauchy type integrals, over semi-infinite smooth paths, of functions which are integrable and have a continuous derivative on those paths. Then, (Pogorzelski [28], Roos [10]), these functions are analytic everywhere, except for a branch point at $\eta = k_0$ (for the $v_n(\eta)$) or at $\eta = -k_0$ (for the $u_n(\eta)$). The branch cuts will be the paths of

integration themselves, and they can be deformed within their respective quadrants, as long as the branches of hyperbola are not crossed, because that would introduce new terms, due to the fact that some of the integrands have poles on those curves.

Attention will now be given to the integrations around k_0 and $-k_0$. It is important to find the dominant few terms of $R_1^*(\xi)$ and $S_1^*(\xi)$ as $\xi \rightarrow \pm k_0$.

Use was made of the series expansion of the Bessel and Hankel functions in ascending powers of the argument (see Watson [29], Chapter 3). For the limit $\xi \rightarrow k_0$, the variable $\zeta = \xi - k_0$ was used, with $\zeta = se^{i\theta}$, s a constant positive real number which vanishes in the limit, and with θ varying from $\pi/2$ to $-3\pi/2$, whence it follows that $\tau_0 = \sqrt{-2k_0\zeta} + O(\zeta^{3/2}) = \sqrt{2|k_0|s} \exp(1/2)(\pi + \arg k_0 + \theta) + O(s^{3/2})$. For the limit $\xi \rightarrow -k_0$, the same variable names were used, but now $\zeta = \xi + k_0$, $\zeta = se^{i\theta}$, θ varying from $3\pi/2$ to $-\pi/2$, $\tau_0 = \sqrt{2k_0\zeta} + O(\zeta^{3/2}) = \sqrt{2|k_0|s} \exp(1/2)(\arg k_0 + \theta)$.

It is known that, γ being a circle centered at k_0 or $-k_0$, and with ζ as defined above,

$$\oint_{\gamma} \zeta^n d\zeta = \begin{cases} -2\pi i & \text{if } n = -1 \\ 0 & \text{for any other integer } n \end{cases}, \quad (\text{B.21})$$

where the integration is carried out in a clockwise direction. Then, of the several terms of the series expansion of the integrand, only the terms of $O(\zeta^{-1})$ behavior contribute to the integral. Though, for $m = 1$, some terms appear that vary as $\zeta^{-1} \ln \zeta$, they cancel each others out and make no contribution.

For $R_1^{*U}(\eta)$, integration (B.8a) is carried out around $\xi = -k_0$, yielding the contribution $K^*/(\eta + k_0)$, where

$$K^* = \frac{A}{i\pi k_0 a^2} \left[\frac{1}{2k_0} + \frac{k_0 a^2}{m(m+1)} + \frac{x^{L'}(-k_0)}{x^L(-k_0)} - \frac{y^{L'}(-k_0)}{y^L(-k_0)} \right] + \frac{iB}{\pi k a^2 (k_0 + \lambda_{m10})} - \frac{iF y^L(-k_0)}{4\pi k_0 a (k_0 + \mu_{m10}) x^L(-k_0)} . \quad (B.22)$$

Likewise, for $S_1^{*U}(\eta)$, integration is carried out around $-k_0$ resulting in

$$\frac{2ik_0^2 a^2 x^L(-k_0)}{m y^L(-k_0)} K^* \frac{1}{\eta + k_0} . \quad (B.23)$$

For $R_1^{*L}(\eta)$, integration (B.8b) is carried out around $\xi = k_0$, producing the contribution $K^{**}/(\eta - k_0)$, where

$$K^{**} = \frac{2A}{i\pi m k_0} \left\{ \frac{k_0}{m} \left[\frac{x^U(k_0)}{y^U(k_0)} \right]^2 - \frac{m}{4k_0 a^2} \right\} + \frac{B}{i\pi k_0 a^2 (\lambda_{m10} - k_0)} + F \frac{k_0 a x^U(k_0)}{i\pi m^2 (k_0 - \mu_{m10}) y^U(k_0)} . \quad (B.24)$$

Similarly, the contribution for $S_1^{*L}(\eta)$ is

$$\frac{i m y^U(k_0)}{2 x^U(k_0)} K^{**} \frac{1}{\eta - k_0} . \quad (B.25)$$

All that is left, now, is to compute the residues due to the poles captured by the deformations of γ_1 and γ_2 .

For $R_1^{*U}(\eta)$, the residues of $R_1^*(\xi)$ at $-\lambda_{mn}$, $n = 1, 2, 3, \dots$, affected by a negative sign, because the integration is carried out in a clockwise direction, will be due to the terms which are multiplied by the constants A and B, and the first term of $f_1(\xi)$ in (3.40a). They contribute

$$\sum_{n=1}^{\infty} \frac{K_n}{\eta + \lambda_{mn}}, \quad \text{with } K_n = \frac{2}{i\pi a^2} \frac{1}{\lambda_{mn}} \left[\frac{A}{\lambda_{mn} - k_0} + \frac{B}{\lambda_{mn} + \lambda_{m10}} \right]. \quad (\text{B.26})$$

The contributions to $S_1^{*U}(\eta)$ will be due to the poles of $S_1^*(\xi)$ in the lower half-plane. These are: at $-\lambda_{mn}$, $n = 1, 2, 3, \dots$, due to the terms multiplied by A and B, and at $-\mu_{mn}$, $n = 1, 2, 3, \dots$, due to the terms multiplied by D and F, and the first term of $f_2(\xi)$ in (3.40b). All the poles are simple, yielding

$$\sum_{n=1}^{\infty} \pi m K_n \lambda_{mn} h_{mn} \frac{1}{\eta + \lambda_{mn}} - \sum_{n=1}^{\infty} K'_n \frac{1}{\eta + \mu_{mn}}, \quad (\text{B.27})$$

where

$$K'_n = - \frac{k_0^2 a}{\pi m \mu_{mn}} \left(\frac{D}{\mu_{mn} - k_0} + \frac{F}{\mu_{mn} + \mu_{m10}} \right) \quad (\text{B.28a})$$

and

$$h_{mn} = \frac{q_{mn}^2 x^U(\lambda_{mn}) J_m(q_{mn}) H_m^{(1)}(q_{mn})}{(m^2 - q_{mn}^2)(k_0 - \lambda_{mn}) y^U(\lambda_{mn})} . \quad (\text{B.28b})$$

Contributions to $R_1^{*L}(\eta)$ come from simple poles of $R_1^*(\xi)$ at $\xi = \lambda_{mn}$, $n = 2, 3, 4, \dots$, and a double pole at $\xi = \lambda_{m10}$. The simple poles come from all the terms of $R_1^*(\xi)$, and their residues yield

$$\sum_{n=2}^{\infty} \frac{K_n''}{\eta - \lambda_{mn}} , \quad (\text{B.29a})$$

where

$$K_n'' = \frac{2}{i\pi a^2 \lambda_{mn}} \left(\frac{A}{\lambda_{mn} + k_0} + \frac{B}{\lambda_{mn} - \lambda_{m10}} \right) + \frac{h_{mn}}{a} \left(\frac{D}{\lambda_{mn} + k_0} + \frac{F}{\lambda_{mn} - \lambda_{m10}} \right) \quad (\text{B.29b})$$

for $n = 2, 3, 4, \dots$

As to the residue at the double pole, λ_{m10} , get

$$K_1'' \frac{1}{\eta - \lambda_{m10}} + \frac{2B}{i\pi \lambda_{m10} a^2} \frac{1}{(\eta - \lambda_{m10})^2} , \quad (\text{B.30a})$$

where

$$K_1'' = \frac{2A}{i\pi a^2 \lambda_{m10} (\lambda_{m10} + k_0)} + B J_m(q_{m1}) \frac{m^2 - q_{m1}^2}{q_{m1}^2} H_m^{(1)}(q_{m1})$$

$$+ \frac{2B}{\pi i} \left[\frac{1}{m^2 - q_{m1}^2} + \frac{3a}{q_{m1}^3} - \frac{1}{2\lambda_{m10}^2 a^2} \right] + \frac{h_{m1}}{a} \left[\frac{D}{\lambda_{m10} + k_0} + \frac{F}{\lambda_{m10} - \mu_{m10}} \right],$$

(B.30b)

with h_{m1} given by (B.28b) by making $n = 1$.

Finally, for $S_1^{*L}(n)$, contributions come from simple poles of $S_1^*(\xi)$ at $\xi = \mu_{mn}$, $n = 2, 3, 4, \dots$ and at $\xi = \lambda_{m10}$, and from a double pole at $\xi = \mu_{m10}$. From the poles at μ_{mn} , $n \geq 2$, get

$$\sum_{n=2}^{\infty} \frac{K_n''''}{n - \mu_{mn}}, \quad \text{where } K_n'''' = \frac{k_0^2 a}{\pi m \mu_{mn}} \left[\frac{D}{\mu_{mn} + k_0} + \frac{F}{\mu_{mn} - \mu_{m10}} \right],$$

(B.31)

for $n = 2, 3, 4, \dots$

From the pole at λ_{m10} , the contribution is

$$4mB \frac{\lambda_{m10} y^U(\lambda_{m10})}{\pi q_{m1}^2 (\lambda_{m10} + k_0) x^U(\lambda_{m10})} \frac{1}{n - \lambda_{m10}}.$$

(B.32)

The contribution from the double pole at μ_{m10} is

$$K_1'''' = \frac{1}{\eta - \mu_{m10}} + \frac{k_0^2 a F}{\pi m \mu_{m10}} \frac{1}{(\eta - \mu_{m10})^2}, \quad (B.33a)$$

where

$$K_1'''' = D \frac{k_0^2 a}{\pi m \mu_{m10} (k_0 + \mu_{m10})} + F \frac{k_0^2 a^3}{\pi m} \left[\frac{1}{p_{m1}^2} - \frac{1}{2\mu_{m10}^2 a^2} - \frac{2\mu_{m10}^2}{k_0^2 p_{m1}^2} - \frac{i\pi}{2} J_m'(p_{m1}) H_m^{(1)'}(p_{m1}) \right]. \quad (B.33b)$$

The final expressions for $R_1^U(\eta)$, $S_1^U(\eta)$, $R_1^L(\eta)$ and $S_1^L(\eta)$ can now be written.

From (B.1), (B.2), (B.17), (B.22) and (B.26), get

$$R_1^U(\eta) = R_C^U(\eta) + \frac{K^*}{\eta + k_0} + \sum_{n=1}^{\infty} \frac{K_n}{\eta + \lambda_{mn}} + \frac{2x^U(k_0)}{\pi a} Au_1(\eta) + \frac{i}{\pi} Bu_2(\eta) + \frac{F}{\pi i} u_3(\eta). \quad (B.34)$$

From (B.3), (B.4), (B.5), (B.6), (B.18), (B.23) and (B.27),

get

$$S_1^U(\eta) = S_G^U(\eta) + S_L^U(\eta) + S_T^U(\eta) + \frac{2ik_0^2 a^2 x^U(k_0)}{m y^U(k_0)} \frac{K^*}{\eta + k_0} + \pi m \sum_{n=1}^{\infty} \frac{K_n h_{mn} \lambda_{mn}}{\eta + \lambda_{mn}} - \sum_{n=1}^{\infty} \frac{K_n'}{\eta + \mu_{mn}} - \frac{4ik_0}{m} x^U(k_0) Au_4(\eta) + \frac{4m}{ia} Bu_5(\eta) - \frac{ik_0^2 a^3}{m} Fu_6(\eta). \quad (B.35)$$

From (B.1), (B.2), (B.19), (B.24), (B.29) and (B.30), and noting that the second term of (B.30a) exactly cancels the first term of (B.1c),

$$R_1^L(\eta) = \frac{K^{**}}{\eta - k_0} + \sum_{n=2}^{\infty} \frac{K_n^{**}}{\eta - \lambda_{mn}} + \frac{K_1^{**} + C \cdot x^{U'}(\lambda_{m10})}{\eta - \lambda_{m10}} - 2Av_1(\eta) - 2Bv_2(\eta) - 2Dv_3(\eta) + 2Fv_4(\eta) \quad . \quad (B.36)$$

Finally, from (B.3), (B.4), (B.5), (B.6), (B.20), (B.25), (B.31), (B.32) and (B.33), and noting that the second term of (B.33a) exactly cancels the first term of (B.5c), and (B.32) exactly cancels (B.3c),

$$S_1^L(\eta) = \frac{imy^U(k_0)}{2x^U(k_0)} \frac{K^{**}}{\eta - k_0} + \sum_{n=2}^{\infty} \frac{K_n^{**}}{\eta - \mu_{mn}} + \left[T \frac{\mu_{m10}^2 + (\mu_{m10} - k_0)^2}{k_0^2} \cdot y^U(\mu_{m10}) + K_1^{**} + T(\mu_{m10} - k_0)y^{U'}(\mu_{m10}) \right] \frac{1}{\eta - \mu_{m10}} - \frac{ik_0^2 a^3}{m} Dv_5(\eta) - \frac{ik_0^2 a^3}{m} Fv_6(\eta) + \frac{4m}{ia} Av_7(\eta) + \frac{4m}{ia} Bv_8(\eta) \quad , \quad (B.37)$$

where $S_1^L(\eta)$ has been incorporated in the terms in T.

APPENDIX C. SOME PROPERTIES OF THE TRANSFORMS OF THE FIELDS FOR $\rho < a$

The Fourier transforms of the z-components of the fields inside the dielectric cylinder are given by (2.12a) and (2.13a). Series expansions of the type (3.1) can be performed, yielding

$$V_z(\eta, \rho) = V_{z0}(\eta, \rho) + V_{z1}(\eta, \rho)\Delta k + \dots \quad (\text{C.1a})$$

and

$$I_z(\eta, \rho) = I_{z0}(\eta, \rho) + I_{z1}(\eta, \rho)\Delta k + \dots, \quad (\text{C.1b})$$

where

$$V_{z0}(\eta, \rho) = V_{z0}^L(\eta) \frac{J_m(\nu_0 \rho)}{J_m(\nu_0 a)}, \quad (\text{C.2a})$$

$$V_{z1}(\eta, \rho) = V_{z1}^L(\eta) \frac{J_m(\nu_0 \rho)}{J_m(\nu_0 a)} + V_{z0}^L(\eta) w(\eta, \rho), \quad (\text{C.2b})$$

$$I_{z0}(\eta, \rho) = I_{z0}(\eta, a-) \frac{J_m(\nu_0 \rho)}{J_m(\nu_0 a)} \quad (\text{C.3a})$$

and

$$I_{z1}(\eta, \rho) = I_{z1}(\eta, a-) \frac{J_m(\nu_0 \rho)}{J_m(\nu_0 a)} + I_{z0}(\eta, a-) w(\eta, \rho), \quad (\text{C.3b})$$

with

$$w(\eta, \rho) = \frac{k_0}{\nu_0} \left\{ \frac{J_m'(\nu_0 \rho)}{J_m(\nu_0 a)} \rho - a \frac{J_m'(\nu_0 a) J_m(\nu_0 \rho)}{[J_m(\nu_0 a)]^2} \right\}. \quad (\text{C.4})$$

In (C.2), $V_{z_0}^L(\eta)$ is given by (3.31b) and (2.53d), and $V_{z_1}^L(\eta)$ is given by (3.36d) and the first order equivalent of (2.53d).

$I_{z_0}(\eta, a^-)$ is given by (2.27), and its series expansion, of the type (3.1), yields $I_{z_0}(\eta, a^-)$ and $I_{z_1}(\eta, a^-)$, given, respectively, by

$$I_{z_0}(\eta, a^-) = \frac{i\pi a v_0}{2} J_m(v_0 a) H_m^{(1)'}(v_0 a) \left[\mathcal{J}_{\phi_0}^U(\eta) + \frac{\alpha_m}{\eta - \lambda_{m10}} \right] \quad (C.5a)$$

and

$$\begin{aligned} I_{z_1}(\eta, a^-) &= \frac{i\pi a v_0}{2} J_m(v_0 a) H_m^{(1)'}(v_0 a) \left[\mathcal{J}_{\phi_1}^U(\eta) + \frac{\alpha_m k_0}{\lambda_{m10}(\eta - \lambda_{m10})^2} \right] \\ &+ \frac{i\pi m k_0 \eta}{\omega \mu v_0^2} J_m(v_0 a) H_m^{(1)}(v_0 a) V_{z_0}^L(\eta) + \frac{i\pi a k_0}{2v_0} \left[\mathcal{J}_{\phi_0}^U(\eta) + \frac{\alpha_m}{\eta - \lambda_{m10}} \right] \\ &\cdot \left\{ a v_0 \frac{J_m'(v_0 a)}{J_m(v_0 a)} + 2 + \frac{\pi a v_0}{2i} \left[v_0 a \frac{m^2 - v_0^2 a^2}{v_0^2 a^2} J_m(v_0 a) \cdot H_m^{(1)}(v_0 a) - 2J_m(v_0 a) \right. \right. \\ &\left. \left. \cdot H_m^{(1)'}(v_0 a) - v_0 a J_m'(v_0 a) H_m^{(1)'}(v_0 a) \right] \right\} J_m(v_0 a) H_m^{(1)'}(v_0 a) \quad (C.5b) \end{aligned}$$

It is the objective of this appendix to show that neither one of the functions (C.2) and (C.3) has branch points in the lower half-plane, $\text{Im } \eta < \text{Im } k_0$. Use will be made of (B.10), wherefrom both $J_m(v_0 \rho)/J_m(v_0 a)$ and $w(\eta, \rho)$ are seen to be free of branch points. Hence, as $V_{z_0}^L(\eta)$ and $V_{z_1}^L(\eta)$ are analytic in the lower half-plane, it is concluded that $V_{z_0}(\eta, \rho)$ and $V_{z_1}(\eta, \rho)$ are free of branch points in the lower half-plane, and their only singularities in that region are poles at $\eta = -\mu_{mn}$, $n = 1, 2, 3, \dots$

A similar conclusion must now be reached concerning $I_{z_0}(\eta, \rho)$ and $I_{z_1}(\eta, \rho)$. From (4.3) it is seen that, using the constants defined in (3.41),

$$\mathcal{U}_{\phi_0}^U(\eta) + \frac{\alpha_m}{\eta - \lambda_{m10}} = \frac{2}{i\pi k_0 a^2} \left(\frac{A}{\eta + k_0} + \frac{B}{\eta - \lambda_{m10}} \right) \frac{x^L(\eta)}{J'_m(\nu_0 a) H_m^{(1)}(\nu_0 a)}. \quad (C.6)$$

Using (C.6) in (C.5a), it follows that $I_{z_0}(\eta, a^-)$ has no branch point in the lower half-plane, its only singularities in that region being poles at $\eta = -\lambda_{mn}$, $n = 1, 2, 3, \dots$

Hence, in the lower half-plane, $I_{z_0}(\eta, \rho)$ has no branch points, it has only poles at $\eta = -\lambda_{mn}$ and $\eta = -\mu_{mn}$, $n = 1, 2, 3, \dots$

$I_{z_1}(\eta, a^-)$, as given by (C.5b), has a possible branch point at $\eta = -k_0$. A branch cut is assumed, like in Fig. B.1, and the discontinuity of (C.5b) across that cut is found, by using (C.6), (3.42a), (2.53d), (3.31b), (3.29b), (4.2) and (4.10). Using (B.10) and definitions (3.41), that discontinuity is found to be

$$\begin{aligned} I_{z_1+}(\eta, a^-) - I_{z_1-}(\eta, a^-) &= -i\pi a \left(\frac{D}{\eta + k_0} + \frac{F}{\eta - \mu_{m10}} \right) \frac{\eta y^L(\eta) [J_m(\nu_0 a)]^2}{\eta - k_0} \\ &- \pi a \left\{ \frac{2x^U(k_0)A}{a} \kappa_1(\eta) + iB \kappa_2(\eta) - iF \kappa_3(\eta) \right\} \frac{\nu_0 x^L(\eta) J_m(\nu_0 a)}{J'_m(\nu_0 a)} \\ &+ i\pi a \left(\frac{A}{\eta + k_0} + \frac{B}{\eta - \lambda_{m10}} \right) \frac{\nu_0 x^L(\eta) J_m(\nu_0 a)}{J'_m(\nu_0 a)} g(\eta), \quad (C.7) \end{aligned}$$

where $g(\eta)$ is given by (B.12).

When the values of $\kappa_n(\eta)$, given by (4.9) and (B.17), are used in (C.7), and after some manipulation, the right-hand side of (C.7) is found to be identically zero along the branch cut. This means that $I_{z_1}(\eta, a_-)$ does not have a branch point at $-k_0$, as (C.5b) would seem to suggest. Rather, its only singularities in the lower half-plane are poles at $\eta = -\lambda_{mn}$ and $\eta = -\mu_{mn}$, with $n = 1, 2, 3, \dots$

It is now concluded that $I_{z_1}(\eta, \rho)$ has no branch points in the lower half-plane, and its only singularities in that region are poles at $\eta = -\lambda_{mn}$ and $\eta = -\mu_{mn}$, $n = 1, 2, 3, \dots$

Concerning the transforms of the other components of the fields, $V_\phi(\eta, \rho)$ and $I_\phi(\eta, \rho)$ are given by (2.9d) and (2.9a), respectively, in terms of $V_z(\eta, \rho)$ and $I_z(\eta, \rho)$. Inside the dielectric cylinder, it follows that

$$V_{\phi 0}(\eta, \rho) = \frac{i}{v_0^2} \left[\omega \mu \rho \frac{\partial I_{z0}(\eta, \rho)}{\partial \rho} + m \eta V_{z0}(\eta, \rho) \right], \quad (C.8a)$$

$$I_{\phi 0}(\eta, \rho) = \frac{1}{i v_0^2} \left[\omega \epsilon_0 \rho \frac{\partial V_{z0}(\eta, \rho)}{\partial \rho} + m \eta I_{z0}(\eta, \rho) \right], \quad (C.8b)$$

$$V_{\phi 1}(\eta, \rho) = -\frac{2ik_0}{v_0^4} \left[\omega \mu \rho \frac{\partial I_{z0}(\eta, \rho)}{\partial \rho} + m \eta V_{z0}(\eta, \rho) \right] + \frac{i}{v_0^2} \left[\omega \mu \rho \frac{\partial I_{z1}(\eta, \rho)}{\partial \rho} + m \eta V_{z1}(\eta, \rho) \right], \quad (C.8c)$$

and

$$I_{\phi 1}(\eta, \rho) = \frac{2ik_0}{v_0^4} \left[\omega \epsilon_0 \rho \frac{\partial V_{z0}(\eta, \rho)}{\partial \rho} + m \eta I_{z0}(\eta, \rho) \right] + \frac{1}{i v_0^2} \left[\frac{2k_0}{\omega \mu} \rho \frac{\partial V_{z0}(\eta, \rho)}{\partial \rho} + \omega \epsilon_0 \rho \frac{\partial V_{z1}(\eta, \rho)}{\partial \rho} + m \eta I_{z1}(\eta, \rho) \right]. \quad (C.8d)$$

Then, the conclusion that has been reached for $V_z(\eta, \rho)$ and $I_z(\eta, \rho)$ implies also that the only singularities of the functions (C.8) in the lower half-plane are poles, and no branch points occur in that region.

From (2.7) and (2.8), a similar conclusion is attained for the ρ -components of the transformed fields inside the dielectric cylinder.

APPENDIX D. SOME PROPERTIES OF THE TRANSFORMS OF THE FIELDS FOR $\rho > a$

The Fourier transforms of the z-components of the fields outside the dielectric cylinder, $\rho > a$, are (2.12b) and (2.13b). Then,

$$V_{z0}(\eta, \rho) = V_{z0}^L(\eta) \frac{H_m^{(1)}(\nu_0 \rho)}{H_m^{(1)}(\nu_0 a)}, \quad (D.1a)$$

$$V_{z1}(\eta, \rho) = V_{z1}^L(\eta) \frac{H_m^{(1)}(\nu_0 \rho)}{H_m^{(1)}(\nu_0 a)}, \quad (D.1b)$$

$$I_{z0}(\eta, \rho) = I_{z0}(\eta, a+) \frac{H_m^{(1)}(\nu_0 \rho)}{H_m^{(1)}(\nu_0 a)} \quad (D.1c)$$

and

$$I_{z1}(\eta, \rho) = I_{z1}(\eta, a+) \frac{H_m^{(1)}(\nu_0 \rho)}{H_m^{(1)}(\nu_0 a)}. \quad (D.1d)$$

It is now remarked that $H_m^{(1)}(\nu_0 a)$ has no zeros in the region of interest, so that $V_{z0}(\eta, \rho)$ and $V_{z1}(\eta, \rho)$ have no poles in the lower half-plane, but have a branch point at $\eta = -k_0$, when $\rho > a$.

With $I_z(\eta, a+)$ given by (2.26), it follows that

$$I_{z0}(\eta, a+) = \frac{1}{k_0 a} \left(\frac{A}{\eta + k_0} + \frac{B}{\eta - \lambda_{m10}} \right) \frac{\nu_0 x^L(\eta) H_m^{(1)}(\nu_0 a)}{H_m^{(1)}(\nu_0 a)}. \quad (D.2)$$

Since $H_m^{(1)'}(v_0 a)$ has no zeros in the region of interest either, it is concluded that $I_{z_0}(\eta, \rho)$ has no poles in the lower half-plane, for $\rho > a$, but has a branch point at $\eta = -k_0$.

Also,

$$\begin{aligned}
 I_{z_1}(\eta, a+) &= \frac{i\pi a v_0}{2} J_m'(v_0 a) H_m^{(1)}(v_0 a) \left[\mathcal{L}_{\phi_1}^U(\eta) + \frac{\alpha_m k_0}{\lambda_{m10}(\eta - \lambda_{m10})^2} \right] \\
 &+ \frac{i\pi m k_0 \eta}{\omega \mu v_0^2} J_m(v_0 a) H_m^{(1)}(v_0 a) v_{z_0}^L(\eta) \\
 &+ \frac{i\pi a k_0}{2v_0} \left[\mathcal{L}_{\phi_0}^U(\eta) + \frac{\alpha_m}{\eta - \lambda_{m10}} \right] \left\{ \frac{m^2 - v_0^2 a}{v_0 a} \frac{J_m(v_0 a)}{J_m'(v_0 a)} \right. \\
 &+ \frac{\pi a v_0}{2i} \left[\frac{m^2 - v_0^2 a^2}{v_0 a} J_m(v_0 a) H_m^{(1)}(v_0 a) - 2J_m(v_0 a) H_m^{(1)'}(v_0 a) \right. \\
 &\left. \left. - v_0 a J_m'(v_0 a) H_m^{(1)'}(v_0 a) \right] \right\} J_m'(v_0 a) H_m^{(1)}(v_0 a) \quad . \quad (D.3)
 \end{aligned}$$

It is noted that

$$\begin{aligned}
 \mathcal{L}_{\phi_1}^U(\eta) + \frac{\alpha_m k_0}{\lambda_{m10}(\eta - \lambda_{m10})^2} &= \left[x^U(\eta) \mathcal{L}_{\phi_1}^U(\eta) + \frac{\alpha_m k_0 x^U(\eta)}{\lambda_{m10}(\eta - \lambda_{m10})^2} \right] \\
 &\cdot \frac{x^L(\eta)}{J_m'(v_0 a) H_m^{(1)'}(v_0 a)} \quad , \quad (D.4)
 \end{aligned}$$

with $\mathcal{L}_{\phi_1}^U(\eta)$ given by (3.42a), whence the first term in the right-hand side of (D.3) has poles for $\eta = -\lambda_{mn}$, $n = 1, 2, 3, \dots$. However, and using (C.6), it is seen that the first term inside the curly brackets of (D.3) also exhibits poles at $\eta = -\lambda_{mn}$, and it can be shown, straightforwardly, that these poles exactly cancel the poles due to the first term of (D.3). It is concluded that $I_{z_1}(\eta, a^+)$ has no poles in the lower half-plane, only a branch point at $\eta = -k_0$. Therefore, the only singularity of $I_{z_1}(\eta, \rho)$ in the lower half-plane, for $\rho > a$, is a branch point at $\eta = -k_0$.

By using the expressions corresponding to (C.8), but now for $\rho > a$, and also from (2.7) and (2.8), it can be concluded that all the ϕ -components and ρ -components of the transformed fields, for $\rho > a$, exhibit a branch point at $-k_0$ as the only singularity in the lower half-plane, and no poles at all in that region.

LIST OF REFERENCES

1. Kiely, D. G., Dielectric Aerials, John Wiley and Sons, Inc., 1953.
2. J. Brown and J.O. Spector, "The Radiating Properties of End-Fire Aerials," Proc. IEE, Vol. 104, Part B, pp. 27-34, 1957.
3. James, J. R., "Theoretical Investigation of Cylindrical Dielectric-Rod Antennas," Proc. IEE, Vol. 114, pp. 309-319, 1967.
4. Yaghjian, A. D. and E. T. Kornhauser, "A Modal Analysis of the Dielectric Rod Antenna Excited by the HE_{11} Mode," IEEE Trans. Antennas Propagat., Vol. AP-20, No. 2, pp. 122-128, 1972.
5. Andersen, J. B., Metallic and Dielectric Antennas, Polyteknisk Forlag, 1971.
6. Yip, G. L., "Launching Efficiency of the HE_{11} Surface Wave Mode on a Dielectric Rod," IEEE Trans. Microwave Theory Tech., Vol. MTT-18, No. 12, pp. 1033-1041, 1970.
7. Jones, D. S., "A Simplifying Technique in the Solution of a Class of Diffraction Problems," Quart. J. Math., Oxford, 2nd Series, Vol. 3, pp. 189-196, 1952.
8. Noble, B., Methods Based on the Wiener-Hopf Technique, Pergamon Press, 1958.
9. Heins, A. E., Chapter VI of J. Schwinger and D. S. Saxon, Discontinuities in Waveguides, Gordon and Breach, 1968.
10. Roos, B. W., Analytic Functions and Distributions in Physics and Engineering, John Wiley and Sons, Inc., 1969.

11. Mittra, R. and S. W. Lee, Analytical Techniques in the Theory of Guided Waves, The MacMillan Co., 1971.
 12. Bailin, L. L., "An Analysis of the Effect of the Discontinuity in a Bifurcated Circular Guide Upon Plane Longitudinal Waves," J. of Res. Nat. Bur. Stand., Vol. 47, pp. 315-335, 1951.
 13. Papadopoulos, V. M., "The Scattering Effect of a Junction Between Two Circular Waveguides," Quart. J. Mech. and Appl. Math., Vol. 10, pp. 191-209, 1957.
 14. Daniele, V. G., I. Montrosset and R. S. Zich, "Wiener-Hopf Solution for the Junction Between a Smooth and a Corrugated Cylindrical Waveguide," Radio Sci., vol. 14, No. 6, pp. 943-955, 1979.
 15. Levine, H. and J. Schwinger, "On the Radiation of Sound from an Unflanged Circular Pipe," Physical Review, Vol. 73, No. 4, pp. 383-406, 1948.
 16. Weinstein, L. A., The Theory of Diffraction and the Factorization Method, The Golem Press, 1969.
 17. Rawlins, A. D., "Radiation of Sound from an Unflanged Rigid Cylindrical Duct with an Acoustically Absorbing Internal Surface," Proc. R. Soc. London, Series A, Vol. 361, pp. 65-91, 1978.
 18. Ledebuer, S., "The Excitation of a Surface Wave by a Coaxial Waveguide," from Electromagnetic Wave Theory (Proc. of a Symposium held at Delft, The Netherlands, Part 1), edited by J. Brown, Pergamon Press, 1967.
-

19. Angulo, C. M. and W.S.C. Chang, "The Excitation of a Dielectric Rod by a Cylindrical Waveguide," IRE Trans. on Microwave Theory Tech., MTT-6, No. 4, pp. 389-393, 1958.
20. Pearson, J. D., "The Diffraction of Electro-Magnetic Waves by a Semi-Infinite Circular Wave Guide," Proc. Camb. Phil. Soc., Vol. 49, pp. 659-667, 1953.
21. Senior, T.B.A., "Diffraction by an Imperfectly Conducting Half-Plane at Oblique Incidence," Appl. Sci. Res., Section B, Vol. 8, pp. 35-61, 1959.
22. Heins, A. E., "Systems of Wiener-Hopf Integral Equations and Their Application to Some Boundary Value Problems in Electromagnetic Theory," Proc. Symposia Appl. Math., Vol. II, pp. 76-81, McGraw-Hill, 1950.
23. Hurd, R. A., "The Wiener-Hopf-Hilbert Method for Diffraction Problems," Can. J. Phys., Vol. 54, pp. 775-780, 1976.
24. Daniele, V. G., "On the Factorization of Wiener-Hopf Matrices in Problems Solvable with Hurd's Method," IEEE Trans. Antennas Propagat., Vol. AP-26, No. 4, pp. 614-616, 1978.
25. Rawlins, A. D., "A Note on the Factorization of Matrices Occurring in Wiener-Hopf Problems," IEEE Trans. Antennas Propagat., Vol. AP-28, No. 6, pp. 933-934, 1980.
26. Heins, A. E., "The Sommerfeld Half-Plane Problem Revisited I: The Solution of a Pair of Coupled Wiener-Hopf Integral Equations," Math. Meth. in the Appl. Sci., Vol. 4, pp. 74-90, 1982.

27. Meixner, J., "The Behavior of Electromagnetic Fields at Edges,"
Res. Report No. EM-72, New York University, Inst. Math. Sci.,
Div. E.M. Res., 1954.
28. Pogorzelski, W., Integral Equations and Their Applications,
Vol. 1, Pergamon Press, 1966.
29. Watson, G. N., Theory of Bessel Functions, 2nd Edition, Cambridge
University Press, 1952.